# CONVERGENT EVOLUTION AND SPECIES BOUNDARIES IN LOMATIUM SPECIES (APIACEAE)

by

Michael Ottenlips

A thesis submitted in partial fulfillment

of the requirements for the degree of

Master of Science in Biology

Boise State University

May 2019

BOISE STATE UNIVERSITY GRADUATE COLLEGE

# DEFENSE COMMITTEE AND FINAL READING APPROVALS

of the thesis submitted by

Michael Ottenlips

Thesis Title: Convergent Evolution and Species Boundaries in *Lomatium* Species (Apiaceae)

Date of Final Oral Examination: 15 February 2019

The following individuals read and discussed the thesis submitted by student Michael Ottenlips, and they evaluated his presentation and response to questions during the final oral examination. They found that the student passed the final oral examination.

| | |
|---|---|
| James F. Smith, Ph.D. | Chair, Supervisory Committee |
| Stephen Novak. Ph.D. | Member, Supervisory Committee |
| Sven Buerki, Ph.D. | Member, Supervisory Committee |
| Donald H. Mansfield, D.A. | Member, Supervisory Committee |

The final reading approval of the thesis was granted by James F. Smith, Ph.D., Chair of the Supervisory Committee. The thesis was approved by the Graduate College.

ACKNOWLEDGEMENTS

I would like to acknowledge the following mentors, collaborators, and friends: My major professor Jim Smith for always being available to discuss research questions, technical problems, and anything else no matter how important or trivial. My graduate committee for providing research guidance, especially Sven Buerki for all the bioinformatics assistance, arranging the visit to Kew Gardens, and providing accesses to his Linux machines. Steve Novak, for his great teaching and guidance on molecular ecology theory. Don Mansfield, for his knowledge of *Lomatium* morphology, ecology, evolution, and geography. Emily Washburne, for her emotional *and* field support, may she never have to dig up another *Lomatium* root again. Kew Gardens and the PAFTOL team, especially Steven Dodsworth and Felix Forest, for arranging my visit and teaching me the molecular techniques in Chapter Two. The Boise State Biology Department for financial assistance and providing a wonderful experience in the form of a teaching assistantship. Finally, the *Lomatium andrusianum* donors for providing funding for this project. This research was truly a team effort and would not have been possible without the people thanked here and many others too numerous to list.

ABSTRACT

Speciation is a complex and ongoing process caused by a variety of forces; this has in part led to a proliferation of species concepts ranging from arbitrary similarity-based concepts such as the morphological species concept to ancestry-based concepts that incorporate the complex nature of gene inheritance. Ancestry-based concepts rely on homologous characters, either molecular or morphological, that share a common origin in order to draw inferences about evolutionary histories and help understand species boundaries. Convergence in morphology and paralogous loci in molecular datasets can cause confusion in understanding if characters are functionally homologous. Other challenges in inferring species boundaries and phylogenies include hybridization, incomplete lineage sorting, and species with a high degree of phenotypic plasticity. Species boundaries and phylogenies complicated by the previously mentioned factors can be understood more readily by incorporating molecular data and associated phylogenetic analysis.

The Perennial Endemic North American clade of Apiaceae (PENA) is one of the largest and least understood plant radiations in Western North America. *Lomatium* is the largest genera in PENA and as traditionally defined is paraphyletic with many cases of homoplasy and morphological convergence. Species boundaries, evolutionary relationships, and field identification are notoriously difficult in this genus. This research proposes to use molecular, morphological, and ecological data sources to investigate species boundaries and evolutionary relationships in two groups within PENA: three

alpine endemics found within the Wallowa and Elkhorn Mountains of eastern Oregon (*Lomatium greenmanii, Lomatium erythrocarpum,* and *Lomatium oreganum*) and the *Lomatium packardiae/anomalum* subcomplex of the larger *Lomatium triternatum* complex found throughout the inland Northwest, intermountain West, and Northern Rocky Mountains.

Convergent evolution is a common phenomenon among alpine plants due to the extreme selective pressures of the environment and the limited number of successful plant body designs that can withstand this environment. In two isolated mountain ranges in eastern Oregon, three morphological similar alpine endemic *Lomatium* exist; these similarities in geographic distribution, habitat preference, and morphology can be ascribed to either shared ancestry or convergent evolution. Previous studies based on limited morphological and molecular data suggested that shared ancestry was the cause of similarities in at least two of these lineages (*L. greenmanii* and *L. oreganum*). In the present study, newly sequenced samples of *L. oreganum L. greenmanii* and *L. erythrocarpum* are included in a phylogeny based on Sanger-sequence data (five plastid markers and two nuclear ribosomal) of the greater PENA clade including about ~200 samples spread across ~70 taxa. Each alpine *Lomatium* occupies a different phylogenetic position indicating that convergence and not shared ancestry is the major force influencing the evolution of similar phenotypes in this group. Increased conservation efforts are urged for these rare taxa as this research indicates that the phylogenetic diversity of the Wallowa and Elkhorn ranges is higher than originally hypothesized.

Inferring species boundaries is a complex effort complicated by many factors including theoretical issues dealing with the nature of the species unit itself and

biological realities which confound field or morphological-based identification. Next-generation sequencing has resulted in a 10 to 100-fold increase in the amount of molecular data available to researchers. The combination of next-generation sequencing and the recent development of complex statistical software that can model the speciation process while incorporating coalescent theory and accounting for incomplete lineage sorting allow researchers to investigate species boundaries and evolutionary relationships accurately in previously recalcitrant taxa. Morphological, ecological, and geographic differences in the *L. anomalum/packardiae* subcomplex do not always agree with monophyletic groups in Sanger-sequence based studies. Hypotheses for the recalcitrant nature of this subcomplex include that the complex is one phenotypically plastic taxa or incomplete lineage sorting is causing the incongruences between morphological, ecological, and molecular data. Fifty-four low copy nuclear introns and whole plastome data sets generated by target-enriched next-generation sequencing were used to generate three types of phylogenies: a concatenated approach for the intron data (MrBayes), a coalescent-based analysis of the intron data (STACEY; ASTRAL-III), and a Bayesian analysis of the whole plastome data (MrBayes). Further, morphological, ecological, environmental, and geographic data were investigated to uncover any unique characteristics which correspond with monophyletic groups. The STACEY coalescent-based phylogeny was the only analysis to uncover monophyletic groups (seven fine scale clades included in three coarser clades) that agree with non-molecular external data including geography and some previously recognized taxonomy. *Lomatium packardiae* was resolved as monophyletic and was the only clade distinct in a PCA of reproductive characters with shorter umbel rays and fruits than other members of the subcomplex.

Incipient speciation with a high degree of incomplete lineage sorting and some phenotypic plasticity appears to be the most likely explanation for the incongruences observed in earlier Sanger-based studies. Currently, geography is the most reliable indicator of phylogenetic placement in the *L. packardiae/anomalum* subcomplex.

TABLE OF CONTENTS

ACKNOWLEDGEMENTS ..... iv

ABSTRACT ..... v

LIST OF TABLES ..... xii

LIST OF FIGURES ..... xiii

CHAPTER ONE: CONVERGENT EVOLUTION AMONG THREE RARE ALPINE ENDEMIC LOMATIUM ..... 1

Abstract ..... 1

Introduction ..... 2

Materials and Methods ..... 8

Sampling, Extractions, PCR, and Sanger Sequencing ..... 8

Phylogenetic Reconstruction ..... 9

Climatic Analysis ..... 10

Geography, Morphology, and Ecology ..... 11

Results ..... 12

Sampling, Extractions, PCR, and Sanger Sequencing ..... 12

Phylogenetic Reconstruction ..... 12

Climatic Analysis ..... 13

Geography, Morphology, and Ecology ..... 13

Discussion ..... 13

Works Cited ..... 34

CHAPTER TWO: INVESTIGATING SPECIES BOUNDARIES IN THE LOMATIUM PACKARDAIE/ANOMALUM SUBCOMPLEX ..... 41

Abstract ..... 41

Introduction ..... 43

Materials and Methods ..... 53

Sample Collection ..... 53

Molecular Methods ..... 54

Bioinformatics Workflow ..... 57

Phylogenetic Reconstruction ..... 59

Ecological, Climatic, and Morphological Analyses ..... 62

Results ..... 64

Sample Collection ..... 64

Assembly Summary ..... 65

Phylogenetic Reconstruction ..... 65

Ecological and Climatic Analysis ..... 67

Morphological Analyses ..... 67

Discussion ..... 68

Reconciling the Chloroplast and Nuclear Phylogenies ..... 69

Environment and Morphological Variation ..... 75

Efficacy of Introns and Coalescent Theory in Shallow-scale Phylogenetic Analysis ..... 77

Conclusions ..... 79

Descriptions of Clades Recovered in STACEY Analysis ..... 80

Works Cited ..... 106

APPENDIX A ..... 116

Samples and Genbank Accession Numbers for Chapter 1 ..... 117

APPENDIX B ..... 129

Table depicting voucher information and which specimens were available for each analysis. (Chapter 2) ..... 130

APPENDIX C ..... 133

Box blot from pilot study of pocket-penetrometer efficacy (Chapter 2) ..... 134

APPENDIX D ..... 135

Raw soil chemistry and physical properties data (Chapter 2) ..... 136

APPENDIX E ..... 138

Climatic variables for each collection (Chapter 2) ..... 138

APPENDIX F ..... 142

Summary of reproductive character measurements. Each cell is the mean of 5 replicate measures. (Chapter 2) ..... 143

APPENDIX G ..... 144

The mean of 5 replicate measurements for leaflet width and length taken from Herbarium collections. (Chapter 2) ..... 145

LIST OF TABLES


Table 1.1 Specimens used in the climatic analysis. Collections denoted with an * where georeferenced.....22

Table 1.2 Specimens reviewed for morphological comparisons.....24

Table 1.3 Results from the Approximately-Unbiased test performed in Consel. p-values < 0.05 were consider significant. The results reject the possibility of the alpine endemics being included within one another.....25

Table 1.4 Bioclimatic variables associated with confirmed populations of the three alpine endemics. Codes correspond to the variable in the key: bio1_12 = Annual Mean Temperature (°C); bio2_12= Mean Diurnal Range (°C); bio3_12 = Isothermality (°C); bio5_12 = Max Temperature of the Warmest Month (°C); bio6_12 = Min Temperature of the Coldest Month (°C); bio7_12 = Temperature Annual Range (°C); bio8_12 = Mean Temperature of the Wettest Quarter (°C); bio9_12 = Mean Temperature of the Driest Quarter (°C); bio11_12 = Mean Temperature of the Warmest Quarter (°C); bio12_12 = Mean Temperature of the Coldest Quarter (°C); bio13_12 = Annual Precipitation (mm); bio14_12 = Precipitation of the Wettest Month (mm); bio16_12 = Precipitation of the Driest Month (mm); bio19_12 = Precipitation of the Wettest Quarter (mm).....26

Table 1.5 Comparison of morphological similarities.....28

Table 2.1 Assembly statistics of the 54 introns. Gene number refers to the unique identifier associated with the Angiosperm 353 bait kit target file. .....102

Table 2.2 MrBayes analysis assembly statistics.....105

LIST OF FIGURES

Figure 1.1 Map of study area. Inset A depicts the Wallowa Mountains, and Inset B depicts the Elkhorn Mountains. Red dots represent L. erythrocarpum populations, green dots represent L. greenmanii populations, and blue dots represent L. oreganum populations. .....29

Figure 1.2. Photographs representing L. greenmanii (A), L. oreganum (B), and L. erythrocarpum (C). Copyright < L. greenmanii (A: Gerald Carr), L. oreganum (B: Bonnie Olson), and L. erythrocarpum (C: Gene Yates)>; courtesy of OregonFlora. .....31

Figure 1.3.A Phylogenetic tree depicting the relationship between the three alpine endemic species. Lomatium greenmanii branches are colored green, L. erythrocarpum red, and L. oreganum blue for emphasis. If more than one individual was sampled for a monophyletic species, the branches were collapsed and replaced with a triangle. The number in parentheses after the species name indicates the number of individuals sampled. Support values indicate are maximum parsimony bootstrap (MPBS), maximum likelihood bootstrap (MLBS), and Bayesian inferences posterior probabilities (BIPP) in following format MPBS/MLBS/BIPP. Values over 75/75/.95 are indicated with a 3 point thickened branch, and maximum support (100/100/1) is indicated by a 6-point thickened branch. .....31

Figure 1.3.B Phylogenetic tree depicting the relationship between the three alpine endemic species. L. greenmanii branches are colored green, L. erythrocarpum red, and L. oreganum blue for emphasis. If more than one individual was sampled for a monophyletic species, the branches were collapsed and replaced with a triangle. The number in parentheses after the species name indicates the number of individuals sampled. Support values indicate are maximum parsimony bootstrap (MPBS), maximum likelihood bootstrap (MLBS), and Bayesian inferences posterior probabilities (BIPP) in following format MPBS/MLBS/BIPP. Values over 75/75/.95 are indicated with a 3 point thickened branch, and maximum support (100/100/1) is indicated by a 6-point thickened branch. .....32

Figure 1.4 PCA depicting the similar climatic niche space of the three Lomatium species. PCA was performed on noncorrelated centered and scale BIOCLIM variables extracted at the 30 arc-second resolution. All known populations of these rare plants within this resolution are included in the analysis. Red dots represented L. erythrocarpum; green L. greenmanii;

blue L. oreganum. Convex frames are drawn to highlight the climatic similarities. ..... 33

Figure 2.1. A. Photograph of wider leaflets suggestive of Lomatium anomalum in the field. B. Photograph of the short narrow leaflets suggestive of Lomatium packardiae. C. Sanger-sequence based analysis of L. anomalum/packardiae subcomplex modified from Smith et al. 2018. Support values are MP/ML/BI with 1-point thickened branches representing support values of (>.75/>.75/>.95) and 2-point thickened branches representing support values of (1/1/1). Purple dots correspond to morphology A. Yellow dots correspond to morphology B. Blue dots represent a third morphology of narrow almost linear leaflets, not shown. ..... 87

Figure 2.2. Bayesian analysis of the concatenated nuclear data set (54 low copy introns). Support values are Bayesian posterior probabilities. Colors correspond to the clades recovered in the STACEY analysis. Pink represents L. packardiae, yellow 'Mann Creek', brown 'Hell's Canyon, green ' East-Central Oregon', blue 'Camas Prairie', black L. triternatum var. triternatum, gray-blue 'Western Montana, and red L. andrusianum. .89

Figure 2.3. Bayesian analysis of the chloroplast data set. Support values are Bayesian posterior probabilities. Colors correspond to the clades recovered in the STACEY analysis. Pink represents L. packardiae, yellow 'Mann Creek', brown 'Hell's Canyon, green ' East-Central Oregon', blue 'Camas Prairie', black L. triternatum var. triternatum, gray-blue 'Western Montana, and red L. andrusianum. ..... 91

Figure 2.4. STACEY analysis of 54 introns. Colors correspond to clades described in the discussion and the morphological and climatic analyses. Support values are posterior probabilities. Values under .50 are collapsed into polytomies. The tree is manually rooted on L. andrusianum. Pink represents L. packardiae, yellow 'Mann Creek', brown 'Hell's Canyon, green ' East-Central Oregon', blue 'Camas Prairie', black L. triternatum var. triternatum, gray-blue 'Western Montana, and red L. andrusianum. Th red dots indicate the taxa with incongruent placements in the concatenated Bayesian analysis which agree with geography in the STACEY analysis. ..... 93

Figure 2.5. Map depicting locations of the samples and the associated clades uncovered in the STACEY analysis. Outgroups (Ottenlips 80; Smith 13048) from the concatenated BI, chloroplast BI, and ASTRAL analyses are included as light green diamonds. The broader STACEY clades are represented by shapes (Circle for 'Andrusianum'; triangle for 'Northern'; and square for 'Southern'). The finer STACEY clades are color coded(Pink represents L. packardiae, yellow 'Mann Creek', brown 'Hell's

Canyon, green ‘ East-Central Oregon’, blue ‘Camas Prairie’, black L. triternatum var. triternatum, gray-blue ‘Western Montana, and red L. andrusianum).....94

Figure 2.6. ASTRAL species tree depicting the relationships between the samples. The three support values on each branch are for the quad partition and show three posterior probabilities for each node: one value for the main topology, one value for probability the clade belongs to the sister group, and one value for the probability that the clade belongs to the outgroup. Colors correspond to the clades recovered in the STACEY analysis. Pink represents L. packardiae, yellow ‘Mann Creek’, brown ‘Hell’s Canyon, green ‘ East-Central Oregon’, blue ‘Camas Prairie’, black L. triternatum var. triternatum, gray-blue ‘Western Montana, and red L. andrusianum. .96

Figure 2.7. Principal components analysis of soil data. Principal components analysis of averaged, centered, and scaled soil physical and chemical characteristics. The broader STACEY clades are represented by shapes (Circle for ‘Andrusianum’; triangle for ‘Northern’; and square for ‘Southern’). The finer STACEY clades are color coded(Pink represents L. packardiae, yellow ‘Mann Creek’, brown ‘Hell’s Canyon, green ‘ East-Central Oregon’, blue ‘Camas Prairie’, black L. triternatum var. triternatum, gray-blue ‘Western Montana, and red L. andrusianum). The red arrow indicates Ottenlips 69in an anomalous position with its placement primarily driven by nitrate and nitrogen content.....97

Figure 2.8. Principal components analysis on 19 centered and scaled bioclimatic variables extracted at 30 arcsecond resolution. The broader STACEY clades are represented by shapes (Circle for ‘Andrusianum’; triangle for ‘Northern’; and square for ‘Southern’). The finer STACEY clades are color coded(Pink represents L. packardiae, yellow ‘Mann Creek’, brown ‘Hell’s Canyon, green ‘ East-Central Oregon’, blue ‘Camas Prairie’, black L. triternatum var. triternatum, gray-blue ‘Western Montana, and red L. andrusianum).....98

Figure 2.9. Scatterplot depicting the average leaflet lengths and widths organized by the clades uncovered in the STACEY analysis. The broader STACEY clades are represented by shapes (Circle for ‘Andrusianum’; triangle for ‘Northern’; and square for ‘Southern’). The finer STACEY clades are color coded(Pink represents L. packardiae, yellow ‘Mann Creek’, brown ‘Hell’s Canyon, green ‘ East-Central Oregon’, blue ‘Camas Prairie’, black L. triternatum var. triternatum, gray-blue ‘Western Montana, and red L. andrusianum).....99

Figure 2.10. Principal components analysis of eight centered and scaled means of reproductive characters (ray length; mature fruit length; mature fruit width; mature pedicel length; length of primary umbel; width of primary

umbel; wing width; fruit length). The broader STACEY clades are represented by shapes (Circle for ‘Andrusianum’; triangle for ‘Northern’; and square for ‘Southern’). The finer STACEY clades are color coded(Pink represents L. packardiae, yellow ‘Mann Creek’, brown ‘Hell’s Canyon, green ‘ East-Central Oregon’, blue ‘Camas Prairie’, black L. triternatum var. triternatum, gray-blue ‘Western Montana, and red L. andrusianum).....100

Figure 2.11 Representative digitized herbarium specimens of the clades uncovered in the STACEY analysis. The coarse clades are labeled with the ‘Northern’ clade on the top row and the ‘Southern’ clade on the bottom row. L. andrusianum is set off to the far right. A represents ‘Camas Prairie’ (Ottenlips 62); B represents Lomatium triternatum var. triternatum (Ottenlips 77); C represents Ottenlips 59; D represents ‘Western Montana’ (Lesica 10541); E represents L. packardiae (Ottenlips 22); F represents ‘Mann Creek’ (Ottenlips 45); G represents ‘Hell’s Canyon (Ottenlips 57); H represents ‘East-Central Oregon’ (Ottenlips 40); I represents L. andrusianum (Mansfield 16031). .....101

# CHAPTER ONE: CONVERGENT EVOLUTION AMONG THREE RARE ALPINE ENDEMIC LOMATIUM

## Abstract

Convergent evolution is the independent origin of similar phenotypes in response to shared environmental pressures, limitations in organismal design, or a combination of both factors. Convergence is especially common in alpine plants due to the limited number of adaptations available in a plants' body design that are able to survive the extreme selective pressures there. Alpine environments harbor a unique biodiversity of relictual genotypes and lineages. Due to the highly specialized adaptations of alpine plants and the vulnerability of their environment to warming, these species are especially prone to extinction due to climate change. Understanding evolutionary relationships is a key first step towards conservation of alpine plants to help preserve their unique adaptations, genotypes, and lineages. *Lomatium* (Apiaceae) is a large genus in the Western North America and as traditionally defined is paraphyletic, riddled with numerous cases of convergence occasionally in characters previously thought to be diagnostic. Three *Lomatium* species (*Lomatium greenmanii*, *Lomatium erythrocarpum*, and *Lomatium oreganum*) are endemic to two isolated mountain ranges in eastern Oregon, the Wallowa and Elkhorn Mountains. Previous studies have suggested that *Lomatium oreganum* and *Lomatium greenmanii* are sister taxa with shared ancestry resulting in their morphological and environmental niche similarities. Using molecular (five plastid loci and two nuclear ribosomal) and environmental (BIOCLIM variables)

data sources, this study aims to investigate evolutionarily relationships between these alpine-adapted species to determine if their similarities are the result of convergent evolution or shared ancestry. These three alpine *Lomatium* species endemic to alpine habitats of northeastern Oregon are included in a phylogeny which includes ~200 samples representing ~70 taxa in the larger clade (PENA) in which *Lomatium* are members. Each alpine endemic occupies a different phylogenetic position and shares a similar environmental niche indicating that convergent evolution, not shared ancestry is responsible for the shared morphologies of these three species. Increased conservation measures are urged for these plants and their habitat because each species represents a unique alpine adapted lineage indicating that the phylogenetic diversity of the Wallowa and Elkhorn Mountains is higher than originally hypothesized.

## Introduction

Morphological similarity is often the first stage in identifying closely related organisms (Nixon and Wheeler, 1990). Most phenotypes shared among taxa are the result of common ancestry. Two species which resulted from allopatric speciation from different ancestors can share a similar environmental niche and associated phenotype even though divergent selection did not occur (Wiens and Graham, 2005). Allopatric speciation is thought to be the main mode of speciation in animals, but may be less common in plants, than in animals (Lande, 1980; Anacker and Strauss, 2014) and occurs when a geographic or geologic barrier prevents certain individuals in a population from reproducing. Geographic separation and allopatric speciation are often associated with adaptive radiation; logperch darters speciated rapidly following the Gulf Coast pattern of endemism observed in many clades of freshwater fishes. Rising sea levels flooded rivers,

isolating populations, and cutting off gene flow to previously connected watersheds (Near and Bernard, 2004). In plants, allopatric speciation has been shown to have occurred in many groups including high-elevation endemics in the Iberian Peninsula and Morocco due to interglacial fragmentation during the Quaternary (Martin-Bravo et al., 2010). Sub-speciation has been documented in *Campunula thyrsoides* from the European Alps following a similar glacial pattern as in the Iberian Peninsula (Kuss et al., 2011). In each of these cases, geographic isolation resulted in taxa that are morphologically akin with similar ecological niches. Allopatric speciation can be a major driver of plant diversity resulting in taxa that share both morphology and ecological niche space.

Convergent evolution can also lead to shared morphology associated with similar ecological niches. The independent origin of similar adaptions in distinct lineages can lead to confusion among taxonomists regarding evolutionary relationships and even species boundaries (Wake, 2003). When convergence occurs in closely related species (i.e. congeners) delimiting taxa and understanding evolutionary relationships can be challenging. Convergence of key innovations to solve common problems such as similar sensory systems in vertebrates and cephalopods are especially well documented (Budelmann, 1995; Montgomery and McFall-Ngai, 1992). Convergent evolution at shallower taxonomic scales is less well-documented. In some cases, convergence occurs in the entire body plan in response to similar selective pressures in the environment. A famous example is the independent origin of succulent life forms in both Cactaceae and Euphorbiaceae in response to the desert biomes of the North American and North African deserts, respectively (Alvarado-Cárdenas et al., 2013).

Alpine environments harbor a biodiversity characterized by a high degree of endemism and a unique flora (Marx et al., 2017; Wang et al., 2009; Billings, 1974). While they are not as species rich as biodiverse tropical environments, alpine habitats are an important reservoir of relictual diversity, where once common, but now rare species or genotypes have found refuge after severe range contractions. Additionally, these environments and their biota are especially sensitive to climate change (Klanderud and Totland, 2005). Mountains can be viewed as island-like due to their isolation from other similar environments and the geological processes implicit in their formation (Hughes and Atchison, 2015). The isolation and common history of mountainous regions serves as a natural laboratory for testing hypotheses about plant community assembly, speciation, and convergence (Anthelme and Lavergne, 2017). Recent studies highlighting this capability include how increasing winter soil temperatures can predict plant community assembly under models of global climate change (Choler, 2018), how endemic plant species diversified in the European Alps (Smyčka et. al 2018), and the convergent development of cushion-plants in the western Peruvian Andes (Schittek et al., 2018).

Phenotypic convergence is especially pronounced in alpine environments due to the limited number of successful adaptions. The alpine environment is characterized by harsh conditions for plant life including: a limited growing season, extreme cold and wind, a high degree of solar radiation, and the potential for mid-season frost. The successful adaptations that have evolved include reduced stature and accelerated ability to flower and set seed (Bliss, 1962) that are found in nearly all alpine plants despite coming from a wide array of plant families (Flora of North America Editorial Committee, eds. 2002). These few adaptations increase the likelihood of convergent evolution. The

evolution of the cushion life form multiple times in *Androsace*, a genus in Primulaceae distributed across the cordillera of Western North America and the Russian Far East (Wang et al., 2009), demonstrates that convergence not only occurs in deep evolutionary time across disparate taxa, but sometimes in short intervals among closely related species. In these cases, the choice of morphological character used to delimit taxa and understand evolution can be unclear due to convergence. The addition of molecular data can help clarify species relationships and boundaries.

Molecular data have been shown to be effective in increasing our understanding of evolution and have frequently resulted in surprising conclusions, such as the higher taxonomic rearrangements promoted by the Angiosperm Phylogeny Group (APG IV, 2016). At finer resolutions, molecular data has helped disentangle a diverse array of evolutionary hypotheses ranging from older techniques such as allozymes and AFLPs to detect cryptic diversity in grape ferns (*Botryhcium*; Williams et al., 2016) to investigating genetic change in endangered species of desert pupfish with next generation sequencing data (Black et al., 2017). Sanger-sequencing of nuclear and chloroplast genes is a common tool used in phylogenetics and has resolved questions as diverse as those about the phylogenetic community assembly of alpine plants in the Alps (Marx et al., 2017) and species boundaries in Apiaceae (Smith et al., 2018).

*Lomatium* is a polyphyletic genus in the larger Perennial Endemic North America clade of Apiaceae (PENA) (George et al., 2014; Sun and Downie, 2010) containing ~200 currently recognized species. Plants in PENA are herbaceous perennials found in a variety of habitats ranging from mesic woodlands to the dry, open sagebrush zone (Hitchcock and Cronquist, 1973; Cronquist et al., 1997). Within *Lomatium* and PENA

there are many examples where morphologies are not reflective of evolutionary history (Feist et al., 2017). Characters traditionally used to delimit taxa such as fruit wings, root morphology, and number of terminal leaflet divisions have been shown to exhibit a high degree of homoplasy (George et al., 2014). Many common "good taxa" have been shown to exhibit cryptic diversity, such as the *Lomatium triternatum* species complex (Smith et al., 2018). Therefore, investigating existing classifications within *Lomatium* using molecular data is a fruitful pursuit to disentangle whether phenotypic similarities are the result of convergence or inheritance.

Three rare high elevation-endemic *Lomatium* species are found in the Wallowa and Elkhorn mountains of the Blue Mountain ecoregion in northeastern Oregon: *Lomatium erythrocarpum* Meinke & Constance, *Lomatium greenmanii* Math., and *Lomatium oreganum* Coult. & Rose (Fig. 1.1; Hitchcock and Cronquist, 2018). The Elkhorns and Wallowa mountains share a similar recent geological history with both ranges once covered by the Wallowa ice cap until its retreat began about 17 kybp (years before present) (Licciardi et al., 2004). Each alpine endemic species exhibits a highly-reduced growth form characteristic of many alpine plants (Figure 1.2; Hitchcock and Cronquist, 2018; Bliss, 1962) including a limited number of leaves, low-growth form, and a short time from flower to seed set. *Lomatium erythrocarpum* is listed as endangered by the state of Oregon (ODA, 2018) and is found only within a three-square mile zone of the subalpine in the Elkhorn Mountains. *Lomatium greenmanii* is listed as threatened by the state of Oregon (ODA, 2018) and is restricted to the alpine of the Wallowa Mountains and is only known from three localities: Redmont Peak, Mount Howard, and Ruby Peak (USDA and USFWS, 2007). *Lomatium oreganum* is found in the alpine zone of both the

Wallowa and Elkhorn mountains. While it is not listed at either the state or federal level, only six populations are known. Early studies based on morphological data suggested that *L. greenmanii* might be a glabrous form of *L. oreganum*, or potentially sister species (Meinke and Constance, 1982). An unpublished molecular study (Schulz and Matthews, 2007) based on limited data (sequences from ITS only) and taxon sampling (15 species) corroborated the suggestion of Meinke and Constance (1982) that *L. oreganum* and *L. greenmanii* are sister taxa.

This study proposes to investigate two contrasting hypotheses (see below) of the evolution of alpine flora in North America using *Lomatium* as a case-study. This will be done by conducting and comparing phylogenetic analyses and climatic niche inferences. Hypotheses for the evolutionary origin of these three alpine species are either convergent evolution or adaptive radiation within the alpine environment. If the three alpine *Lomatium* species are scattered across the phylogeny, convergent evolution is the primary force influencing the morphological and ecological affinities of these species. If they share a common ancestor, an adaptive radiation within the alpine environment is likely responsible for the observed similarities in morphology and ecological preferences. Due to ongoing taxonomic revisions and high degrees of homoplasy within the PENA clade uncovered with molecular sequence data, this study also proposes to confirm species boundaries by testing the independent monophyly of each of the three alpine-endemic *Lomatium* species in the Wallowa and Elkhorn Mountains of Eastern Oregon. Understanding the relationships and taxonomy of these species is especially important given their rarity and state listed status. Based on preliminary molecular and morphological data, one hypothesis suggests that *L. oreganum* and *L. greenmanii* are

similar due to inheritance (Meinke and Constance, 1982; Schulz and Matthews, 2007). *Lomatium erythrocarpum* has never been proposed as a close relative of either *L. oreganum* or *L. greenmanii* but given its affinities and distribution it could potentially be formed from allopatric speciation of an alpine adapted common ancestor. Another hypothesis, based on recent molecular studies indicating a high degree of homoplasy within PENA (George et al., 2014; Smith et al., 2018), suggests convergence is responsible for the morphological and ecological affinities in these three species. Our study incorporates new samples of alpine *Lomatium* into a phylogeny of the PENA clade to understand whether the species endemic to the high elevations of the Wallowa and Elkhorn Mountains share an alpine adapted common ancestor or are the result of convergent evolution.

## Materials and Methods

### Sampling, Extractions, PCR, and Sanger Sequencing

The PENA clade was widely sampled to determine the phylogenetic position of the Blue Mountain endemic *Lomatium* species. Five individuals of *L. greenmanii*, two individuals of *L. erythrocarpum*, and five individuals of *L. oreganum* were included in the analysis. All new leaf material was obtained from herbarium specimens. All previously published and many unpublished sequences were used in this analysis culminating in the broadest sampling yet of the PENA clade. Total sampling efforts included 209 individuals spread across approximately 79 taxa including outgroups (Appendix A).

DNA from the leaf tissue removed from herbarium samples were extracted with the Qiagen DNeasy plant mini kit (Qiagen, Valencia, California) following the protocol

recommended by the manufacturer and minor modifications according to Smith et al. (2018). Two nuclear ribosomal genes (ETS and ITS) and five chloroplast regions (*rps16* intron, *trnD-trnT*, *ndhA* intron, $trnL_{UAG}$ and *psbA-trnH*) were amplified using primers previously published in George et al. (2014) and Smith et al. (2018).

Successful amplifications were determined via UV visualization of ethidium bromide stained DNA run on 1% agarose gels. Exo-Sapit (Affymetrix, Cleveland, Ohio) was used to purify successful amplifications. Successful purified amplifications were sent to GeneWiz (Plainfield, New Jersey) for Sanger-sequencing. Assembly and editing of the raw data from chromatograms were performed in PhyDE (Müller et al. 2010).

Phylogenetic Reconstruction

Each gene region was manually aligned individually in PhyDE (Müller et al. 2010) and then concatenated them into one supermatrix for downstream phylogenetic analysis. The python package AMAS (Borowiec, 2016) was used to calculate basic alignment statistics: number of variable sites, and number of parsimony informative sites. Maximum parsimony(MP) was performed using PAUP* (Swofford, 2001) with 1000 bootstrapping replicates using the TBR method and a ratchet input derived from PAUPRat (Müller et al., 2010). Maximum likelihood (ML) was performed using RAxML (Stamatakis, 2006); bootstrapping was stopped automatically using the default autoMRE. The AIC calculations from jModelTest 2 (Darriba et al., 2012) determined the best fit model of molecular evolution and base pair substitution rate priors for subsequent Bayesian analysis.

Two independent runs of MrBayes (Ronquist and Huelsenbeck, 2003) each consisting of 4 chains, a burn-in of 5000 trees, and 10,000,000 total generations using the

TVM + I + G model and other priors suggested by following the results of jModelTest2 were used to conduct the Bayesian inference (BI) analysis. To determine if estimated priors had been adequately sampled, we evaluated ESS values (>=200) using Tracer v1.7.1 (Rambaut et al. 2014). MrBayes, RAxML, and jModelTest2 were all performed on the CIPRES Science Gateway (Miller et al., 2011).

Trees generated from each MrBayes analysis were imported into MEGA7 (Kumar et al. 2016) to generate majority rule (50% cutoff) consensus trees. All trees were rooted with the outgroup: *Angelica lineariloba*. The Bayesian tree was used as the base topology and support values from the other analyses were imported using TreeGraph2 (Stóver and Müller, 2010).

Alternative topology tests were used to confirm that the alpine species were not reciprocally included within each other. Each species pair was constrained to be monophyletic by manually editing the partitioned Bayesian newick tree using a text editor. PAUP* (Swofford, 2001) was used to determine site-log likelihoods for each constraint tree. Approximately unbiased (AU) tests were performed in Consel (Shimodaira and Hasegawa, 2001) using the site-log likelihoods exported for each of the constraint trees by PAUP*.

Climatic Analysis

Geographic information was obtained by downloading herbarium records from the Consortium of Pacific Northwest Herbaria database (http://www.pnwherbaria.org/index.php). Only one specimen/coordinate set from each known population was retained by comparing localities with known occurrences of *L. greenmanii* and *L. erythrocarpum* provided by the United States Fish and Wildlife

Service and United Stats Forest Service (USDA and USFWS, 2007), *Lomatium oreganum* is not monitored by any federal or state agency which makes determining the exact number of populations difficult. Collections with no GPS coordinates were georeferenced using Township, Range, Section, and other geographic markers such as mountain peaks on Google Earth Pro (https://www.google.com/earth/). Manual analysis of locations of herbarium records suggests six populations. All localities included in the climatic analysis are represented by herbarium vouchers (Table 1). BIOCLIM variables at 30 arc-second resolutions were downloaded from the UC-Davis biogeography repository (https://biogeo.ucdavis.edu/projects.html). BIOCLIM variables were extracted for each set of coordinates with the package *raster* (Hijmans et al., 2017) and checked for correlation using Pearson's correlation co-efficient in the package *Hmisc* (Harrell and Dupont, 2008). Five correlated variables were removed ($p < 0.05$). A principal component analysis (PCA) was performed in base R on the remaining BIOCLIM variables and visualized using *ggplot2* (Wickham, 2011) and ggfortify (Horikoshi and Tang, 2016). All climatic analyses were performed in R version 3.5.1 – "Feather Spray" (R Core Team, 2018). R code for the climatic analysis is available at https://github.com/ottenlipsmv/alpine_lom.

Geography, Morphology, and Ecology

Herbarium specimens (Table 2) were reviewed to investigate overlapping geographic, morphological, and ecological characters. All specimens were viewed via databased images available on the Consortium of Pacific Northwest Herbaria website (http://www.pnwherbaria.org/index.php). Species descriptions (Meinke and Constance, 1982), the regional flora (Hitchcock and Cronquist, 2018), and USFWS internal

documents (USDA and USFWS, 2007) were also reviewed to make observations regarding the shared geographic range, morphology, and ecology of this group.

## Results

### Sampling, Extractions, PCR, and Sanger Sequencing

We successfully extracted DNA for all samples and only included individuals with at least five of the seven gene regions amplified. All Sanger sequence runs were successful for the newly extracted alpine *Lomatium*. Detailed information about the success of other amplifications and subsequent alignments can be found in the Appendix A. The final alignment after concatenating all DNA regions was 7941 base pairs with 1854 variables sites (23%) and 928 parsimony informative sites (12%).

### Phylogenetic Reconstruction

The consensus trees generated from the three phylogenetic reconstruction techniques (MP, ML, BI) were largely congruent with one another differing only in the placement of a few individuals, none of which are the three alpine endemics of interest. The BI analysis resolved clades with the highest nodal support and has the most realistic model of molecular evolution therefore it is presented as the base tree in Fig. 1.3. Maximum parsimony and maximum likelihood bootstrap values are plotted alongside the posterior probabilities for shared nodes. Maximum parsimony analysis resulted in 196 most parsimonious trees (length = 4339 steps, consistency index (CI) excluding uninformative positions = 0.4187, retention index (RI) = 0.7754, rescaled consistency index (RC) = 0.4187). The log-likelihood (lnL) for each of the MrBayes runs had the following ESS values: 1,440 and 1,208. The two independent runs of MrBayes resulted in trees with an identical topology. Trees from all three analyses were congruent in their

placement of the three alpine endemics and strongly supported them as monophyletic species. The AU tests reject ($p < 0.005$) the possibility of *L. greenmanii* being sister to *L. erythrocarpum*, *L. oreganum* being sister in *L. greenmanii*, and *L. erythrocarpum* being sister in *L oreganum* (Table 3).

Climatic Analysis

Table 4 shows the values for each BIOCLIM variable according to collection. A PCA of non-correlated BIOCLIM variables reveals similar niche space between all three-alpine endemic *Lomatium* species with *L. greenmanii* and *L. erythrocarpum* contained with *L. oreganum* (Fig. 1.4). PC1 explains 89.92% of the variance in the data and PC2 explains an additional 5.74% of variance. The major drivers of placement in the PCA determined by plotting the eigen values are temperature and rainfall variables.

Geography, Morphology, and Ecology

A review of imaged herbarium specimens and scientific literature reveals a suite of overlapping geographic, morphological (Table 5), and ecological characters. Most apparent is the restriction of the three species to a limited geographic area contained entirely within the Wallowa and Elkhorn ranges of the Blue Mountain Ecoregion in Eastern Oregon (Fig. 1.1). All species have a low growing habit, with thickened dissected leaflets, and similar shaped umbellets (Fig. 1.2; Table 1.5). *Lomatium oreganum* and *L. greenmanii* are found at slightly higher elevations than *L. erythrocarpum*, but all three species are restricted to the alpine or sub-alpine zone.

## Discussion

Our results indicate that the three alpine-adapted *Lomatium* species endemic to the Blue Mountains of eastern Oregon are distantly related unique taxonomic entities.

This result supports the hypothesis that convergence played a key role in the evolution of these species. None of the tree building methods we utilized (MP, ML, or BI) support the idea that any combination of *L. oreganum*, *L. greenmanii*, and *L. erythrocarpum* evolved from a common alpine-adapted ancestor. Approximately-unbiased (AU) tests further reject the hypothesis of a single independent origin of alpine-adaptions in the *Lomatium* species of the Wallowa and Elkhorn Mountains. Further, the climatic niche analysis confirms the hypothesis that these three species share similar ecological niche space.

Two previous studies (Meinke and Constance, 1982; Schulz and Matthews, 2007) suggested that *L. oreganum* and *L. greenmanii* may potentially be sister species. Meinke and Constance (1982) utilized a traditional taxonomic study with evidence largely derived from shared morphological characters, such as "caespitose development from a fibrous multicipital caudex surmounting a deep taproot, oblong to lanceolate pinnately dissected leaves, reduction of the inflorescence to a solitary terminal umbel with only 1-3 fertile umbellets, each bearing 1-6(-8) short-pedicellate fruits, yellow flowers, and dorsally flattened fruits" (Meinke and Constance, 1982; p. 14). However, the authors contend that the observed similarities between these two taxa and other alpine Apiaceae "Perhaps … means only that most alpine Umbelliferae tend to resemble one another" (Meinke and Constance, 1982; p. 17). The *Lomatium greenmanii* candidate conservation agreement prepared for the United States Fish and Wildlife Service (USDA and USFWS, 2007) to determine if it was appropriate to place this taxon on the endangered species list was more confident in the assertation that the two *Lomatium* species were sister. As part of the assessment, they performed a phylogenetic analysis of a regional sampling of *Lomatium* species with the goal of including any potential sister taxa of *L. greenmanii*. In

their study, maximum parsimony analysis using the DNA sequences from the ITS region corroborates the suggestion that *L. oreganum* and *L. greenmanii* are sister. However, this study relied on limited taxon sampling (14 species), limited data (based on one gene region, albeit a common pratice for the time) inadequate phylogenetic reconstruction techniques (maximum parsimony with no evidence of support), the samples included in the study are of unknown origin (no voucher information), and finally, to our knowledge, the data were not deposited in an accessible database such as GenBank. Our study encompassed a much wider sampling scheme (209 individuals spread across approximately 70 taxa), more sophisticated phylogenetic reconstruction techniques (ML and BI), and six additional molecular markers. Further, attempts to recreate their results by limiting our taxon sampling, data, and methodologies to only those that they used did not return the same results (unpublished results). Therefore, we feel strongly that we cannot rely on this study and conclude that *L. greenmanni* and *L. oreganum* share no phylogenetic affinity and that alpine Apiaceae are frequently morphologically similar despite uncommon ancestry as Meinke and Constance (1982) speculated.

Data from the original species descriptions, Meinke and Constance (1982), and herbarium material show many morphological and ecological similarities between the taxa including a low growing stature, short period from flowering to seed set, thickened rootstock, and a preference for a similar substrate (Fig. 1.1; Table 1.5; Hitchcock and Cronquist, 2018; Meinke and Constance, 1982). Many of these morphological convergences are common adaptations found among alpine plants from a variety of lineages (Billings, 1974).

Climatic analysis using BIOCLIM variables indicate that *L. greenmanii, L. oreganum*, and *L. erythrocarpum* share a similar environmental niche (Fig. 1.4). We did not further model or project the climatic niche of these species because all known populations were included in the analysis. The commonly employed D and I statistics (Warren et al., 2008) lack statistical power at low sample sizes and are designed for use in distribution modeling scenarios. Schulz and Matthews (2007) created species distribution models (SDMs) for *L. greenmanii* in an attempt to locate new populations. Using their models as guides, they were able to locate one new population of *L. greenmanii*. The combination of these SDMs and associated field work, restricted habitat type, overall rarity, and ongoing monitoring of these species by the USFWS (USDA and USFWS, 2007; Schulz and Matthews, 2007) increases our confidence that there are no, or few populations that have not been included in this analysis, thus no further modeling or projection of potential distribution is warranted. The similar climatic niche and morphological overlap of these species, considering their phylogenetic position, further supports our claim that these three alpine endemics represent a case of convergent evolution.

In addition to our study highlighting the importance of convergence in the evolution of these three species, our results also provide insight into alpine plant phylogenetic community assembly, convergence in closely related lineages, the biogeography of the flora of the Wallowa and Elkhorn Mountains, rare plant conservation, and the molecular systematics of the PENA clade. Convergent evolution is thought to be especially common in alpine communities due to the limited number of feasible adaptations plants can evolve to survive in such a stressful environment (Billings

and Mooney, 1968). While convergence is oftentimes viewed as one of the leading lines of evidence for natural selection, others have proposed it is simply the result of structural limitations inherent in an organisms' body plan (Wake, 2003). Both hypotheses share degrees of validity, and biological reality is likely a combination of both aspects. The harsh environment of the alpine in combination with limited plant architecture leads to a flora frequently consisting of distantly related species that share similar adaptions (Chabot and Billings, 1972; Mansfield, 2000; Billings and Mooney,1968). In studying the alpine flora of the French alps, Marx et al. (2017) found that species neutral processes, such as colonization and extirpation, can also play a role in shaping alpine plant communities. The independent origins of alpine adaptions observed in this study suggests that extreme selective pressure and colonization are both factors in the formation of the plant communities in the Wallowa and Elkhorn Mountains.

While alpine habitats do not exhibit the sheer number of species and unique niches of traditionally biodiverse habitats, such as tropical rainforests, they display their own unique type of biodiversity featuring a high degree of endemism (Wang et al., 2009; Billings, 1974). The frequent endemism and isolation of mountain ranges leads to their comparison with island biogeography and their characterization as 'sky islands' (Marx et al., 2017). The Wallowa and Elkhorn mountains of eastern Oregon are relatively isolated from other major mountain ranges with only the Seven Devils of western Idaho sharing a similar geological history, both being a disjunct fragment of the insular belt that created the Cascades and Coast Ranges located over 300 kilometers to the west (Townsend and Figge, 2002). They do not share a similar geology with the closer batholith-derived mountains of central Idaho. The historic geographic isolation of this environment helps

guide the development of the hypothesis of how the alpine endemics evolved: Did they allopatrically speciate from an alpine-adapted common ancestor; or did they converge on this morphology from different ancestors? Further, we can infer the isolation between the Wallowa and Elkhorn mountains led to a potential lack of gene flow and subsequent genetic structuring of the northern Wallowa and southern Elkhorn populations which are weakly/moderately supported as reciprocally monophyletic in our phylogenetic analysis (Fig. 1.3). The alpine endemic *Lomatium* species of the Wallowa and Elkhorn mountains contribute to a unique endemic biodiversity characteristic of sky-island environments.

Convergent evolution can occur across both shallow and deep evolutionary time scales. Some of the most well-known and exciting examples of convergence, such as the independent origin of pitcher traps in *Nepenthes* and the Sarraceniaceae, occurred across great phylogenetic distance (Thorogood et al., 2018). Deep convergence plays a unique role in shaping alpine floras; most alpine taxa share a specialized suite of traits that makes them uniquely adapted to their environment (Billings, 1974). The increase in the ubiquity and affordability of molecular sequence data has allowed for a proliferation of studies highlighting convergence among more closely related taxa at shallower time scales (Huiet et al. 2018; Wang et al., 2009). Without molecular data it can be difficult to infer homology between characters in closely related lineages. Recently, molecular data has shown that leaf blade architecture in maiden-hair ferns (*Adiantum* species) is the result of convergence and not shared ancestry as previously assumed based on morphology alone (Huiet et al., 2018). In carnivorous pitcher plants, the evolutionary history is more nuanced than originally inferred; many small structural convergences such as minute trap design details have been uncovered with the help of molecular

resources (Thorogood et al., 2018). The addition of molecular data has allowed for the observation that similarities in leaf morphology, rootstock, and other morphological characters among the alpine *Lomatium* species have convergently evolved in relatively closely related lineages. This phenomenon has been observed in other alpine plant groups such as the multiple independent origins of the cushion lifeform in the genus *Androsace* (Wang et al., 2009). Our study lends support to the importance of shallow scale (within generea) convergence in the evolution of alpine plant community assembly.

The PENA clade is one of the largest plant radiations in western North America only surpassed by *Penstemon* and *Astragalus*. Species of PENA have successfully colonized a wide range of habitat types ranging from *Cymopterus ripleyi* found only in western desert environments to *Ziza aurea* common in wet meadows throughout the United States. While there are other taxa in Apiaceae and PENA found in the alpine: *Lomatium cusickii,* and various species of *Cymopterus*, they have not diversified as rapidly or substantiality in this environment as other genera such as the artic-alpine genus *Cassiope* (Ericaceae) (Hou et al., 2016) or *Androsace* (Primulaceae; Wang et al, 2009). The evolutionary history of *L. greenmanii*, *L. oreganum*, and *L. erythrocarpum* offers further evidence to the high degree of observed homoplasy of many characters in the PENA clade, including those previously thought to be taxonomically informative including root morphology, fruit wings, and leaflet width to length ratios (George et al., 2014; Smith et al., 2018). The convergence of leaf morphology and life-history strategies was expected given similar observations in this clade. This study is part of an ongoing effort to unmask homoplasy and investigate the evolutionary history of PENA.

Further, these results highlight the importance of rare plant conservation and research. Previous workers (Schulz and Matthews, 2007; Meinke and Constance, 1982) entertained the possibility that some of these taxa might represent a monophyletic group and therefore one independent alpine-adapted lineage. This work shows that each of the three-alpine *Lomatium* species endemic to the Wallowa and Elkhorn mountains represent their own unique evolutionary lineage. Further, *L. greenmanii* does not fall out with other *Lomatium* species, but rather in a different clade within PENA and in need of taxonomic revision. Therefore, the phylogenetic diversity of this area is higher than originally hypothesized by the treatment of these taxa in the most common reference for the region, the Flora of the Pacific Northwest (Hitchcock and Cronquist, 1973). While the agencies responsible for placing protections on plant species and conservation do not directly take phylogenetic diversity into account, they do prioritize conservation of threatened/endangered taxa if they are monotypic or in smaller genera. Additionally, one of the three known populations of *L. greenmanii* is located at the top of the Wallowa Lake tramline, a public gondola that brings tourists to the summit of Mount Howard in the summer months. This *L. greenmanii* population is sensitive to trampling and other anthropogenic disturbances caused by summer visitors (Schulz and Matthews, 2007). Sadly, due to this species superficial affinity with the more common *Lomatium cous* and *Lomatium cusickii* it has been misidentified in the field and many individuals have been collected from the Mount Howard population for herbarium inclusion under the wrong species name (http://www.pnwherbaria.org/).

In conclusion, this study widely samples from across the PENA clade including 209 individuals spread across approximately 70 taxa with higher resolution than any

previously published studies. In addition to the convergence among the three alpine species investigated here, there are many other cases of convergent evolution represented in this clade including similarities in leaflet morphology among *L. simplex* and the *L. triternatum* species complex (Smith et al., 2018). The three alpine taxa of focus are not the result of shared ancestry but have converged on similar morphologies and life-history strategies from different phylogenetic positions within the PENA clade. These rare taxa represent unique lines of evolution and thus warrant increased conservation measures especially in the face of anthropogenic disturbance and climate change. The three independent origins could only be uncovered with molecular data and a wide sampling scheme. In addition to improving the reconstruction of the evolutionary history of PENA, our results provide insight into alpine plant phylogenetic community assembly, convergence in closely related lineages, and the biogeographical history of the flora associated with the Wallowa and Elkhorn mountains.

**Table 1.1 Specimens used in the climatic analysis. Collections denoted with an * where georeferenced**

| Species | Collection | Collection Date | Location | Latitude | Longitude | Accession # |
|---|---|---|---|---|---|---|
| *Lomatium greenmanii* | *Michael Mancuso 3606* | 6/14/2010 | Redmont Peak; Wallowa Mountains | 45.2204 | -117.13 | ID 163719 |
| *Lomatium greenmanii* | *Jessie Johanson 02-118** | 7/20/2002 | Mount Howard; Wallowa Mountains | 45.2557 | -117.18 | OSC 229580 |
| *Lomatium greenmanii* | *Julie Kierstead 84-33** | ??/??/1984 | Ruby Peak; Wallowa Mountains | 45.3512 | -117.37 | OSC 166057 |
| *Lomatium oreganum* | *Rachel Sines sn** | 8/??/1983 | Hurwal Divide; Wallowa Mountains | 45.2711 | -117.26 | OSC 160894 |
| *Lomatium oreganum* | *Morton Eaton Peck 18536** | 7/??/1934 | Summit West of Ice Lake; Wallowa Mountains | 45.2286 | -117.3 | OSC 17765 |
| *Lomatium oreganum* | *Georgia Mason 6489** | 8/12/1963 | On summit of Eagle Cap. ; Wallowa Mountains | 45.1588 | -117.3 | OSC 124517 |
| *Lomatium oreganum* | *Peter Zika 10430A ** | 8/??/1987 | Imnaha River headwaters. ; Wallowa Mountains | 45.1336 | -117.25 | OSC 188525 |
| *Lomatium oreganum* | *Ann Kratz sn** | 8/10/1987 | Maxwell Pk, 400' E of | 44.8694 | -118.08 | ID 77376 |

| | | | | | | |
|---|---|---|---|---|---|---|
| | | | summit; Elkhorn Mountains | | | |
| *Lomatium oreganum* | *Roy Sines sn** | 8/10/1982 | West side of Hunt Mtn; Elkhorn Mountains | 44.8708 | -118.07 | OSC 159357 |
| *Lomatium erythrocarpum* | *Andy Kratz sn** | 8/21/1982 | Cougar Basin; Elkhorn Mountains | 44.8389 | -118.1 | WS 291027 |
| *Lomatium erythrocarpum* | *Robert Meinke 3114** | 8/2/1983 | In saddle between Pine Creek and Cougar Basin; Elkhorn Mountains | 44.8262 | -118.1 | WTU 303772 |
| *Lomatium erythrocarpum* | *Michael Murray sn** | 7/19/2001 | South of Rock Creek Butte; Elkhorn Mountains | 44.8117 | -118.11 | OSC 197364 |

**Table 1.2 Specimens reviewed for morphological comparisons**

| Species | Collection | Accession number |
|---|---|---|
| *Lomatium greenmanii* | *Michael Mancuso 3606* | ID 163719 |
| *Lomatium greenmanii* | *Jessie Johanson 02-118* | WTU 360976 |
| *Lomatium greenmanii* | *Michael R. Hays 1028* | ID 129405 |
| *Lomatium greenmanii* | *Robert J. Meinke 2433* | ID 84401 |
| *Lomatium greenmanii* | *Ruth Martin Hansen 4611* | HPSU 14885 |
| *Lomatium greenmanii* | *Dr. David French 3456* | HPSU 14884 |
| *Lomatium greenmanii* | *William C. Cusick 2458* | RM 31457 |
| *Lomatium oreganum* | *Rachel Sines s.n.* | ID 81385 |
| *Lomatium oreganum* | *Ann Kratz s.n.* | WTU 286971 |
| *Lomatium oreganum* | *C. L. Hitchcock 21423* | WTU 209449 |
| *Lomatium erythrocarpum* | *Jon Titus s.n.* | WTU 336905 |
| *Lomatium erythrocarpum* | *R. Meinke 3114* | WTU 303772 |

**Table 1.3 Results from the Approximately-Unbiased test performed in Consel. p-values < 0.05 were consider significant. The results reject the possibility of the alpine endemics being included within one another.**

| Topology | Rank | AU score |
|---|---|---|
| Maximum Parsimony Tree | 1 | 1 |
| (*Lomatium greenmanii, Lomatium erythrocarpum*) | 3 | 3.00E-05 |
| (*Lomatium oreganum, Lomatium greenmanii*) | 4 | 6.00E-07 |
| (*Lomatium erythrocarpum, Lomatium oreganum*) | 2 | 4.00E-06 |

**Table 1.4 Bioclimatic variables associated with confirmed populations of the three alpine endemics. Codes correspond to the variable in the key: bio1_12 = Annual Mean Temperature (°C); bio2_12= Mean Diurnal Range (°C); bio3_12 = Isothermality (°C); bio5_12 = Max Temperature of the Warmest Month (°C); bio6_12 = Min Temperature of the Coldest Month (°C); bio7_12 = Temperature Annual Range (°C); bio8_12 = Mean Temperature of the Wettest Quarter (°C); bio9_12 = Mean Temperature of the Driest Quarter (°C); bio11_12 = Mean Temperature of the Warmest Quarter (°C); bio12_12 = Mean Temperature of the Coldest Quarter (°C); bio13_12 = Annual Precipitation (mm); bio14_12 = Precipitation of the Wettest Month (mm); bio16_12 = Precipitation of the Driest Month (mm); bio19_12 = Precipitation of the Wettest Quarter (mm)**

| Species | Collection | bio1_12 | bio2_12 | bio3_12 | bio5_12 | bio6_12 | bio7_12 | bio8_12 | bio9_12 | bio10_12 | bio11_12 | bio12_12 | bio13_12 | bio14_12 | bio16_12 | bio19_12 |
|---|---|---|---|---|---|---|---|---|---|---|---|---|---|---|---|---|
| *Lomatium greenmanii* | *Michael Mancuso 3606* | -1.2 | 14 | 3.9 | 19 | -16.1 | 35.1 | -8.4 | 7.8 | 7.8 | -9.5 | 79.3 | 10.4 | 2.8 | 29.5 | 28.2 |
| *Lomatium greenmanii* | *Jessie Johanson 02-118* | -2.9 | 13.6 | 3.9 | 16.7 | -17.4 | 34.1 | -9.8 | 5.9 | 5.9 | -10.9 | 86.4 | 11.4 | 3.1 | 32.4 | 31 |
| *Lomatium greenmanii* | *Julie Kierstead 84-33* | -2.3 | 13.8 | 3.9 | 17.7 | -16.9 | 34.6 | -9.2 | 6.6 | 6.6 | -10.4 | 83.1 | 11 | 3 | 31.1 | 29.7 |
| *Lomatium oreganum* | *Rachel Sines sn* | -1.5 | 14.1 | 4 | 18.6 | -16.5 | 35.1 | -8.7 | 7.4 | 7.4 | -9.9 | 79.5 | 10.5 | 2.8 | 29.8 | 28.4 |
| *Lomatium oreganum* | *Morton Eaton Peck 18536* | 0.2 | 14.2 | 4 | 20.5 | -14.9 | 35.4 | -7.3 | 9.2 | 9.2 | -8.4 | 70.6 | 10 | 2.4 | 27.7 | 26 |
| *Lomatium oreganum* | *Georgia Mason 6489* | -0.3 | 14.1 | 4 | 19.8 | -15.2 | 35 | -7.7 | 8.6 | 8.6 | -8.7 | 73.2 | 10.3 | 2.5 | 28.7 | 27 |
| *Lomatium oreganum* | *Peter Zika 10430A* | -1.6 | 14.1 | 4 | 18.6 | -16.6 | 35.2 | -8.8 | 7.4 | 7.4 | -9.9 | 80.3 | 10.5 | 2.9 | 29.8 | 28.5 |

| | | | | | | | | | | | | | | | | |
|---|---|---|---|---|---|---|---|---|---|---|---|---|---|---|---|---|
| *Lomatium oreganum* | *Ann Kratz sn* | -1.3 | 14.1 | 4 | 18.9 | -16.2 | 35.1 | -8.5 | 7.7 | 7.7 | -9.6 | 79.6 | 10.4 | 2.8 | 29.5 | 28.2 |
| *Lomatium oreganum* | *Roy Sines sn* | -0.4 | 14 | 4 | 19.7 | -15.3 | 35 | -7.8 | 8.5 | 8.5 | -8.9 | 76.9 | 10.1 | 2.7 | 28.7 | 27.3 |
| *Lomatium erythrocarpum* | *Andy Kratz sn* | -0.6 | 14 | 4 | 19.5 | -15.5 | 35 | -7.9 | 8.3 | 8.4 | -8.9 | 74 | 10.4 | 2.5 | 28.9 | 27.2 |
| *Lomatium erythrocarpum* | *Robert Meinke 3114* | -1.2 | 13.9 | 4 | 18.7 | -16 | 34.7 | -8.4 | 7.6 | 7.6 | -9.5 | 76.8 | 10.8 | 2.6 | 30.1 | 28.3 |
| *Lomatium erythrocarpum* | *Michael Murray sn* | -0.6 | 14.1 | 4 | 19.5 | -15.6 | 35.1 | -8 | 8.3 | 8.3 | -9.1 | 73.9 | 10.3 | 2.5 | 28.8 | 27.1 |

**Table 1.5 Comparison of morphological similarities**

| Character | *Lomatium greenmanii* | *Lomatium oreganum* | *Lomatium erythrocarpum* | Citation |
|---|---|---|---|---|
| Leaflet margins entire | Yes | No | Yes | Hitchcock and Cronquist, 2018 |
| Yellow flowers | Yes | Yes | No | Meineke and Constance, 1982 |
| Caespitose development | Yes | Yes | Yes | Meineke and Constance, 1982; Hitchcock and Cronquist, 2018 |
| Dissected leaves | Yes | Yes | Yes | Hitchcock and Cronquist, 2018 |
| Deep taproot | Yes | Yes | Yes | Hitchcock and Cronquist, 2018 |
| Developed involucel | Yes | Yes | Yes | Hitchcock and Cronquist, 2018 |
| Reduced terminal inflorescence | Yes | Yes | No | Meineke and Constance, 1982 |
| Dorsally flattened fruits | Yes | Yes | No | Meineke and Constance, 1982 |

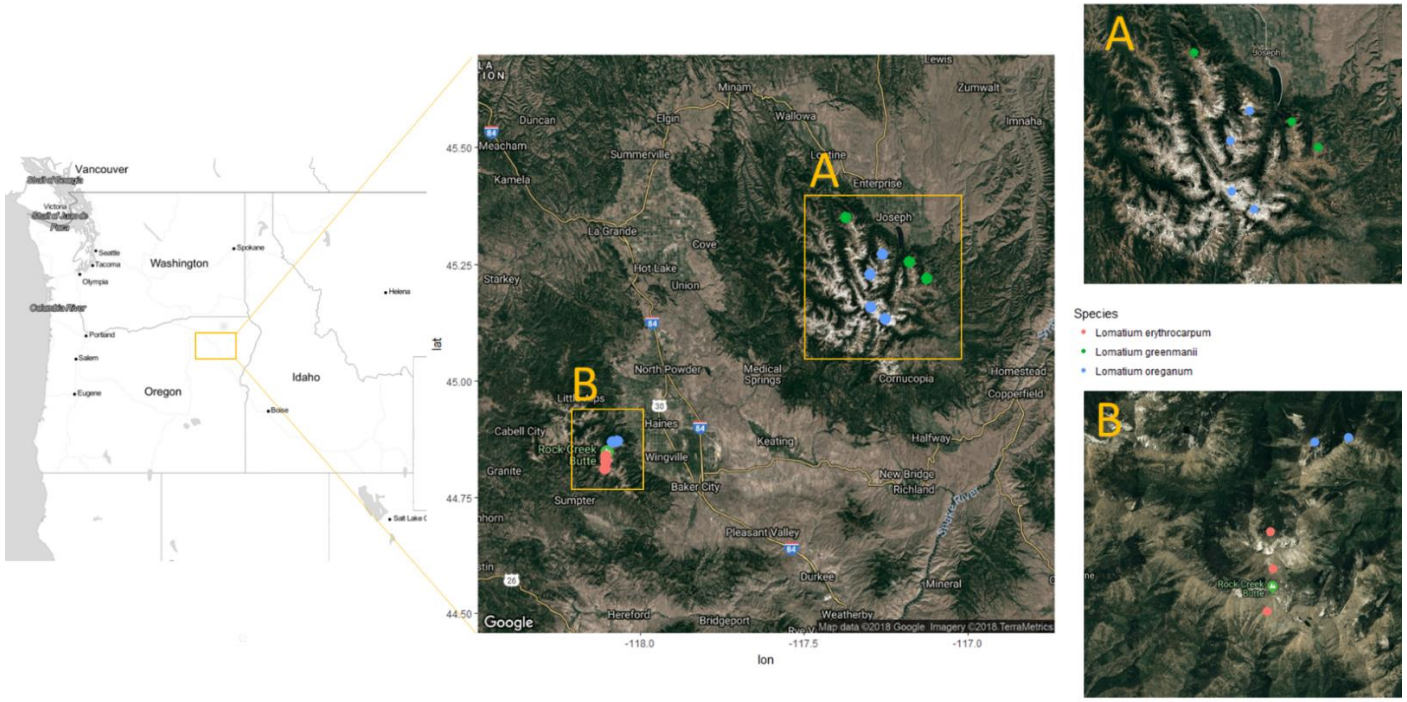


**Figure 1.1 Map of study area. Inset A depicts the Wallowa Mountains, and Inset B depicts the Elkhorn Mountains. Red dots represent L. erythrocarpum populations, green dots represent L. greenmanii populations, and blue dots represent L. oreganum populations.**

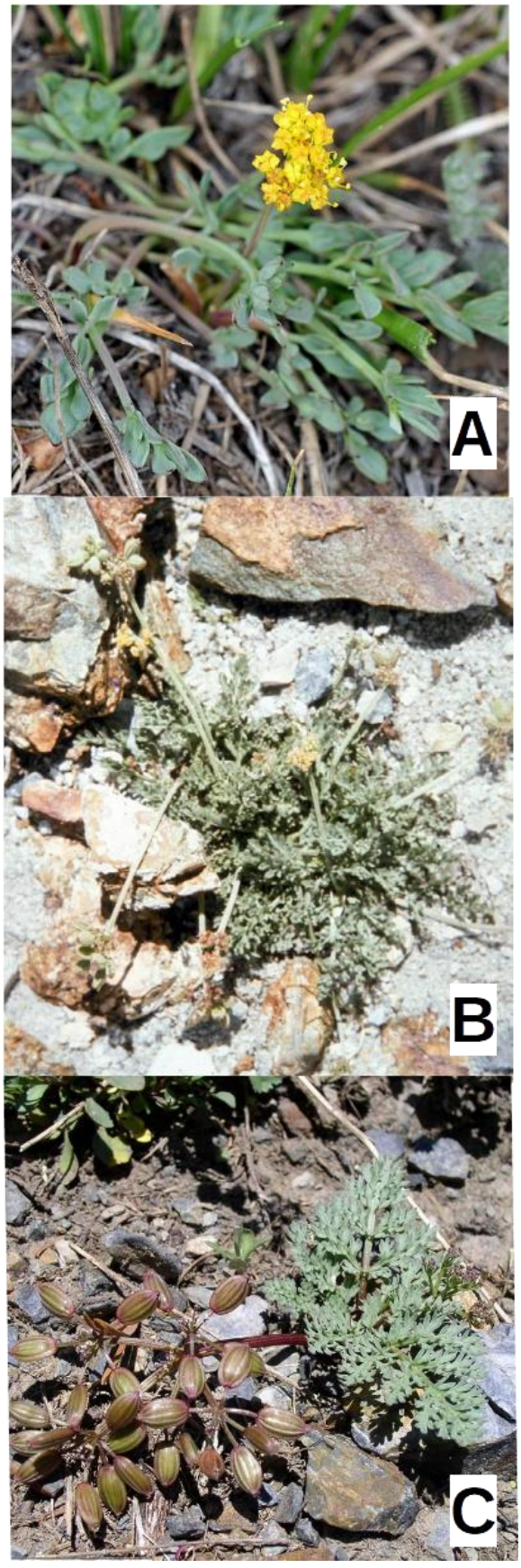
A
B
C

**Figure 1.2. Photographs representing L. greenmanii (A), L. oreganum (B), and L. erythrocarpum (C). Copyright < L. greenmanii (A: Gerald Carr), L. oreganum (B: Bonnie Olson), and L. erythrocarpum (C: Gene Yates)>; courtesy of OregonFlora.**

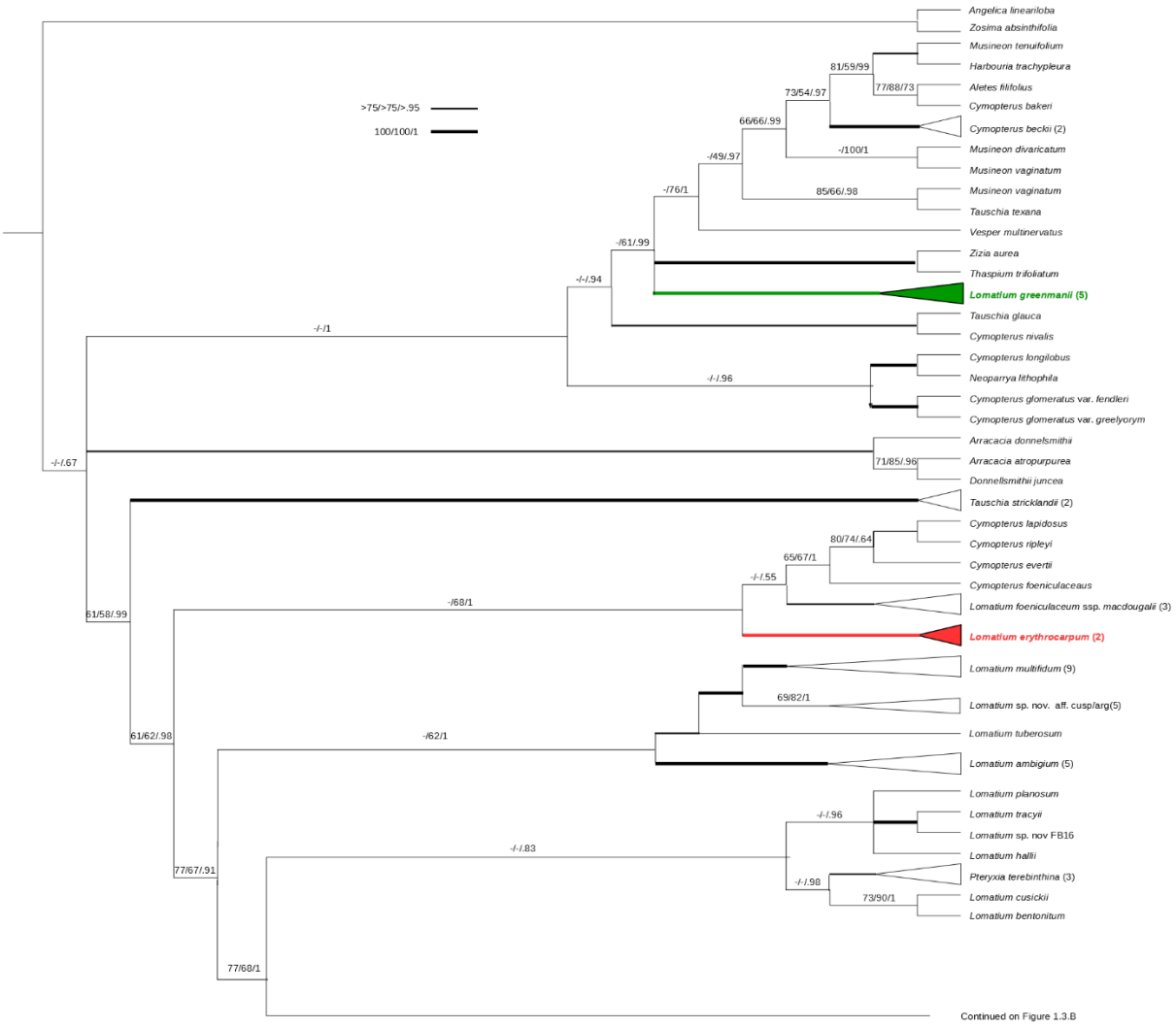


**Figure 1.3.A Phylogenetic tree depicting the relationship between the three alpine endemic species. Lomatium greenmanii branches are colored green, L. erythrocarpum red, and L. oreganum blue for emphasis. If more than one individual was sampled for a monophyletic species, the branches were collapsed and replaced with a triangle. The number in parentheses after the species name indicates the number of individuals sampled. Support values indicate are maximum parsimony bootstrap (MPBS), maximum likelihood bootstrap (MLBS), and Bayesian inferences posterior probabilities (BIPP) in following format MPBS/MLBS/BIPP. Values over**

**75/75/.95 are indicated with a 3 point thickened branch, and maximum support (100/100/1) is indicated by a 6-point thickened branch.**

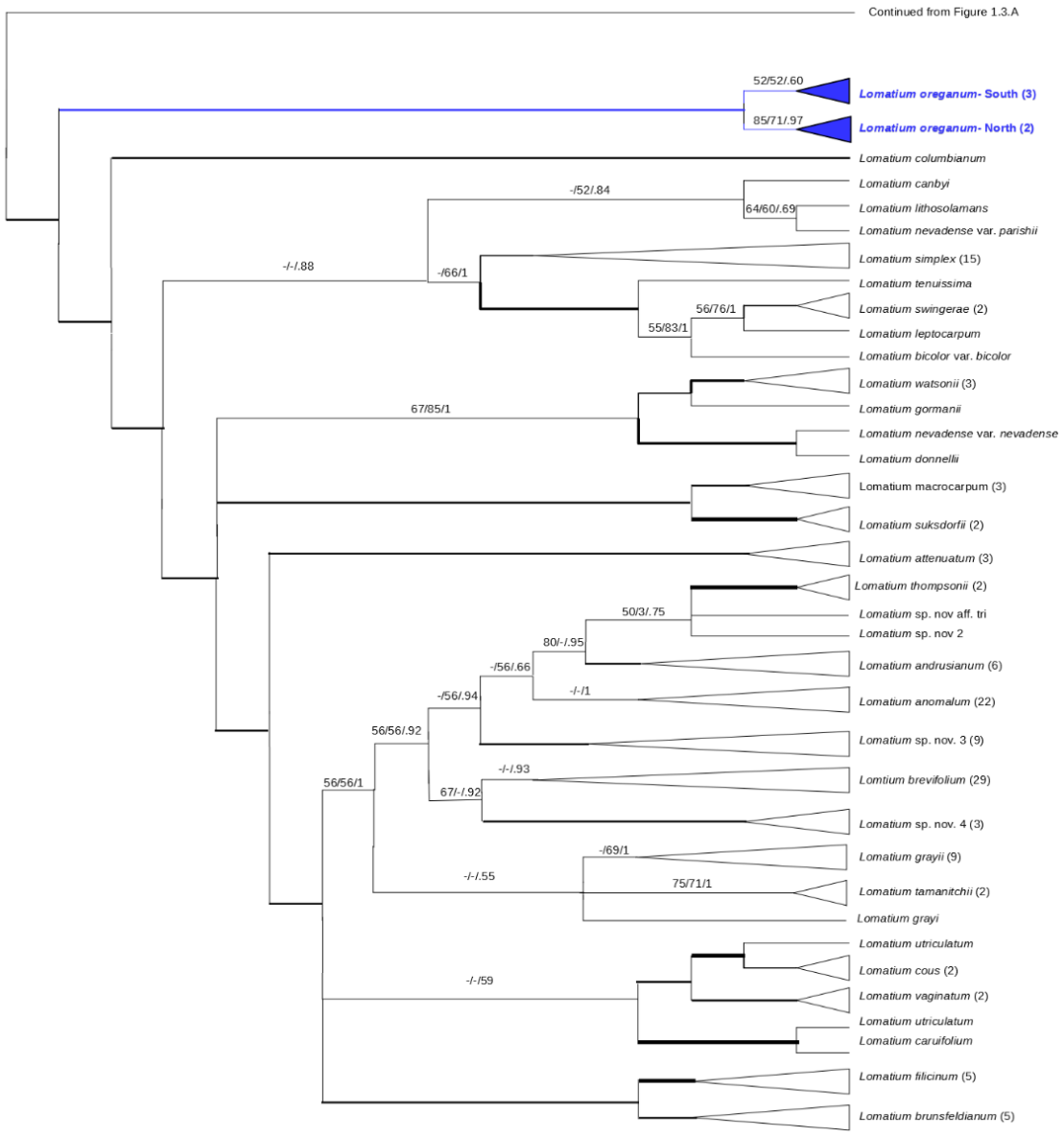


**Figure 1.3.B Phylogenetic tree depicting the relationship between the three alpine endemic species. L. greenmanii branches are colored green, L. erythrocarpum red, and L. oreganum blue for emphasis. If more than one individual was sampled for a monophyletic species, the branches were collapsed and replaced with a triangle. The number in parentheses after the species name indicates the number of individuals**

**sampled. Support values indicate are maximum parsimony bootstrap (MPBS), maximum likelihood bootstrap (MLBS), and Bayesian inferences posterior probabilities (BIPP) in following format MPBS/MLBS/BIPP. Values over 75/75/.95 are indicated with a 3 point thickened branch, and maximum support (100/100/1) is indicated by a 6-point thickened branch.**

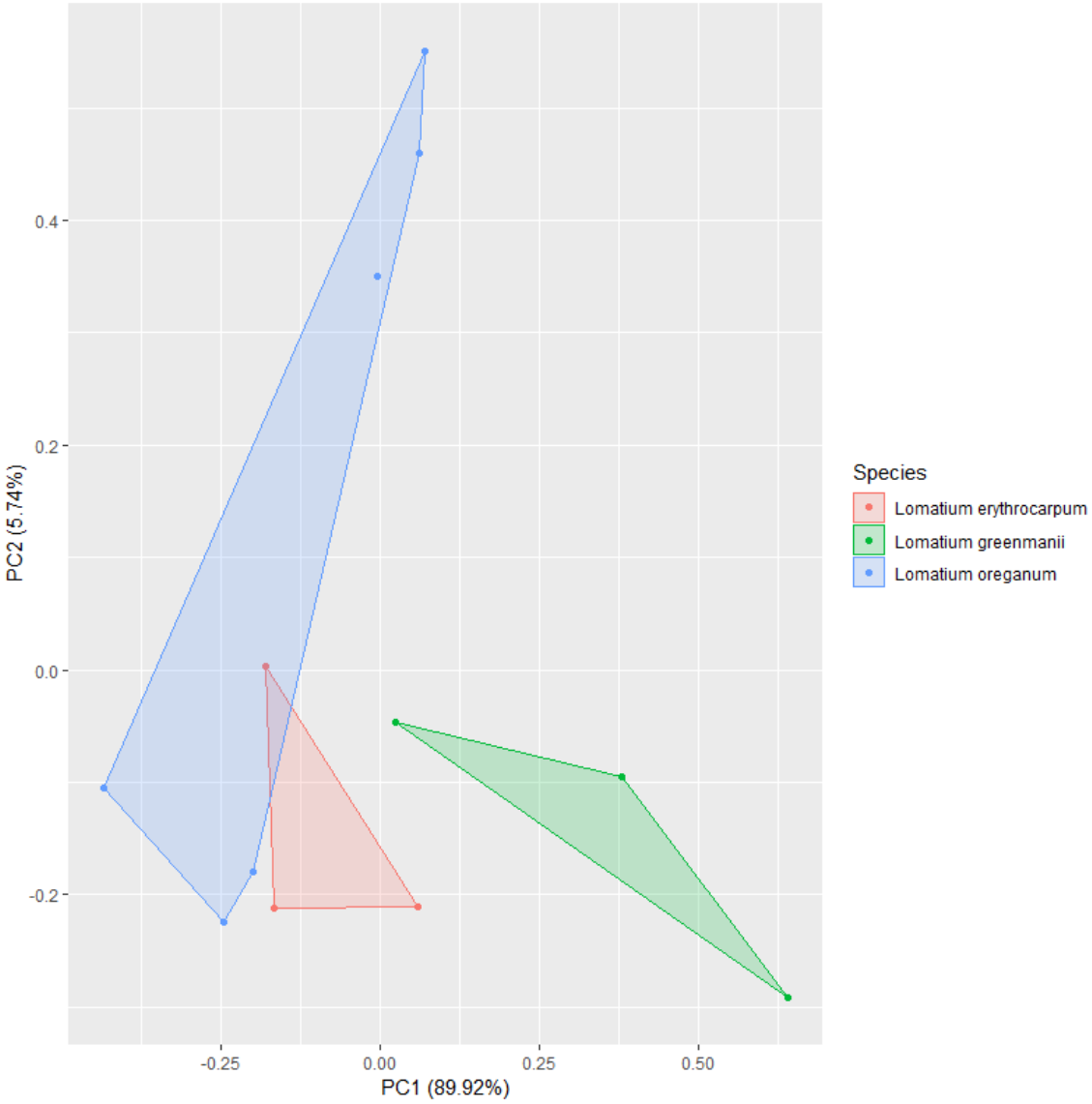


**Figure 1.4 PCA depicting the similar climatic niche space of the three Lomatium species. PCA was performed on noncorrelated centered and scale BIOCLIM variables extracted at the 30 arc-second resolution. All known populations of these rare plants within this resolution are included in the analysis. Red dots represented L. erythrocarpum; green L. greenmanii; blue L. oreganum. Convex frames are drawn to highlight the climatic similarities.**

## Works Cited

Alvarado-Cárdenas, L. O., Martínez-Meyer, E., Feria, T. P., Eguiarte, L. E., Hernández, H. M., Midgley, G., & Olson, M. E. (2013). To converge or not to converge in environmental space: testing for similar environments between analogous succulent plants of North America and Africa. *Annals of botany*, *111*(6), 1125-1138.

Anacker, B. L., & Strauss, S. Y. (2014). The geography and ecology of plant speciation: range overlap and niche divergence in sister species. *Proceedings of the Royal Society of London B: Biological Sciences*, *281*(1778), 20132980.

Anthelme, F., & Lavergne, S. (2017). Alpine and arctic plant communities: a worldwide perspective. *Perspectives in plant ecology, evolution and systematics* (1433-8319), 30, p. 1.

APG IV (2016). An update of the Angiosperm Phylogeny Group classification for the orders and families of flowering plants: APG IV. *Botanical Journal of the Linnean Society,* 181(1), 1-20.

Billings, W. D. (1974). Adaptations and origins of alpine plants. *Arctic and alpine research*, *6*(2), 129-142.

Billings, W. D., & Mooney, H. A. (1968). The ecology of arctic and alpine plants. *Biological reviews*, *43*(4), 481-529.

Black, A. N., Seears, H. A., Hollenbeck, C. M., & Samollow, P. B. (2017). Rapid genetic and morphologic divergence between captive and wild populations of the endangered Leon Springs pupfish, Cyprinodon bovinus. *Molecular ecology*, *26*(8), 2237-2256.

Bliss, L. C. (1962). Adaptations of arctic and alpine plants to environmental conditions. *Arctic*, *15*(2), 117-144.

Borowiec, M. L. (2016). AMAS: a fast tool for alignment manipulation and computing of summary statistics. *PeerJ*, *4*, 1660.

Budelmann, B. U. (1995). Cephalopod sense organs, nerves and the brain: adaptations for high performance and life style. *Marine and Freshwater Behavior and Physiology*, *25*(1-3), 13-33.

Chabot, B. F., & Billings, W. D. (1972). Origins and ecology of the Sierran alpine flora and vegetation. *Ecological Monographs*, *42*(2), 163-199.

Choler, P. (2018). Winter soil temperature dependence of alpine plant distribution: Implications for anticipating vegetation changes under a warming climate. *Perspectives in Plant Ecology, Evolution and Systematics*, *30*, 6-15.

Cronquist, A. J., Holmgren, N. H., & Holmgren, P. K. (1997). Intermountain flora: Vascular plants of the intermountain west, USA Volume three, part A, subclass Rosidae (except Fabales). *New York: New York Botanical Garden. ISBN*, *893273759*.

Darriba, D., Taboada, G. L., Doallo, R., & Posada, D. (2012). jModelTest 2: more models, new heuristics and parallel computing. *Nature methods*, *9*(8), 772.

Feist, M. A. E., Smith, J. F., Mansfield, D. H., Darrach, M., Mcneill, R. P., Downie, S. R., ... & Wilson, B. L. (2017). New combinations in *Lomatium* (Apiaceae, Subfamily Apioideae). *Phytotaxa*, *316*(1), 95-98.

Flora of North America Editorial Committee (Ed.). (2002). *Flora of North America: Volume 23: Magnoliophyta: Commelinidae (in Part): Cyperaceae* (Vol. 23). Oxford University Press on Demand.

George, E. E., Mansfield, D. H., Smith, J. F., Hartman, R. L., Downie, S. R., & Hinchliff, C. E. (2014). Phylogenetic analysis reveals multiple cases of morphological parallelism and taxonomic polyphyly in Lomatium (Apiaceae). *Systematic Botany*, *39*(2), 662-675.

Harrell, F. E., & Dupont, C. (2008). Hmisc: harrell miscellaneous. *R package version*, *3*(2).

Hijmans, R. J., & van Etten, J. (2014). raster: Geographic data analysis and modeling. *R package version*, *2*(8).

Hitchcock, C. L., & Cronquist, A. (1973). *Flora of the Pacific Northwest: an illustrated manual*. University of Washington Press.

Hitchcock, C. L., & Cronquist, A. (2018). *Flora of the Pacific Northwest: an illustrated manual*. University of Washington Press.

Horikoshi, M., & Tang, Y. (2016). ggfortify: Data visualization tools for statistical analysis results. *R package version 0.2. 0 URL: http://CRAN. R-project. org/package= ggfortif*.

Hou, Y., Nowak, M. D., Mirre, V., Bjorå, C. S., Brochmann, C., & Popp, M. (2016). RAD-seq data point to a northern origin of the arctic–alpine genus Cassiope (Ericaceae). *Molecular phylogenetics and evolution*, *95*, 152-160.

Hughes, C. E., & Atchison, G. W. (2015). The ubiquity of alpine plant radiations: from the Andes to the Hengduan Mountains. *New Phytologist*, *207*(2), 275-282.

Huiet, L., Li, F. W., Kao, T. T., Prado, J., Smith, A. R., Schuettpelz, E., & Pryer, K. M. (2018). A worldwide phylogeny of *Adiantum* (Pteridaceae) reveals remarkable convergent evolution in leaf blade architecture. *Taxon*, *67*(3), 488-502.

Klanderud, K., & Totland, Ø. (2005). Simulated climate change altered dominance hierarchies and diversity of an alpine biodiversity hotspot. *Ecology*, *86*(8), 2047-2054.

Kumar, S., Stecher, G., & Tamura, K. (2016). MEGA7: molecular evolutionary genetics analysis version 7.0 for bigger datasets. *Molecular biology and evolution*, *33*(7), 1870-1874.

Kuss, P., Armbruster, G. F. J., Ægisdóttir, H. H., Scheepens, J. F., & Stöcklin, J. (2011). Spatial genetic structure of *Campanula thyrsoides* across the European Alps: indications for glaciation-driven allopatric subspeciation. *Perspectives in plant ecology, evolution and systematics*, *13*(2), 101-110.

Lande, R. (1980). Genetic variation and phenotypic evolution during allopatric speciation. *The American Naturalist*, *116*(4), 463-479.

Licciardi, J. M., Clark, P. U., Brook, E. J., Elmore, D., & Sharma, P. (2004). Variable responses of western US glaciers during the last deglaciation. *Geology*, *32*(1), 81-84.

Mansfield, D. H. (2000). Flora of Steens Mountain. Oregon State University Press.

Martín-Bravo, S., Valcárcel, V., Vargas, P., & Luceño, M. (2010). Geographical speciation related to Pleistocene range shifts in the western Mediterranean mountains (*Reseda* sect. Glaucoreseda, Resedaceae). *Taxon*, *59*(2), 466-482.

Marx, H. E., Dentant, C., Renaud, J., Delunel, R., Tank, D. C., & Lavergne, S. (2017). Riders in the sky (islands): Using a mega-phylogenetic approach to understand plant species distribution and coexistence at the altitudinal limits of angiosperm plant life. *Journal of biogeography*, *44*(11), 2618-2630.

Meinke, R. J., & Constance, L. (1982). Lomatium oreganum and L. greenmanii (Umbelliferae), two little known alpine endemics from northeastern Oregon. *Madroño*, 13-18.

Miller, M. A., Pfeiffer, W., & Schwartz, T. (2011, July). The CIPRES science gateway: a community resource for phylogenetic analyses. In *Proceedings of the 2011 TeraGrid Conference: extreme digital discovery* (p. 41). ACM.

Montgomery, M. K., & McFall-Ngai, M. J. (1992). The muscle-derived lens of a squid bioluminescent organ is biochemically convergent with the ocular lens. Evidence for recruitment of aldehyde dehydrogenase as a predominant structural protein. *Journal of Biological Chemistry*, *267*(29), 20999-21003.

Müller, J., Müller, K., Quandt, D., & Neinhuis, C. (2010). PhyDE–phylogenetic data editor, version 0.995. *Available from: www.phyde de*

Near, T. J., & Benard, M. F. (2004). Rapid allopatric speciation in logperch darters (Percidae: *Percina*). *Evolution*, *58*(12), 2798-2808.

Nixon, K. C., & Wheeler, Q. D. (1990). An amplification of the phylogenetic species concept. *Cladistics*, *6*(3), 211-223.

Oregon Department of Agriculture (ODA) (2018). Oregon's threatened, endangered, and candidate plants. *Available from: www.oregon.gov/ODA/programs/PlantConservation/Pages/AboutPlants.aspx*

R Core Team (2018). R Foundation for Statistical Computing; Vienna, Austria: 2014. *R: A language and environment for statistical computing*, 2013.

Rambaut, A., Drummond, A. J., & Suchard, M. (2014). Tracer v1.6 *Available from:* www.beast.bio.ed ac.uk.

Ronquist, F., & Huelsenbeck, J. P. (2003). MrBayes 3: Bayesian phylogenetic inference under mixed models. *Bioinformatics*, *19*(12), 1572-1574.

Schittek, K., Forbriger, M., Berg, D., Hense, J., Schaebitz, F., & Eitel, B. (2018). Last millennial environmental dynamics in the western Peruvian Andes inferred from the development of a cushion-plant peat hillock. *Perspectives in Plant Ecology, Evolution and Systematics, 30*, 115-124.

Schulz, J. and Matthews, J. (2007). *Lomatium greenmanii* Candidate Conservation Agreement- Appendix D: Research, Monitoring, and Predictive Habitat Modeling.

Shimodaira, H., & Hasegawa, M. (2001). CONSEL: for assessing the confidence of phylogenetic tree selection. *Bioinformatics*, *17*(12), 1246-1247.

Smith, J. F., Mansfield, D. H., Stevens, M., Sosa, E., Feist, M. A. E., Downie, S. R., ... & Darrach, M. (2018). Try Tri again? Resolving species boundaries in the *Lomatium triternatum* (Apiaceae) complex. *Journal of Systematics and Evolution*, 56(3), 218-230.

Smyčka, J., Roquet, C., Renaud, J., Thuiller, W., Zimmermann, N. E., & Lavergne, S. (2017). Disentangling drivers of plant endemism and diversification in the European Alps–A phylogenetic and spatially explicit approach. *Perspectives in Plant Ecology, Evolution and Systematics*, 28, 19-27.

Stamatakis, A. (2006). RAxML-VI-HPC: maximum likelihood-based phylogenetic analyses with thousands of taxa and mixed models. *Bioinformatics*, *22*(21), 2688-2690.

Stöver, B. C., & Müller, K. F. (2010). TreeGraph 2: combining and visualizing evidence from different phylogenetic analyses. *BMC bioinformatics*, *11*(1), 7.

Sun, F. J., & Downie, S. R. (2010). Phylogenetic analyses of morphological and molecular data reveal major clades within the perennial, endemic western North American Apiaceae subfamily Apioideae. *The Journal of the Torrey Botanical Society*, 133-156.

Swofford, D. L. (2002). PAUP*. Phylogenetic analysis using parsimony (* and other methods). *Version*, *4*, b10.

Thorogood, C. J., Bauer, U., & Hiscock, S. J. (2018). Convergent and divergent evolution in carnivorous pitcher plant traps. *New Phytologist*, *217*(3), 1035-1041.

Townsend, C. L., & Figge, J. T. (2002). Northwest Origins | Burke Museum. Retrieved from http://www.burkemuseum.org/geo_history_wa/

U.S.D.A. Forest Service, Eagle Cap Ranger District U.S.D.A. Forest Service, Wallowa-Whitman National Forest U.S. Fish and Wildlife Service, La Grande Field Office U.S. Fish and Wildlife Service, Oregon Fish and Wildlife Office (USDA and USFSWS) (2007). Candidate Conservation Agreement for *Lomatium greenmanii*: Greenman's Desert Parsley.

Wake, D. B. (2003). Homology and homoplasy. Keywords and concepts in evolutionary developmental biology, 191-201.

Wang, L., Abbott, R. J., Zheng, W. E. I., Chen, P., Wang, Y., & Liu, J. (2009). History and evolution of alpine plants endemic to the Qinghai-Tibetan Plateau: Aconitum gymnandrum (Ranunculaceae). *Molecular Ecology*, 18(4), 709-721.

Warren, D. L., Glor, R. E., & Turelli, M. (2008). Environmental niche equivalency versus conservatism: quantitative approaches to niche evolution. *Evolution*, *62*(11), 2868-2883.

Wickham, H. (2011). ggplot2. Wiley Interdisciplinary Reviews: Computational Statistics, 3(2), 180-185.

Wiens, J. J., & Graham, C. H. (2005). Niche conservatism: integrating evolution, ecology, and conservation biology. *Annu. Rev. Ecol. Evol. Syst.*, *36*, 519-539.

Williams, E. W., Farrar, D. R., & Henson, D. (2016). Cryptic speciation in allotetraploids: Lessons from the Botrychium matricariifolium complex. *American Journal of Botany*, *103*(4), 740-753.

# CHAPTER TWO: INVESTIGATING SPECIES BOUNDARIES IN THE LOMATIUM PACKARDAIE/ANOMALUM SUBCOMPLEX

**Abstract**

Speciation is a process that exists on a continuum beginning with genetic structuring to incipient speciation and finally distinct species. Understanding where to draw species boundaries is complicated by many factors ranging from theoretical issues dealing with the nature of the species unit itself to biological realities which confound field or morphological-based identification. The genealogical species concept, employed in this study, focuses on uncovering the relative contribution of reticulate and divergent evolution in monophyletic groups and explicitly incorporates coalescent theory. Modern advances in genomics, including next-generation sequencing, bioinformatics processing, and phylogenetic reconstruction, allow researchers to model speciation under this concept more accurately than ever before. Biological issues including phenotypic plasticity and convergent evolution can confound species delimitation based on morphological and ecological evidence. The Perennial Endemic North American clade of Apiaceae (PENA) is one of the largest and least understood plant radiations in Western North America. *Lomatium* is the largest genera and as traditionally defined is polyphyletic. Recent Sanger-sequence based studies have resolved many evolutionary relationships and revealed a homoplasy in previously thought to be taxonomically informative characters. The *Lomatium packardiae/anomalum* subcomplex embedded within the larger *Lomatium triternatum* complex could not be resolved with Sanger-sequencing and traditional

concatenated-based phylogenetic analysis. The observed morphological, ecological, and geographic differences in the *L. anomalum/packardiae* subcomplex do not ascribe to monophyletic groups in Sanger-sequence based studies. Hypotheses for the recalcitrant nature of this subcomplex include that the complex is one phenotypically plastic taxa or incomplete lineage sorting (ILS) is causing the incongruences between morphological, ecological, and molecular data. An NGS target-enrichment approach was used to sequence 353 Angiosperm-wide genes which have been shown to perform consistently across a wide range of plant families. Reads were mapped to reference genes and de novo assembled with the Hyb-Piper pipeline. Fifty-four introns flanking the genes were then extracted for downstream analysis. Unmapped reads were used to generate entire plastomes with a reference-based assembly-method. STACEY, a Bayesian coalescent based species tree analysis which takes ILS into account, and a concatenated approach with MrBayes were performed on the intron dataset. The whole plastome data were also analyzed with MrBayes. The STACY analysis uncovered three coarse and seven fine scale clades that correspond with geographic distributions and some previously recognized taxonomy. The concatenated data set was incongruent with geography and previously recognized taxonomy. Phylogenetic analysis of the whole plastome dataset revealed a stochastic pattern. Climatic factors, morphological characters, and soil variables were measured in an attempt to provide additional support to uncover any unifying features of monophyletic groups. Climatic niche and leaflet width and length were to some degree predictive of coarse phylogenetic structure. *Lomatium packardiae* was found to be monophyletic in the molecular data and distinct in the PCA of reproductive characters with measurably shorter umbels rays and fruit than other

members of the subcomplex. The comparison of chloroplast and low copy nuclear intron analyses leads to the conclusion that recent stochastic events through either prehistoric super-floods or seed dispersal by indigenous peoples and incomplete lineage sorting are the two primary culprits causing the contrasting patterns observed in the molecular data. A possible explanation is that the clades recovered with the STACEY analysis are the result of incipient speciation, which is cryptic due to the lack of any consistently reliable diagnostic traits besides geography. Additionally, the comparison between morphological, environmental, and phylogenetic datasets show that local gene flow mediated through small-insect pollination and short-distance dispersion can play a large role in shaping the morphologies of populations within this group. Currently, the best predictor of phylogenetic placement is geography.

## Introduction

Speciation is frequently associated with morphological change especially in reproductive characters such as the flowers and fruits of Angiosperms. This can be due to changes in pollination syndrome and the subsequent secession of gene flow between populations. Darwin (1862) predicted the existence of an increasingly long proboscis in moths (*Xanthopan morgani* ssp. *praedicta*) after the observation of unusually long nectar spurs in an orchid (*Angraecum sesquipedale*). The discovery of the moth occurred 61 years after his prediction (Whitall and Hodges, 2007). Darwin's theory that co-evolutionary patterns between pollinators and flowers can drive the speciation process was further confirmed by a molecular phylogeny of columbine (*Aquilegia*) species mapped with nectar spur lengths by Whitall and Hodges (2007) whereby pollinator morphology shifts causes nectar spurs to rapidly evolve in a punctuated fashion during

speciation. Morphological changes do not always occur in reproductive characters. In allopatric speciation, gene flow can cease due to the formation of a geographic reproductive barrier. Subsequent natural selection or genetic drift can result in the formation of species which differ morphologically in vegetative characters. Many wind-pollinated species such as alders (*Alnus* spp.) and pines (*Pinus* spp.) have highly conserved reproductive features with the major taxonomically informative distinctions occurring in vegetative characteristics such as the bark, leaves, and buds (Hitchcock and Cronquist, 1973).

Plant speciation is not always associated with morphological change, as is the case in cryptic speciation. Cryptic species occur when no clear morphological character delimits species boundaries (Paris et al., 1989) and harbor a unique diversity that is underreported in many traditional taxonomic treatments based solely on morphology. Cryptic species exist across a wide range of taxa including butterflies (Hebert et al., 2004), limpets (Johnson et al., 2008), and plants (Williams et al., 2016) and are potentially common in many other lineages (Bickford et al., 2007). In the well-documented, example of grape ferns (*Botrychium* spp.), species boundaries are not clearly defined by any obvious morphological character (Williams et al., 2016; Paris et al., 1989). There is a great deal of overlap between pinnae and sporangium size and shape across different species. In these cases, the choice of morphological character used to delimit taxa can be difficult or impossible making additional data necessary to adequately determine species boundaries. Frequently, molecular data are used to fill this void. In the *Botrychium matricarifolium* complex, amplified fragment length polymorphisms and allozymes were used to help delimit species which corresponded to minute

morphological differentiation difficult to detect without the guidance of molecular data (Williams et al., 2016). When the speciation process is recent or ongoing (incipient speciation), substantial morphological differences may not have had time to accrue leading to lineages which are challenging to distinguish morphologically. This was shown in a population genetics study of the Western Diamondback Rattlesnake (*Crotalus atrox*) where the eastern and western extremes of the range are genetically distinct with a large admixture zone in-between, and while local variation exists, no morphological characters clearly distinguishes the eastern versus western genetic groups (Schield et al., 2015). Molecular data are a common tool used to increase the amount of data available to systematists for species delimitation and phylogenetic reconstruction; it is especially vital in cases of cryptic, recent, and incipient speciation.

Over the last decade, next-generation sequencing (NGS) has resulted in a proliferation of molecular data available to researchers when compared with traditional Sanger sequencing (Metzker, 2010). Increases in computing power and software developments have allowed systematists to merge NGS data and bioinformatics to create higher resolution phylogenies than previously available. Restriction-site associated DNA sequencing (Rad-seq), a type of NGS technology, have helped untangle a complicated evolutionary history and a biogeographic account of *Quercus* (Fagaceae) which is riddled with ancient and ongoing introgression (Hipp et al., 2014; Eaton et al., 2015). At shallower evolutionary time-scales, NGS technologies have been used to test species boundaries in *Lepanthes horrida* (Orchidaceae; Bogarin et al., 2018), *Micranthes* (Saxifragaceae; Stubbs et al., 2018), and *Campanula* (Campanulaceae; Crowl et al., 2017). Population-level evolutionary processes can also be investigated with NGS;

replacing a field that was once dominated by microsatellites and other variable taxon-specific markers (Davey and Blaxter, 2010). Next-generation sequencing and associated bioinformatics tools have revolutionized the fields of molecular ecology and systematics.

While high-resolution molecular data have been effective at resolving recalcitrant evolutionary relationships at both deep and shallow taxonomic ranks these data are not without their own challenges. Incongruences between molecular data, morphology, ecology, and geography can be caused by many factors including paralogous loci, hybridization, incomplete lineage sorting (ILS), and ongoing gene flow among populations especially in morphologically variable and phenotypically plastic species. Paralogous loci can be accounted for in the bioinformatic processing steps of a study, with the remaining factors broken into a simple dichotomy: subtle differences in morphology and ecology can be caused by either historic evolutionary processes (ILS; introgression) or present-day phenomena, such as phenotypic plasticity, morphological variation, and ongoing gene flow. Interplay between these factors can complicate morphology and taxonomic understanding even further.

Inferring homology across loci can be challenging due to the potential for paralogs arising from gene duplication events. Many procedures that target low-copy nuclear genes cannot assure a lack of paralogs until downstream bioinformatics filtering. Comparing paralogous or other non-homologous loci when building a phylogeny will lead to incorrect inferences about evolutionary history. Non-taxon specific target-enrichment protocols (Johnson et al., 2018; Faircloth et al., 2015, Léveillé-Bourret et al., 2017) target exons or other highly conserved regions which are easier to align and ensure homology across disparate taxa. However, these targeted highly conserved regions may

not have enough variation to be suitable for specific or population level studies. Recent bioinformatics developments (Johnson et al., 2016) allow for increased ease of extracting flanking intronic regions which are theoretically more variable and useful at shallow taxonomic levels. However, to our knowledge this theory has yet to be demonstrated practically.

Additional complications with molecular data include varying histories of different genes and genomes sometimes caused by reticulate evolution. The chloroplast genome is maternally inherited and can have a different evolutionary history than the nuclear genome in instances of hybridization, ongoing gene flow, extensive ILS, ancient dispersal events, and range contractions (Soltis et al., 2004; Degnan and Rosenburg, 2009; Hooker, 2018; Meng et al., 2015). These factors can be untangled by incongruences in phylogenies based on nuclear versus chloroplast data and concatenated versus coalescent-based analyses. A well-documented example of hybrid speciation (Ownbey, 1950) was repeatedly shown by Soltis et al. (1989, 1995, 2004) in *Tragopogon* of western North America. Variation in the inheritance of individual genes within a whole genome can also lead to the observation of contrasting gene trees. Incomplete lineage sorting poses a problem for phylogenetics when a gene used for reconstructing evolutionary history coalesces in a lineage that is not the most recent common ancestor (Degnan and Rosenburg, 2009). Incomplete lineage sorting can appear as reticulate evolution in genomic datasets. Recent development of bioinformatics software that can reconstruct phylogenies while accommodating ILS, such as ASTRAL-III and STACEY, (Zhang et al., 2017; Jones, 2014) have eased this issue. A study by Morales-Briones et al. (2018) investigating hybridization in *Lachemilla* (Rosaceae) have shown the utility and

possibility of accurately reconstructing phylogenies despite extensive ILS and introgression. Stochastic ancient long-distance dispersal events (Hooker, 2018) and range contractions with subsequent population isolation (Meng et al., 2015) have also been shown to leave conflicting patterns in nuclear versus chloroplast histories. In these cases, additional data sources, such as climate and morphology, are needed to resolve potential factors causing the conflicting patterns. The vast increase in molecular data and subsequent bioinformatic applications allows researchers to reconstruct phylogenies in previously recalcitrant taxa with complex evolutionary histories.

Ongoing gene flow, phenotypic plasticity, and morphological variation are additional factors that can cause incongruities between molecular data and other potentially taxonomically informative characters. When gene-flow is ongoing between a group of populations, phylogenies will not be well-resolved and the populations should be considered members of the same species. In the case of phenotypic plasticity, individuals within the same species can be morphologically differentiated when they occur in different environments. Delimiting species boundaries in this scenario is difficult not because of complex evolutionary histories, but because species with the ability to adapt to a wide range of conditions can have morphologies that vary accordingly. This is a well-documented phenomenon among plants: After a wildfire, an increase in open ground to colonize and essential nutrients such as nitrogen, may cause certain species to grow more robustly, such as the proliferation of *Chamaenerion angustifolium* after disturbances in the western United States (Cook and Halpbern, 2018). In species with ranges that span an environmental or ecological gradient, those found in wetter or warmer environments may exhibit different morphologies than those found in cooler or drier

environments, such as in the highly polymorphic Hawaiian tree species *Metrosideros polymorpha* with differing leaf morphologies and other traits that vary depending on the substrate, rainfall regime, and other environmental parameters (Cordell et al., 1998; Izuno et al., 2017). The speciation process exists on a continuum from genetic structuring to incipient speciation and finally distinct species. In some cases, including the previously mentioned *M. polymorpha*, observations of varying morphology at the environmental or geographic extremes of a species range/tolerance can be associated with incipient speciation or extensive genetic structuring such as in cichlid fishes (Meyer, 1987) and *Mimulus* (Sobel and Streisfeld, 2014). The increase in the availability of highly variable NGS-based molecular markers and associated bioinformatics tools makes investigations into phenotypic plasticity and its relationship with genetic structure and incipient speciation worthwhile.

Species delimitation is a complex task that must consider a variety of data sources (molecular, morphological, ecological, and geographic) in addition to a wide range of theory dealing not only with evolutionary processes such as introgression and lineage sorting, but also the nature of the species unit itself. Speciation is an intricate and ongoing process caused by a variety of forces. This has in part, led to a proliferation of species concepts ranging from similarity-based concepts such as the morphological species concept (Burger, 1975) to ancestry-based concepts that incorporate the complex nature of gene inheritance, such as the genealogical species concept (Baum and Shaw, 1995). The genealogical species concept is one type of phylogenetic species concept that defines species among other criteria as being a monophyletic group. This concept also incorporates the process of coalescence stating that “species reside at the boundary

between reticulate and divergent genealogy" (Baum and Shaw, 1995). Since the acceptance of the theory of evolution, similarity-based concepts are rarely explicitly evoked. However, the monophyly of most species has not been tested with molecular data, and it is difficult to guarantee that many morphological characters used to delimit species are taxonomically informative from an ancestry-based perspective.

The perennial endemic North America (PENA) clade of Apioideae (Apiaceae) is one of the largest land plant radiations in western North America and has been shown to have many examples of apparent homoplasy of previously thought to be taxonomically informative characters when viewed with molecular sequence data (George et al., 2014; Sun and Downie, 2010). Mature fruit characters such as dorsal wings and number of oil tubes have traditionally been used to delimit taxa at both the specific and generic level in this group. *Lomatium,* the largest genus composed of approximately 80 species, has been described as distinct from *Cymopterus* based on its lack of dorsal rib winging on mature fruits (Hithcock and Cronquist, 1973). Sanger-sequencing of the ITS region revealed *Cymopterus,* as traditionally described, is polyphyletic (Sun and Downie, 2010). The recent recognition of *Cymopterus glomeratus* var. *concinnus* shows convergence in seed morphology, a trait previously thought to be diagnostic (George et al., 2014). The dissolution of *Orogenia* and its inclusion into *Lomatium* based on molecular data is another example of morphological-based taxonomy that is not reflective of evolutionary history in this clade (Feist et al., 2017). Since molecular studies have revealed such a high degree of homoplasy in traditionally 'taxonomically informative' characters, revisiting existing species boundaries with the addition of molecular data is warranted throughout the PENA clade.

Recent investigations into the *Lomatium triternatum* species complex have revealed a suite of homoplasy and incongruences between morphological and molecular data. *Lomatium simplex,* once considered a variety of *L. triternatum*, has been elevated to the rank of species because it occupies a different phylogenetic position from the rest of the complex. The triternate leaf morphology most likely represents yet another case of convergence within the PENA clade. *Lomatium triternatum* as described in the Flora of the Intermountain West (Cronquist et al., 1997) is distributed throughout the northwestern United States, neighboring Canadian provinces, and the northern Great Basin and Rocky Mountains. The *Lomatium anomalum/packardiae* subcomplex is part of the larger *L. triternatum* complex and consists of two traditionally recognized taxa with different morphologies and ecological preferences: *Lomatium packardiae* was originally described as existing solely on "volcanic ash that has yet to weather into clay" and with a morphology akin to *L. triternatum* var. *triternatum* except for leaflets with a different aspect (Cronquist, 1992). *Lomatium anomalum* has been at various points in time described as its own species, a variety, and a sub-species of *L. triternatum; L. anomalum* has substantially wider leaflets than any other described entity in the complex making it readily identifiable in the field (Hitchcock and Cronquist, 1973; Cronquist et al., 1997). It is frequently found in more mesic habitat types associated less with sagebrush and more with prairie-like conditions. While many populations of *L. anomalum* are readily differentiated based on morphology, there are populations and even individuals which exhibit both wider *L. anomalum*–like leaves and narrower *L. triternatum* var. *triternatum* or *L. packardiae* type leaves. The *L. packardiae/anomalum* subcomplex is taxonomically

confusing when viewed solely with the lens of morphological, ecological, and geographic data.

To untangle the confusion caused by morphological, ecological, and geographic data, Smith et al. (2018) used a set of seven Sanger-sequenced loci (two nuclear ribosomal and five plastid) to investigate species boundaries in the larger *L. triternatum* species complex. While many problematic taxa were resolved, such as the previously mentioned *L. simplex*, they found that the observed morphological, ecological, and geographic differences in the *L. anomalum/packardiae* subcomplex do not ascribe to monophyletic groups. Wide leaflet plants from prairies in central-western Idaho fall out in the same clade with narrow leaflet plants found in and around ash beds in Southeastern Oregon (Fig. 2.1). The observed incongruences between molecular data, geography, ecology, and morphology can be attributed to two main hypotheses: (1) individuals within the *L. anomalum/packardiae* sub-complex are highly morphologically variable and/or phenotypically plastic with different morphologies caused by varying environmental conditions, or (2) historic evolutionary processes such as ILS and introgression are failing to be reconciled by the Sanger-based dataset and differences can be explained by populations belonging to separate taxa. Both of these hypotheses can act in conjunction, such that the subcomplex consists of some morphologically fixed species and other variable species could further confound delimitation. The goal of this study is to use ecological, morphological, and molecualr information to ascertain species boundaries and understand the role of complex evolutionary scenarios and phenotypic plasticity in the evolution of the *L. anomalum/packardiae* subcomplex. In order to resolve species boundaries, the genealogical species concept will be employed with the molecular

data and any monophyletic groups uncovered will be validated with external data sources, such as morphology and ecology to help better establish species boundaries.

## Materials and Methods

### Sample Collection

To obtain fresh leaf material for molecular methods, collect ecological data, and acquire specimens for morphometric analysis and herbarium vouchers, populations in the *L. packardiae/anomalum* species complex were visited between April and July of the 2017 and 2018 growing seasons. Prior to collecting, known localities of populations within the species subcomplex were identified via morphology and geography on the Consortium of Pacific Northwest Herbaria (http://www.pnwherbaria.org/) and through discussions with local *Lomatium* experts (Don Mansfield; Jim Smith). Additional populations were collected opportunistically en route to known locations. Areas of known genetic diversity and sources of taxonomic confusion as revealed by Smith et al. (2018) (Succor Creek drainage of eastern Oregon; Camas Prairie outside Grangeville, Idaho; Asotin County in Southeastern Washington) based on preliminary Sanger-sequencing and morphological data (Smith et al. 2018) were sampled more heavily to obtain sufficient material to clarify taxonomic relationships. Individuals of uncertain identity were keyed in the Flora of the Pacific Northwest (Hitchcock and Cronquist, 2018) and/or the Intermountain Flora (Cronquist et al., 1997). At each location, fresh leaf material was dried in silica gel. Herbarium vouchers of representative plants were collected and deposited at SRP with duplicates at CIC (Appendix B).

## Molecular Methods

### Sample Choice and DNA Extraction

Forty-eight samples were chosen for molecular analysis including previously collected material which had been preserved in silica gel and newly collected material from the 2017 field season (Appendix B). Populations which had been included in Smith et al. (2018) were used to reconstruct the backbone of the broader *Lomatium triternatum* species complex in which newly collected individuals could be placed (Appendix B). New samples were included to expand the range of collections, decrease the geographic distance between previously collected individuals, and include more morphological intermediates between narrow and wider leaflet populations. More samples also included additional representatives from under-sampled locations and sources of taxonomic confusion including Asotin County Washington, Camas Prairie Idaho, and the Owyhee region of southeastern Oregon/southwestern Idaho. DNA was extracted from silica dried leaf material using the Qiagen DNAeasy plant minikit (Valencia, California) following the manufacturer's recommended protocol with slight modifications as described in Smith et al. (2018) and George et al. (2014). Post-extraction, DNA concentration was quantified using a Qubit 4 Fluorometer with the dsDNA HS assay kit (Thermo Fisher Scientific, Waltham, Massachusetts). A sub-set of 15 samples were randomly chosen for analysis on the Agilent 4200 Tape Station (Agilent Technologies, Santa Clara, California) using a genomic DNA tape to determine the molecular weight of the samples to ascertain if the DNA was degraded. Degraded samples do not need to be further sheared in the sonication step. Output graphs were visually inspected to identify if there

was a peak of around 20 kbp indicating the genomic DNA was of high molecular weight and in need of shearing.

DNA Shearing

DNAs were sheared using a Covaris ME 220 Focused-ultrasonicator (Covaris, Woburn, Massachusetts) with 58 ul of input DNA per sample, a duration of 65 seconds, with a peak power of 40 watts, an average power of 4 watts, a duty factor of 10%, and 1000 cycles per burst. Eight samples were sonicated at a time for 8 minutes and 40 seconds at an average temperature of 20 degrees C.

Library Preparation

Libraries were prepared with the NEBNext Ultra II kit (New England BioLabs, Ipswich, Massachusetts) according to the manufacturer's recommendations with the following modifications: dual-index (i5 and i7) primers were used for barcodes, and size selection was performed with 30 ul of SPRIselect beads (Beckman Coulter, Brea, California) for a target insert size length of 400-500 base pairs. The Agilent 4200 Tape Station was used to check the fragment size distribution of the libraries; 2 ul of the high sensitivity buffer provided by the manufacturer, and 2 ul of the sample were included in each well. Four D100 High Sensitivity (HS) tapes were placed in the machine. Since no D100 HS ladder was available, 1 ul of the D100 (non-HS) buffer was diluted in 20 ul of neutral buffer. The machine was run according to the manufacture's specifications for the D100 HS kit. To quantify the concentration of double-stranded DNA in each sample, a Quantas Flurometer (Promega, Madison, Wisconsin) was used following the manufacturer's recommended protocol.

Hybridization/Target Enrichment

All prepared libraries (100 ng of DNA each) were pooled into a single tube for one hybridization reaction (only one reaction was required because samples were closely related members of the same species complex) utilizing the Angiosperm 353 bait kit manufactured by MYcroarry (Ann Arbor, Michigan). The hybridization reaction was performed following the MYbaits user manual Version 3.02 (MYcroarray, 2016) with an incubation period of 24 hours in a Hybex Microsample Incubator (SciGene, Sunnyvale, California) at 65 degrees C. The final product was amplified for 10 cycles using a KAPA HiFi 2X HotStart ReadyMix PCR Kit (Roche, Basel, Switzerland). NebNext beads (New England BioLabs, Ipswich, Massachusetts) at a 1:1 DNA to bead ratio were used to clean the final PCR reaction. The final fragment size distribution and DNA concentration were quantified using the D100 HS kit on an Agilent 4200 Tape Station and a Quantus Flurometer, respectively.

Next-Generation Sequencing

Sequencing was performed on an Illumina MiSeq L1000 (San Diego, California) with the MiSeq reagents kit v3 following manufacturer's recommendations to dilute the final concentration of DNA to 16.5 pM in a 600 ul solution of the IlluminaHT1 reagent. One lane of the machine was used to sequence 2 x 300 paired-end reads.

DNA extractions were performed at Boise State University. All other laboratory work was performed at the Sackler Center for Phlyogenomics at Kew Gardens in London, U.K.

## Bioinformatics Workflow

### Trimming

Raw reads were demultiplexed with Illumina's included software before downloading data from the MiSeq. Demultiplexed reads were checked for quality and adapter content with FastQC (Andrews, 2010). The paired-end reads were combined and trimmed to remove leftover adapter fragments and low-quality base pair calls (phred<33) with TRIMMOMATIC (Bolger et al., 2014) utilizing the following parameters {-phred33; ILLUMINACLIP:TruSeq3-PE-2.fa:2:30:7:2:true MAXINFO:40:0.7 CROP:290 MINLEN:36}.

### Nuclear Loci Assembly

The HybPiper pipeline was used to assemble the 353 genes targeted in the Angiosperm 353 kit. The pipeline maps individual reads to a target file using bwa (Li and Durbin, 2010) or BLAST (McGinnis et al., 2004) before performing a *de novo* assembly of each gene individually from the mapped reads with SPAdes (Bankevich et al., 2012) and annotating intron/exon boundaries sequences with Exonerate (Slater and Birney, 2005). The target files, provided by the developers of Angiosperm 353 (https://github.com/mossmatters/Angiosperms353), contained reference genes from a wide range of Angiosperm taxa ensuring its ability to map reads to each gene effectively across wide phylogenetic ranges. A benefit of this assembly method versus a solely reference-based approach is the capture of the more variable flanking intronic regions. The pipeline was run twice using different target files consisting of nucleotide (bwa method) or amino acid data (BLAST method). Theoretically, an amino acid target file will allow for greater variance in the mapped reads resulting in assemblies with more

depth and coverage. Hyb-Piper was used to output both the exonic and intronic region(s) for each gene, separately. Loci were aligned individually with mafft (Katoh and Standley, 2013) {parameters: -localpair --maxiterate 1000 --adjustdirectionaccurately} and alignments were cleaned to remove ambiguous regions with BMGE (Criscuolo and Gribaldo, 2010) with the default settings. Block Mapping and Gathering with Entropy (BMGE) uses calculations that simulate entropy to distinguish between random variation and biologically probable base pair substitutions thereby removing regions which are misaligned.

Nuclear Loci Filtering

Basic alignment statistics including sequence length, percent missing data, percent variable sites, and percent parsimony informative sites were calculated with AMAS (Borowiec, 2016), a Python package with standard phylogenetic utilities. Loci were chosen for downstream analysis based on the following criteria adapted from Gernandt et al. (2018): all 48 samples present, less than 10% missing data, an alignment length of greater than or equal to 200 base pairs, less than 15% variable sites; and no paralog warnings generated by Hyb-piper. Loci criteria were applied using the custom script genepicker.R (https://github.com/ottenlipsmv/lom_pack_anom) on introns and exons, independently.

Whole Chloroplast Assembly

The MITObim (Hahn et al., 2013) plastid baiting and iterative mapping assembler was used to reconstruct whole chloroplast genomes using reads which did not hybridize to the target loci. MITObim performs numerous iterations of the MIRA short-read assembler (Chevreux, 2007) from a starting sequence seed and stops when it reaches a

stable assembly. The starting seed can be as short as one chloroplast region, such as *matK*, or a whole closely related reference plastome. A previously assembled *Foeniculum vulgare* plastid genome (GenBank #: KR011054.1) was available as a reference and used as the starting seed for the MITObim assembly. *Foeniculum vulgare* is in the same subfamily (Apiodeae) of Apiaceae as the *L. packardiae/anomalum* species subcomplex (Peery, 2015).

All scripts used in the assembly workflow including any detailed parameters unspecified in the methods can be found at https://github.com/ottenlipsmv/lom_pack_anom.

## Phylogenetic Reconstruction

### Concatenated Analysis

A Bayesian analysis was performed on a dataset consisting of a concatenated alignment of the 54 introns filtered by the criteria identified above. Concatenation was performed by AMAS and alignments by mafft {parameters: -localpair --maxiterate 1000}. A concatenated analysis assumes gene trees are identical to the overall species tree, and thus does not account for ILS. The model of molecular evolution (GTR+I+G) and base pair substitution rates were identified via jModeltest2's AIC calculations (Darriba et al., 2012) and input as priors into MrBayes (Ronquist et al., 2012) with the following MCMC parameters: two independent runs consisting of 20,000,000 generations sampling every 1000 generations with a burn-in of 25% and four chains. *L. brevifolium Smith 13048* was set as the outgroup. Tracer (Rambaut and Drummond, 2003) was used to evaluate effective sample size (ESS) values, burn-in period and convergence of other priors.

Chloroplast Genomes

The whole plastid assemblies generated by the MITObim assembler were used to reconstruct the plastid history of the samples in this species subcomplex. Mafft {parameters: -localpair --maxiterate 1000} was used to align the chloroplast genomes, and misaligned regions were removed with BMGE utilizing the default settings. Phylogenies were reconstructed using MrBayes with the model (GTR+I+G) and prior parameters suggested by the AIC calculation output of jModelTest2. MCMC settings are identical to the settings used for the concatenated nuclear analysis, and Tracer was used to evaluate ESS values.

Species Tree Analyses

STACEY (Jones, 2014) is a BEAST2 (Bouckaert et al., 2014) package that models the speciation process incorporating coalescent theory. Species tree analyses do not have the same assumption that gene trees share the same species tree of concatenated methods making this methodology more effective in rapid and/or recent radiations which are expected to have a high degree of ILS. Outgroup samples (*Lomatium brevifolium Smith 13048* and *Lomatium thompsonii Ottenlips 80*) were excluded from this analysis because preliminary STACEY runs suggested that the more distantly related outgroups were drastically increasing computing time by causing MCMC mixing problems. Runs with fewer generations that included outgroups had similar topologies to those presented here, but inadequate ESS values. Five independent chains of STACEY were run for 5,000,000,000 generations each with a collapse height set to .0001, a Yule-death rate, and the JC69 molecular evolution model allowing STACEY to estimate the base pair substitution rate. The BEAST2 .xml file with additional unspecified priors and MCMC

parameters is available at https://github.com/ottenlipsmv/lom_pack_anom. Logcombiner (Rambaut and Drummond, 2013) and loganalyzer (Bouckarert et al., 2014) were used to evaluate ESS values for all priors and parameters. A burn-in of 50% was implemented for all log and tree files based on inspection of outputs from loganalyzer. Tree files were combined using logcombiner and then annotated, visualized, and edited with treeannotater (maximum clade credibility tree; Rambaut and Drummond, 2013), Figtree (manually re-rooted on *L. andrusianum* clade; Rambaut, 2007) and TreeGraph2 (collapsed nodes with <50% support into polytomies; Stöver and Müller, 2010)

ASTRAL-III (Zhang et al., 2017) is a species tree analysis program that measures gene tree discordance while estimating a species tree given a set of gene trees. ASTRAL-III outputs three support values (posterior probabilities) for each node: one value for the main topology, one value for the probability the clade belongs to the sister group, and one value for the probability that the clade belongs to the outgroup(https://github.com/smirarab/ASTRAL/). Input gene trees were generated with RAxML (Stamatakis, 2014) stopping bootstrapping automatically using the auto-MRE feature. The ASTRAL-III analysis includes the outgroup samples excluded from the STACEY analysis.

The bioinformatics pipeline and all evolutionary history reconstruction techniques with the exception of MrBayes were performed on a machine running Linux Ubuntu with 32 Intel Xeon Gold 6130 CPUs and 48 GB of RAM. MrBayes was run on the CIPRES Science Gateway (Miller et al., 2011). All Linux scripts used in the phylogenetic reconstruction workflow including any parameters/settings not specified in the methods can be found at https://github.com/ottenlipsmv/lom_pack_anom.

## Ecological, Climatic, and Morphological Analyses

### Soil Data Collection and Analysis

Soil data was collected for five replicate individuals at each population. Five soil compaction readings were taken with a pocket penetrometer (Forestry Suppliers, Jackson, Mississippi) in the four corners and at the center of each quadrat. Individual readings can be highly variable due in part to the small piston, so it is advisable to make multiple readings per site (unpublished results; Appendix C). Additionally, about 200-500 grams of soil were collected from the upper horizons at each replicate for further laboratory analysis. Soils were airdried inside a greenhouse at Boise State University. Dried soils were ground with a mortar and pestle and gravels were separated from fines with a 2 mm sieve to determine the gravel fraction. The hydrometer method (Bouyoucos, 1962) was used to determine the fines fraction. Due to calibration issues with the hydrometer, the fraction between sand and silt could not be determined. All soil particle analyses were performed at the soil laboratory in the Department of Geosciences at Boise State University. About 150-200 grams of dried, ground, and sieved soil were sent to the Soil and Forage Analysis lab at the University of Wisconsin-Madison for routine and base saturation tests (soil pH, P, K, Ca, Mg, cation exchange capacity (CEC), organic matter(OM)) and other additional soil tests (sulfate, soluble salts, N, Nitrate, Ammonia). Raw soil chemistry, compaction, and particle size data is available as Appendix D.

Soil characteristics were analyzed with principal component analysis (PCA) to uncover distinct groupings that might correspond to monophyletic groups and/or distinct populations. Soil chemistry, compaction, and particle size data were centered and scaled

and a PCA performed on the combined dataset. Some individuals were collected by outside collaborators and therefore ecological variables were not available (Appendix B).

Climatic Data Collection and Analysis

Climate data were downloaded using the R package *raster* (Hijmans and van Etten, 2014) in the form of 19 BIOCLIM variables (Fick and Hijmans, 2017) at the 30 arc second resolution (~1 $km^2$) from the UC-Davis Biogeography webserver (http://biogeo.ucdavis.edu/data/climate/worldclim/). BIOCLIM variables were extracted for the GPS coordinates for each of the 48 individuals included in the molecular analysis using the 'extract' function from the R package *raster*. The data were centered and scaled, and a PCA performed. Raw BIOCLIM variables for each collection are available as Appendix E.

Morphological Data Collection and Analysis

Both vegetative and reproductive morphological characters were measured from herbarium specimens. Each measurement was replicated five times and the means from each specimen were calculated. Leaflets and umbels which were completely visible with no overlap from other material on the herbarium sheet were chosen for measurements. The following reproductive traits were quantitively measured: ray length, mature fruit length, mature fruit width, mature pedicel length, length of primary umbel, width of primary umbel, wing width, and fruit length. Fruiting material was only available for 17 populations, however at least one populations for each fine scale clade identified in STACEY was available (Appendix F). A PCA was performed on the centered and scaled reproductive character means. Vegetative traits, leaflet width and length, were visualized separately by constructing a scatterplot with width on the y axis and length on the x axis.

Preliminary analysis on additional vegetative characters (adapted from George et al., 2014) were uninformative, so only leaflet width and length were retained. Morphological data as averages are available as Appendices 5 and 6 for reproductive and vegetative data, respectively.

All data curation and analysis for ecological, morphological, and climatic variables was performed in R version 3.5.1 (R Core Team, 2018) and visualized using *ggplot2* (Wickham, 2016) and *ggfortify* (Tang et al., 2016). Principal components analyses were performed in base R. All R scripts used in the soil, climatic, and morphometric analyses including any parameters not specified in the methods can be found at https://github.com/ottenlipsmv/lom_pack_anom.

## Results

### Sample Collection

Herbarium specimens and ecological data were collected for a total of 69 populations in flower between April and July of the 2017 field season; twelve populations were revisited later in 2017 and in 2018 to obtain fruiting material. Notable collections included repeat visits to the type specimens of *Lomatium packardiae* and *Lomatium triternatum* var. *triternatum*: *Ottenlips 20* and *Mansfield 16078*, respectively. Forty-eight specimens that represent the morphological, ecological, genetic, and geographic variation of the sub-complex were chosen from material that was collected in the 2017 field season and previously-collected samples from Smith et al. (2018) for inclusion in the target-enrichment NGS methods.

Assembly Summary

Approximately 13% of the reads mapped back to the target genes. An average of 121 genes for each sample were at least 75% the target gene length. Fifty-four introns met the filtering criteria to be included in downstream phylogenetic analysis (Table 1).

Phylogenetic Reconstruction

Concatenated Analysis

The total length of the concatenated alignment was 55,152 characters (Table 2). The two independent runs of MrBayes resulted in trees with identical topologies and ESS values of 7,447 and 7,570, respectively with a combined value of 15,197. All nodes were resolved with > .99 posterior probabilities with the exception of one with a support value of .64 (Fig. 2.2). Clades recovered in the concatenated analysis were mostly congruent with geographic separation and the species tree analyses with multiple notable exceptions, including the placement of three samples from Washington County, Idaho and adjacent Oregon (*Stevens 123, Stevens 121, Ottenlips 57*) , two samples from the foothills Northwest of Boise, Idaho (*Mansfield 16031* and *Mansfield 16033*), one sample from the Salmon River Canyon in Western Idaho (*Ottenlips 69*), four samples from southeastern Oregon and adjacent Idaho (*Ottenlips 25, Ottenlips 32, George 58*), and two samples from Asotin County, Washington (*Ottenlips 76, Ottenlips 77*).

Chloroplast Genomes

The total length of the post-BMGE whole plastid alignment was 150,591 characters (Table 2). Prior to alignment and cleaning by BMGE, the chloroplast genomes were between 153,286 and 153,741 base pairs long. The two runs resulted in identical

topologies with ESS values of 133 and 5135, respectively and a combined value of 198. Figure 2.3 shows the Bayesian consensus tree with branches < .50 PP collapsed.

Species Tree Analyses

The five combined runs of STACEY with a burn-in of 50% for each run had ESS values of 631 for the posterior probability and 779 for the species-tree Coalescent model. All other estimated parameters had ESS values between 230 and 2,500 (https://github.com/ottenlipsmv/lom_pack_anom). The combined STACEY runs resulted in seven moderately to extremely well-supported sub-clades (posterior probabilities = .83 to 1.0; 'Hell's Canyon', 'Mann Creek', one corresponding to the previously recognized *L. packardiae*, 'East-Central Oregon', 'Camas Prairie', 'Western Montana', and one corresponding to the previously recognized *L. triternatum* var. *triternatum*) that agree with the geography and some of the traditionally recognized taxa within this species complex (Figs. 2.4 and 2.5). At a coarser scale, three larger clades ('Northern', 'Southern', and one corresponding to the previously recognized *L. andrusianum*) are evident which split the species complex into northern and southern populations with the exception of the previously recognized *L. andrusianum* found in the Rocky Mountain foothills Northwest of Boise, Idaho which forms its own unique clade.

The ASTRAL-III species tree (Fig. 2.6) was to some degree congruent with the STACEY analysis with lower posterior probabilities for the main topology indicating a high degree of gene tree discordance. The main discrepancies occurred in the larger coarse 'Southern' clade from the STACEY analysis including the placement of 'Andrusianum' within the 'Southern' clade and the inclusion of individual samples from 'Hell's Canyon' within 'East-Central-Oregon'.

## Ecological and Climatic Analysis

### Soils

Principal components 1 and 2 explain 24.3% and 20.9% of the variation in the data, respectively (Fig. 2.7). No clear patterns are evident that agree with the sub-clades distinguished by the STACEY analysis (Figs. 2.6 and 2.7). Collections *Ottenlips 69* and *Ottenlips 72* are outliers and are both found near the Camas Prairie outside Grangeville, Idaho with their placement in the PCA driven primarily by nitrate, total nitrogen, organic matter, and soluble salts content.

### Climate

Principal components 1 and 2 explain 44.05% and 24.86% of the variation in the climatic data, respectively. Two clear clusters are evident in the analysis: the 'Northern' and 'Southern' clades with some overlap in the 'East-Central Oregon' populations (Fig. 2.8).

## Morphological Analyses

### Reproductive Characters

Principal components 1 and 2 explain 41.82% and 24.86% of the variation in the fruit morphology data. The *L. packardiae* populations cluster together all sharing similarities in ray length and fruit size. Other previously recognized taxa, such as *Lomatium andrusianum*, are not evident in our fruit morphology analysis (Fig. 2.10). Appendix F contains the morphological data matrix as averages.

### Vegetative Characters

Most 'Northern' populations have longer and wider leaflets than 'Southern' populations, however there is substantial overlap in length and width primarily in the

clades from Washington County ('Hell's Canyon' and 'Mann Creek'). Most populations from 'Camas Prairie' are separated from all others in the scatterplot of leaflet width versus leaflet lengths distinguished by their longer and wider leaves. (Fig. 2.9) Appendix G contains the average leaflet length and width for each specimen sampled.

## Discussion

The STACEY phylogeny, a Bayesian coalescent-based analysis, performed on 54 introns was the only method to recover clades consistent with external non-molecular data (Figs.2. 4, 2.5, and 2.8). Conflict within the molecular data can be resolved through a comparison of different phylogenetic methodologies with varying assumptions and models. Geography and to some degree morphology and previously recognized taxonomy are the best predictors of phylogenetic position in the STACEY analysis. The observation of conflicting placements of populations in the concatenated nuclear analysis and the chloroplast phylogeny in conjunction with external data sources, such as morphology, life-history, and geography, indicate extensive ILS and stochastic seed dispersal are major factors influencing the evolution of this subcomplex.

The STACEY phylogeny reveals a coarse geographic split between Northern and Southern populations; this split is also observed in the other coalescent-based methodology, ASTRAL-III, but not in the concatenated Bayesian nuclear analysis or the chloroplast phylogeny. This comparison of phylogenetic methods reveals ILS is a major driver of the evolutionary patterns within the subcomplex. Within the larger clades, STACEY uncovers seven finer clades that correspond directly with geography and to some degree morphology and previously recognized taxonomy, such as the recovery of *L. packardiae* as monophyletic with molecular data and distinct with a PCA of reproductive

characters (Fig. 2.10). Neither the ASTRAL-III, concatenated nuclear Bayesian, or chloroplast analysis recognize the fine clades with as little conflict or as much support as the main STACEY topology (Figs. 2.2, 2.3, 2.4, and 2.6). Further, STACEY also distinguishes *L. andrusianum* as separate from the coarse Northern and Southern clades. This distinction is not evident in other analyses, however *L. andrusianum* is highly supported (pp= ~.95) as monophyletic in the ASTRAL-III analysis but is embedded within the coarse Southern clade. The conflicting nuclear and chloroplast genomes in conjunction with external data and coalescent-based methodologies reveal the complex evolutionary history and biology of the *L. packardiae/anomalum* subcomplex.

Reconciling the Chloroplast and Nuclear Phylogenies

While the chloroplast and nuclear genomes of the *L. packardiae/anomalum* species sub-complex are in conflict, they can be reconciled through a comparison of concatenated and coalescent-based phylogenetic reconstruction techniques in conjunction with environmental, geographic, and morphological data. These comparisons allow for the disentanglement of the major factors influencing the evolution of the subcomplex. The whole chloroplast topology uncovers similar clades to those recognized in earlier Sanger-based analyses of primarily plastid regions (Smith et al., 2018). Many of these clades are highly supported, but do not agree with geographic, morphological, or ecological variables (Fig. 2.3). A plastid phylogeny in disagreement with other characters has two basic explanations: there is either ongoing gene-flow through modern seed movement or the stochastic pattern is ancient and derived through prehistoric seed exchange or range contraction/isolation. Many species for which ongoing geneflow through seed movement influences evolution have obvious dispersal mechanisms such as

hooks, sticky trichomes, edibility, or wind-dispersal structures (Nathan et al., 2008). In the *L. packardiae/anomalum* sub-complex, there is little biological evidence to suggest a high degree of modern ongoing seed dispersal (Cronquist, 1992; Cronquist et al., 1997). Other criteria that suggest that gene flow is not ongoing include the chloroplast is inherited as a single locus with no recombination which could cause it to be more severely affected by ILS than nuclear genes. Incomplete lineage sorting is especially prevalent in more recent radiations (Degnan and Rosenburg, 2009). The PENA clade evolved fairly recently, under five million years ago (Banasiak et al., 2013), and this sub-complex is found on long-branches deep within PENA (Smith et al., 2018). Further, many populations occupy sites which are geologically young, such as ash deposits in the Owyhee desert (Cronquist, 1992; Perkins and Nash, 2002). The Bayesian analysis conducted on the whole plastid alignment does not take ILS into account and therefore results must be treated cautiously. Other studies (Soltis et al., 1995; Rautenberg et al., 2010; Albaladejo et al., 2005) have emphasized caution in drawing taxonomic conclusions from the recovery of monophyletic groups in phylogenies derived solely from chloroplast data.

Chloroplast genomes frequently retain a geographic signature that is not reflective of the nuclear phylogeny or previously recognized taxonomy. Rautenberg et al. (2010) described a northeastern and southwestern dichotomy of chloroplast haplotypes that disagrees with nuclear evidence and taxonomy in *Silene* section *Melandrium* found throughout Europe. Albaladejo et al. (2005) observed a similar pattern in *Phlomis* spp. of the Iberian Peninsula. Both concluded that widespread hybridization and backcrossing resulted in these conflicting patterns. While no hybrids have yet to be observed in

*Lomatium* and cannot be ruled out, further studies into breeding systems, reproductive barriers, and potential hybridization are necessary. The genomes of the *L. packardiae/anomalum* sub-complex have a seemingly opposite pattern than that observed in the previously mentioned studies: where nuclear introns reflect geographic structure, but not the chloroplast. Smith et al. (2018) presented a much wider sampling scheme based on predominantly chloroplast regions and showed a general pattern of northeast and southwest geographic separation in the broader *Lomatium triternatum* species complex. Some authors delimit the southwestern members as *Lomatium brevifolium*, occupying southwestern Oregon, Nevada, and California (Hitchcock and Cronquist, 2018). The rest of the complex (including the *L. packardiae/anomalum* subcomplex) occupies the Northeastern part of the range (Idaho, Montana, eastern Washington). However, the chloroplast structure *within* the *L. packardiae/anomalum* sub-complex is seemingly random and not associated with any broad geographic split, previously recognized taxonomy, environmental, or ecological factors.

Range contraction and subsequent isolation can leave a stochastic genetic signature on a chloroplast-based phylogeny creating contrasting patterns in chloroplast and nuclear genomes. Because chloroplasts are haploid, they have smaller effective population sizes that can be more severely affected by genetic drift causing high differentiation between populations and potentially stochastic patterns (Birky et al., 1989). *Pinus cembra* was once widespread throughout eastern Europe and western Asia in the Holocene, but due to climatic shifts is now restricted to isolated high elevation refugia. Chloroplast genes in this pine are more diverse than the nuclear genes and help assign individuals to genetic populations (Lendvay et al., 2014). Other similar studies

(Meng et al., 2015; Wan et al., 2017) have shown that chloroplast haplotypes can be used to group individuals into populations after a severe range contraction. While the geographic structure that consistently assigns individuals to broader populations such as that observed in the nuclear intron-based STACEY analysis is not evident in the chloroplast phylogeny, some local populations in close proximity to each other do form monophyletic groups in the chloroplast phylogeny including, *Lesica 10552* and *Lesica 10541* from western Montana and *Mansfield 16033* and *Mansfield 16031* from the Rocky Mountain foothills outside Boise, Idaho (Fig. 2.3). It is possible that some isolated extant populations from a once wide-ranging species have undergone genetic drift that has resulted in the fixation of alleles creating unique haplotypes only apparent in some adjacent populations. However, our sampling scheme is not dense enough to properly investigate these population-level phenomena.

The lack of broad geographic patterns observed in the chloroplast phylogeny could also be explained by geologic or anthropogenic factors. A possible geological event that could have caused the pattern with the chloroplast genomes is repeated massive flooding caused by the sudden releases of glacial Lake Missoula and the subsequent backflows up the tributaries to the Columbia including the Snake and its tributaries (Bretz, 1925; Denlinger and O'Connell, 2010; Lopes and Mix, 2009). Hooker (2018) hypothesized that flooding caused by glacial lake Missoula has influenced genetic diversity of *Synthyris* species in the channeled scablands of eastern Washington. Another potential explanation is prehistoric seed movement by native peoples. Tubers of many *Lomatium* species including the *Lomatium triternatum* complex are a known food source for native Americans, notably the Sahaptin of the interior Columbia basin (Hunn and

French, 1981), and it is plausible that nomadic tribes brought plants with them from place to place planting them either accidentally or to provide a more widespread food source. Lepofsky and Letzman (2008) reviewed evidence that tribes in the modern-day Northwestern United States and British Columbia strategically managed their plant resources including tuberous vegetables, such as *Camassia* and *Balsamorhiza*. These root vegetables were widely eaten by people that also consumed *Lomatium* tubers (Hunn and French, 1981). Geological events or anthropogenic movement could have potentially caused the random pattern observed in the chloroplast phylogeny.

However, without greater sampling and increased knowledge of the biogeographic history of the PENA clade it is uncertain whether the stochastic nature of the chloroplast phylogeny is the result of gene flow through ongoing dispersal, ancient stochastic migration events facilitated by super-floods, planting by indigenous peoples, or range contraction and isolation caused by habitat fragmentation. The lack of dispersal mechanisms and the nuclear intron evidence suggest the latter two hypotheses are more likely. While the chloroplast genome might help draw conclusions about ancient or ongoing maternal geneflow, it provides little information about current day geneflow through pollen exchange and local seed dispersal that might be causing the broad geographic structuring observed in the introns.

The geographically consistent nuclear intron phylogeny is a stark contrast to the randomly structured chloroplast phylogeny and provides insight into modern-day geneflow likely mediated through pollination and local dispersal. The incongruent placements from the concatenated Bayesian analysis, which do not agree with geographic, morphological, or environmental parameters, are concentrated in Washington

County, Idaho and adjacent Oregon. Some of the individuals sampled from this area contain both narrow leaflets which are suggestive of the morphology predominant in the southern range of the sub-complex and wider leaflets which are more common in the northern range (such as, *Mansfield 7551*). The observation of intermediate morphologies and geography in conjunction with discordance in the nuclear genome implies hybridization between northern and southern individuals. However, there are other incongruent placements of individuals which are not morphological or geographic intermediates (*Mansfield 16031*; *Ottenlips 25*; *George 58*). The incongruent clades from the concatenated Bayesian analysis cluster geographically when using models that take ILS into account (Figs. 2.2 and 2.3). The recovery of monophyletic groups that correspond with geography in the STACEY analysis supports the hypothesis that ILS, not hybridization, is leading to extensive gene tree discordance in the dataset. However, hybridization cannot be ruled out at this time without further study and analysis. Species tree approaches, such as STACEY and ASTRAL-III, first reconstruct the history of individual genes and then build phylogenies with models that incorporate coalescent theory thereby accounting for ILS (Jones, 2014; Zhang et al., 2017). The lack of coalescence seems to be mostly affecting *L. andrusianum*, both clades from Washington County, and *L. packardiae* as evident by the contrasting placements in the concatenated versus species tree topologies. The two species tree methods (ASTRAL-III and STACEY) share a similar dichotomous split between the Northern and Southern clades with the exception of *L. andrusianum* which is included in the Southern clade in ASTRAL-III (Fig 2.6). Additionally, the finer clades recognized by STACEY are not clearly evident in part due to low support across most of the ASTRAL-III phylogeny.

ASTRAL-III generates three support values for each quad-partition surrounding a branch (https://github.com/smirarab/ASTRAL/). While the main topology generally has more support (>.33) than any of the alternatives, the probabilities are not overwhelming (>.95) indicating a high degree of gene tree discordance in the dataset (Fig. 2.6). STACEY incorporates robust Bayesian models which allow for greater flexibility in parameterization than ASTRAL-III (Jones, 2014). Additionally, STACEY was run five independent times from different starting seeds and always converged on the same topology with high support and strong (>200) ESS values. The STACEY analysis was the only phylogenetic reconstruction technique to recognize groups which agreed with geography, environmental variables, and some previously recognized taxonomy. The observation that the incongruent placements in the concatenated Bayesian analysis are resolved with regards to geography and to some degree morphology in the STACEY species tree approach leads to the conclusion that ILS is playing a large role in the evolution of these clades. The contrast between the STACEY analysis, the nuclear concatenation results, and the whole plastome Bayesian reconstruction suggests that the *L. packardiae/anomalum* sub-complex is defined by geographic population structure caused by pollination-mediated geneflow and local seed dispersal with high amounts of ILS and a chloroplast phylogeny with a stochastic history.

Environment and Morphological Variation

A comparison of environmental, morphological, and phylogenetic data reveals that morphologies of some of the clades are genetically determined, while others exhibit morphological variation and potentially plasticity in response to ecological and environmental parameters. The environment of the ‘Northern’ clade has cooler and wetter

temperatures than the ‘Southern’ clade (Fig. 2.8; Appendix E). Most populations found in the north have wide leaflets resembling the traditionally recognized taxa *Lomatium anomalum*. The ‘Southern’ clade’s environment is hotter and drier (Fig. 2.8; Appendix E). Populations found in the south generally have short narrow leaflets and many have been previously circumscribed as *L. packardiae* (Figs. 2.9, 2.11) These environmental factors correspond to the overall genetic structure of the group, but the ‘Southern’ clade is only moderately (STACEY pp = .76) supported as monophyletic (Fig. 2.4). Further, because the environmental factors are correlated with geography it is difficult to fully ascertain whether the morphology of clades found in the north is a plastic response to the environment or genetically derived. However, not all populations in the north share the wide *anomalum*-like leaflet morphology. Individuals from the sub-clade corresponding to *L. triternatum* var. *triternatum*, especially those found in Asotin County, Washington exhibit narrow leaflets more evocative of the previously recognized taxa *L. triternatum* var. *platycarpum* (now recognized as *L. simplex*) and *L. triternatum* var. *triternatum*. Also, individuals from Washington County which are members of the ‘Southern’ clade have wider leaflets in contrast to the more representative squat narrow leaflets from the north. The observation that morphology is not fully associated with environmental parameters or the plastid history suggests that the nuclear genome and local gene flow via pollination and short-distance dispersal plays a large role in shaping the morphologies and possibly the ecological tolerances of the sub-clades. Further evidence to support this hypothesis include observations by Schlessman (1982) that pollination in *Lomatium* is mostly performed by small flies, bees, and beetles with limited ability to transfer pollen long distances. Environmental and genetic factors in conjunction determine the

morphology of individuals within the *L. packardiae/anomalum* sub-complex and their multifaceted interplay has been a primary source of taxonomic confusion.

To summarize, the contrasting chloroplast and nuclear histories indicate stochastic seed dispersal, potentially either through ancient events or ongoing migration. The recovery of geographically separated and occasionally morphologically distinguishable sub-clades with nuclear coalescent-based approaches, but not concatenated analysis indicate that ILS has prevented previous recognition of distinct clades within this sub-complex. A possible explanation is that the clades recovered with the STACEY analysis are the result of incipient speciation, which is cryptic due to the lack of any consistently reliable diagnostic traits besides geography. The comparison between morphological, environmental, and phylogenetic datasets show that local gene flow mediated through small-insect pollination and short-distance dispersion can play a large role in shaping the morphologies of populations within this group. However, phenotypic plasticity in response to differing environmental variables also shapes local morphologies confounding field identification. Until we have sampled more widely within this species complex using the methodology presented in this paper, we hesitate to recognize any new or even existing species boundaries within the *L. anomalum/packardiae* sub-complex. Currently, the best predicter of phylogenetic position is geography.

Efficacy of Introns and Coalescent Theory in Shallow-scale Phylogenetic Analysis

This investigation into the evolutionary history of the *L. packardiae/anomalum* sub-complex is the first study to our knowledge to demonstrate the efficacy of extracting the flanking intronic regions from a target-enrichment approach at shallow species-complex level scales. Authors including the developers of both the wet-lab techniques

(Johnson et al., 2018) and the bioinformatics pipeline (Johnson et al., 2016) have discussed the theoretical practicality of using the highly variable introns at population or species-complex levels, but this study is the first to demonstrate the effectiveness of this approach. Most similar studies at this taxonomic scale utilize presence/absence data including RAD-seq derived SNPs or microsatellites. Examples include investigations into speciation with gene-flow in lake whitefishes with RAD-seq data (Gagnaire et al, 2013) and the creation of a genetic linkage map using microsatellites in the *Mimulus guttatus* species complex (Fishman et al., 2001). However, presence/absence data may not fully account for ILS due to the lack of full sequence data for intact genes. Some methodologies such as SVDQuarterts can model coalescence without intact genes or generating individual gene trees, however simulation studies (Chou et al., 2015) have shown SVDQuartets to be less effective at accurately uncovering species trees than programs which do require individual gene trees, such as ASTRAL-III and STACEY. Coalescent-based methodologies have been shown to outperform concatenated approaches in recovering accurate evolutionary relationships especially at short-time scales where ILS may be more common (Degnan and Rosenburg, 2009). Additionally, coalescent models more accurately represent biological reality, the speciation process, and the genealogical species concept when compared with concatenation by allowing for the possibility that individual gene trees have a different evolutionary history than the species tree and that some genes have coalesced in lineages that are not the most recent common ancestor (Baum and Shaw, 1995). Concatenation of data ignores this biological reality and instead assumes that all genes share the same history. Our sampling scheme of multiple individuals from nearby sometimes adjacent populations allows STACEY to

more accurately estimate the population size parameter of the coalescent-based model. Effective population size is an important parameter that can greatly affect the time it takes for coalescence to occur. ASTRAL-III is not a Bayesian model and is thus unable to estimate this parameter like STACEY. Additionally, no previous studies have demonstrated the use of STACEY with such a large number (54) of loci derived from NGS data due to intense computational demand. Introns contain enough variation to be useful at shallower levels but have the added benefit of being easily incorporated into coalescent based models.

Conclusions

The evolutionary history and morphological variation of the *L. packardiae/anomalum* subcomplex is likely a combination of ancient or ongoing seed dispersal, ILS caused by incipient or recent speciation, phenotypic plasticity in response to ecological parameters, and geographic structuring in the nuclear genome mediated by small-insect pollination and local seed dispersal. Whole plastome, concatenated nuclear, coalescent-based, morphometric, and ecological analyses provide evidence to help understand the evolutionary history and morphological variation. Denser sampling of morphological and environmental parameters should help untangle the role of ecologically determined plasticity, especially in the 'Camas Prairie' and *L. triternatum* var. *triternatum* clades. Further investigations into potential hybridization are also necessary. Bayesian coalescent-based phylogenetic reconstruction techniques performed on introns extracted from target-enrichment NGS protocols were crucial to understanding these recalcitrant taxa, and this technique could be more broadly applied in ongoing and

recent radiations at the species complex and population level in a wide variety of Angiosperm groups.

Descriptions of Clades Recovered in STACEY Analysis

The following is a description of each clade recovered in the STACY analysis and how their distribution, morphological traits, currently recognized taxonomy and evolutionary histories compare (Fig. 2.11).

'Southern'

The 'Southern' clade is recognized in the species tree analysis with moderate support (STACEY pp = .76) but is not evident in the concatenated analysis indicating high amounts of ILS and extensive gene tree discordance (Figs. 2.2 and 2.4). Most individuals and populations in this clade have short squat leaflets akin to the previously recognized *L. packardiae* and *L. tamanitchii*. Some individuals such as those found in both sub-clades from Washington County ('Hell's Canyon' in the northern half of the county and 'Mann Creek' in the southern half) have wider leaflets that more closely resemble the morphology common in the 'Northern' clade. Sometimes this variation exists on the same plant (*Mansfield 7551*), further complicating taxonomic treatment. The environment of the 'Southern' clade is hotter and drier with a longer growing season than the 'Northern' clade. Populations are found throughout Eastern Oregon and adjacent Idaho. This clade is probably not fully sampled and future work should include specimens that are identified as *L. brevifolium* which extends further south into Northern Nevada and California and west into western Washington.

*L. packardiae*

The clade comprising *L. packardiae* is the most compatible with previously recognized taxonomy and contains a revisit (*Ottenlips 20*) to the type locality of *L. packardiae*. This is a surprising result because this clade was not evident in previous Sanger-based studies and its resolution was one of the primary motivations for the research presented here. Additionally, *L. packardiae* is the only clade apparent in the PCA of reproductive characters featuring smaller fruits and shorter umbel rays than other members of the sub-complex. Most populations within this clade have the characteristic squat leaflets with a unique aspect as described in the original circumscription of the taxa (Cronquist, 1992) with some additional variation uncovered here including an increase in leaflet length. However, not all populations that share this morphology are found in this clade; it is restricted to the Owyhee region of Idaho and Oregon with an extension further west near the town of Drewsey, Oregon. The incongruent placements between the STACEY and the concatenated analysis, notably the contrasting placements of populations from the Succor Creek Canyon of southeastern Oregon lead to the conclusion that ILS has played a large role influencing the evolution of the group.

'Mann Creek'

Populations found in this clade have leaflet widths and lengths that are intermediate between the morphologies common to the 'Northern' and 'Southern' clades. The population represented by *Mansfield 16036* is thought to be the closest to the type locality for *L. anomalum* collected by Marcus Jones at Indian Valley in western Idaho. However, the morphology of this clade is not fully compatible with the *L. anomalum* descriptions from the two dominant regional floras: The Flora of the Pacific Northwest

and The Intermountain Flora (Hitchcock and Cronquist, 1973; Cronquist, Holmgren, and Holmgren, 1997). This clade was one of the most problematic in the concatenated analysis and has likely been heavily affected by ILS (Fig. 2.2). The possibility of this clade being of hybrid origin hypothesized by the observation of intermediate morphologies and contrasting nuclear and chloroplast phylogenies merits further investigated.

‘Hell’s Canyon’

The isolation of this clade from ‘Mann Creek’ is a surprising result due to its geographic proximity and morphological similarity. There is no obvious rationale for the split between these two groups. ‘Hell’s Canyon’ shares a similar pattern and history of ILS that is also observed in ‘Mann Creek’. The ‘Hell’s Canyon’ and ‘Mann Creek’ clades are found in northern and southern Washington County, Idaho, respectively.

‘East-Central Oregon’

Two populations in this clade from Franklin Hill near Heppner, Oregon were previously recognized as disjunct populations of *L. tamanitchii* based solely on morphological characteristics (Darrach et al., 2010). Subsequent molecular analysis showed the *L. tamanitchii* lineage did not contain the disjunction in eastern Oregon and the affinity is convergent rather than diagnostic (Smith et al., 2018; George et al., 2014). Otherwise, this analysis was the first to recognize the ‘East-Central Oregon’ clade as distinct. Previous workers have also included these populations with either *L. triternatum* var. *triternatum* or *L. packardiae.* While these populations mostly have the short and narrow *L. packardiae*-type leaflets common in the ‘Southern’ clade, they exist in a climatic niche that is intermediate between the ‘Northern’ clade and the rest of the

‘Southern’ clade. This observation lends further support to the hypothesis that short-distance seed dispersal and pollen mediated gene-flow play a role in shaping the nuclear genomes and local morphologies in this sub-complex.

‘Northern’

The ‘Northern’ clade is highly supported in the STACEY (pp = 1.0) analysis and moderately supported in the ASTRAL-III analysis (pp = 0.75) but is not recovered in the concatenated topology. Incomplete lineage sorting is likely a major factor influencing the evolution of this group. The environment of the ‘Northern’ clade is cooler and wetter (Fig 2.8). Plants generally have longer and wider leaves than the squat narrow leaves more prevalent in the south. However, a wide range of variation exists within the ‘Northern’ clade especially in the ‘Camas Prairie’ and *L. triternatum* var. *triternatum* sub-clades (Fig. 2.11). Because the type population (*Mansfield 16078*; a revisit to the Merriweather Lewis type locality near the confluence of the Potlatch and Clearwater Rivers) is included in this clade and the high support of monophyly, this clade could be circumcised as *L. triternatum* and the local variation treated at the subspecific or varietal level. Further sampling into eastern Montana and Southern Canada could help resolve this group to determine its eastern and northern boundaries.

‘Camas Prairie’

The monophyly of the samples from the Camas Prairie outside Grangeville, Idaho has long been suspected based on preliminary Sanger-sequencing and shared morphology of extremely wide leaflets (Don Mansfield, personal communication; Stevens et al., 2018). The incongruent placement of *Mansfield 16064* and other populations in earlier work (Smith et al., 2018) hindered its recognition until now. In conjunction with the

populations from ‘Western Montana’, these individuals most closely resemble *L. anomalum* as described in Intermountain Flora and Flora of the Pacific Northwest (Hitchcock and Cronquist, 1973; Cronquist, Holmgren, and Holmgren, 1997). However, the type locality in Indian Valley, Idaho of that taxon is not included with this clade. The populations with the widest-leaflets are found in the Camas Prairie while a population with more narrow leaflets is found in the rugged nearby Salmon River Canyon region (*Ottenlips 69*) suggesting that morphological variation or plasticity in response to ecological parameters may be affecting morphologies in this clade (Figs. 2.9, 2.11). *Ottenlips 69* occupies a distinct position in the soils PCA with its placement driven primarily by high nitrogen content (Fig. 2.7). In the climatic analysis, *Ottenlips 69* is also separated from the populations found in the Camas Prairie (Fig. 2.8). More collections and analyses are required to better understand phenotypic plasticity in response to environmental and ecological parameters in this clade.

‘Western Montana’

This clade had been previously recognized as ‘sp. nov. 3’ in Smith et al. (2018)’s investigation into the broader *L. triternatum* species complex. The current study expands this clade’s range into the Idaho panhandle. These plants are similar morphologically to the “Camas Prairie” clade, however the terminal angle formed by the apex of the leaflet is more acute. We have no soil-based ecological data for this clade and limited collections. Further investigations into its range, ecology, and morphology are necessary.

L. triternatum var. triternatum

The type locality (*Mansfield 16078*) of *L. triternatum* var. *triternatum* is included within this clade. A wide range of morphological variation is present including

individuals with long narrow leaflets that are reminiscent of *L. simplex* and squatter leaflets akin to *L. triternatum* var. *triternatum*. All populations in this sub-clade share a similar environment (Fig. 2.8). For populations for which fruiting material is available, individuals key to *L. triternatum* var. *triternatum* based on reproductive characters. However, this similarity is not evident in our PCA of reproductive characters indicating the analysis potentially does not fully measure diagnostic or taxonomically informative traits (Fig 2.10).

'Ottenlips 59'

*Ottenlips 59* is the only individual which is not assigned to a clade in the STACEY analysis (Fig. 2.4). It is geographically closest to the 'Camas Prairie' clade (Fig. 2.5) and most morphologically similar to 'Western Montana'. In addition to the extensive gene tree discordance, high amounts of ILS, and overlapping morphologies, the placement of this population is one of the primary lines of evidence towards incipient or ongoing speciation in this group.

L. andrusianum

*Lomatium andrusianum* was recently described on the basis of characteristic plastid, ecological, geographic, and morphological features (Stevens et al., 2018). The current study recovers this clade as monophyletic with regards to the nuclear genome but does not find evidence that it occupies a distinct ecological niche or has a unique morphology when compared to the rest of the sub-complex (Figs. 2.4, 2.5 ,2.7 ,2.8,2. 9, 2.10, 2.11). However, our sampling scheme was limited in scope (three individuals) compared to the 13 that were sequenced and approximately 80 that were examined morphologically in Stevens et al. (2018). The population (*Ottenlips 60* from the same

population as *Smith 13033*) from Squaw Butte northwest of Boise, Idaho was not part of this clade in earlier Sanger-based studies but had been hypothesized to be a member based on geographic and morphological observations. In the nuclear intron data, it is assigned to the 'Andrusianum' clade for the first time. This clade does not appear to be as affected by chloroplast stochasticity as much as the other clades in the sub-complex the reason for this is unknown.

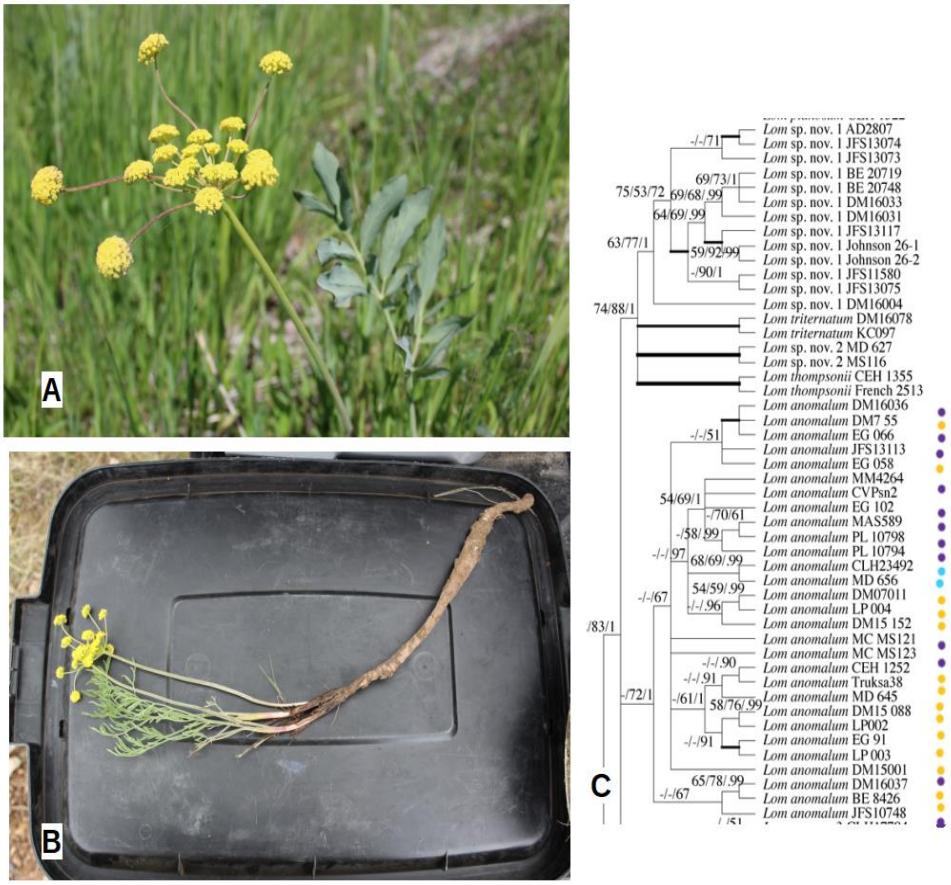


**Figure 2.1. A. Photograph of wider leaflets suggestive of Lomatium anomalum in the field. B. Photograph of the short narrow leaflets suggestive of Lomatium packardiae. C. Sanger-sequence based analysis of L. anomalum/packardiae subcomplex modified from Smith et al. 2018. Support values are MP/ML/BI with 1-point thickened branches representing support values of (>.75/>.75/>.95) and 2-point thickened branches representing support values of (1/1/1). Purple dots correspond to morphology A. Yellow dots correspond to morphology B. Blue dots represent a third morphology of narrow almost linear leaflets, not shown.**

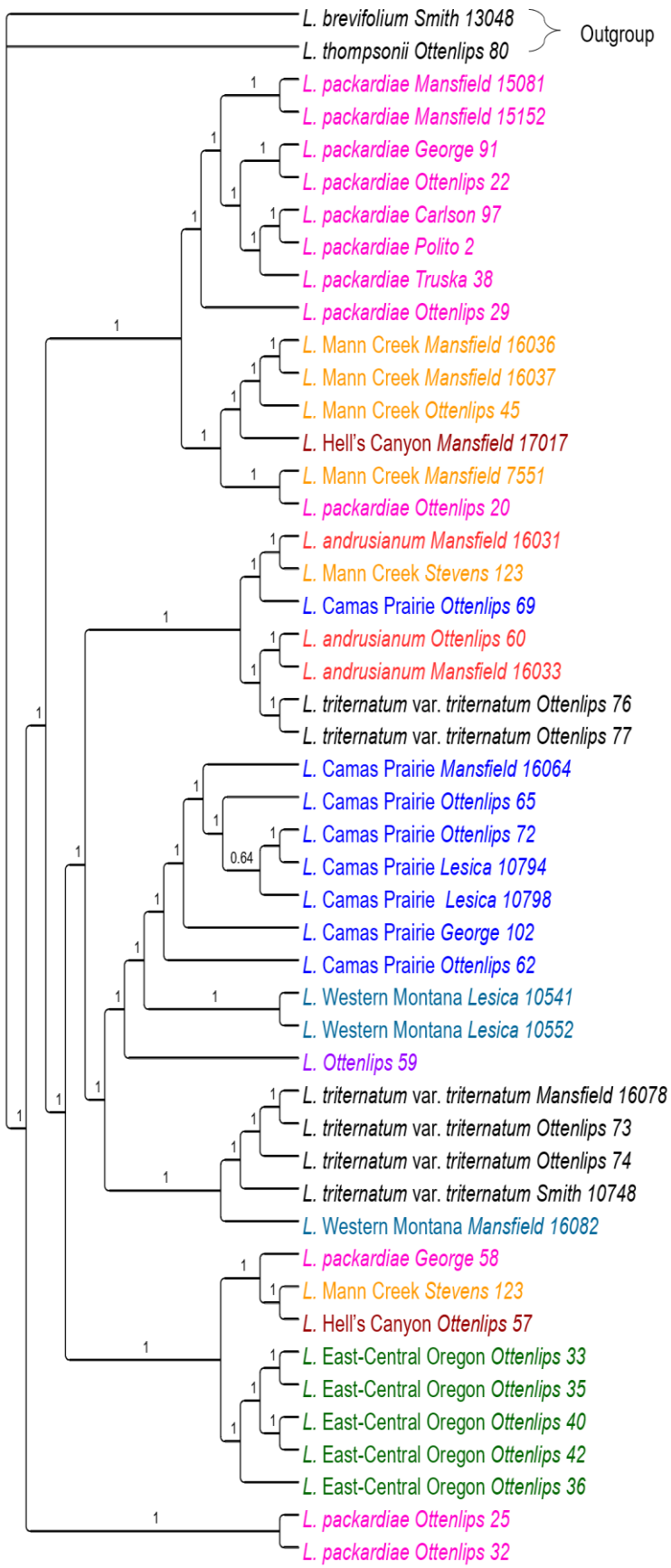
L. brevifolium Smith 13048
L. thompsonii Ottenlips 80
Outgroup
L. packardiae Mansfield 15081
L. packardiae Mansfield 15152
L. packardiae George 91
L. packardiae Ottenlips 22
L. packardiae Carlson 97
L. packardiae Polito 2
L. packardiae Truska 38
L. packardiae Ottenlips 29
L. Mann Creek Mansfield 16036
L. Mann Creek Mansfield 16037
L. Mann Creek Ottenlips 45
L. Hell's Canyon Mansfield 17017
L. Mann Creek Mansfield 7551
L. packardiae Ottenlips 20
L. andrusianum Mansfield 16031
L. Mann Creek Stevens 123
L. Camas Prairie Ottenlips 69
L. andrusianum Ottenlips 60
L. andrusianum Mansfield 16033
L. triternatum var. triternatum Ottenlips 76
L. triternatum var. triternatum Ottenlips 77
L. Camas Prairie Mansfield 16064
L. Camas Prairie Ottenlips 65
L. Camas Prairie Ottenlips 72
L. Camas Prairie Lesica 10794
L. Camas Prairie Lesica 10798
L. Camas Prairie George 102
L. Camas Prairie Ottenlips 62
L. Western Montana Lesica 10541
L. Western Montana Lesica 10552
L. Ottenlips 59
L. triternatum var. triternatum Mansfield 16078
L. triternatum var. triternatum Ottenlips 73
L. triternatum var. triternatum Ottenlips 74
L. triternatum var. triternatum Smith 10748
L. Western Montana Mansfield 16082
L. packardiae George 58
L. Mann Creek Stevens 123
L. Hell's Canyon Ottenlips 57
L. East-Central Oregon Ottenlips 33
L. East-Central Oregon Ottenlips 35
L. East-Central Oregon Ottenlips 40
L. East-Central Oregon Ottenlips 42
L. East-Central Oregon Ottenlips 36
L. packardiae Ottenlips 25
L. packardiae Ottenlips 32
0.64

**Figure 2.2. Bayesian analysis of the concatenated nuclear data set (54 low copy introns). Support values are Bayesian posterior probabilities. Colors correspond to the clades recovered in the STACEY analysis. Pink represents L. packardiae, yellow 'Mann Creek', brown 'Hell's Canyon, green ' East-Central Oregon', blue 'Camas Prairie', black L. triternatum var. triternatum, gray-blue 'Western Montana, and red L. andrusianum.**

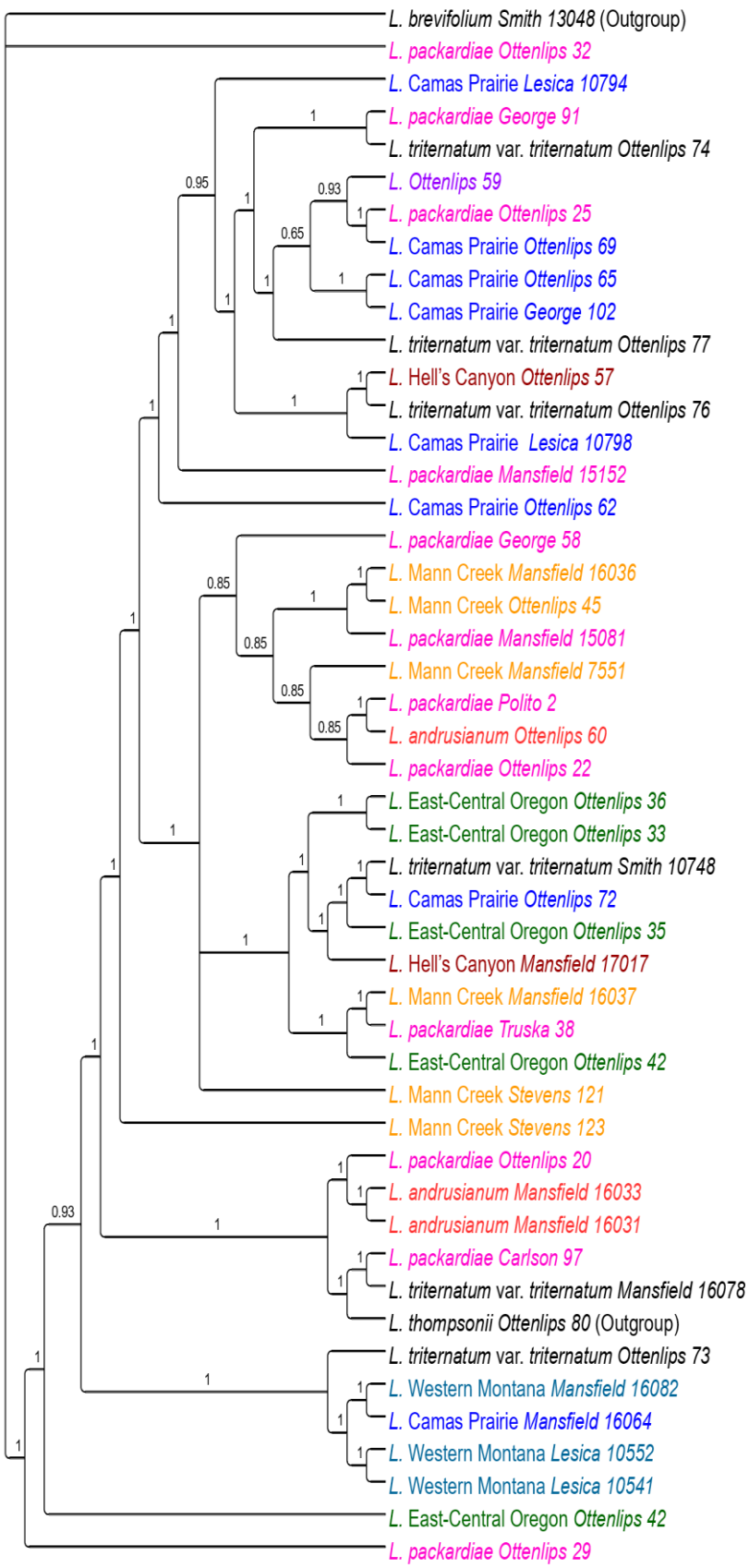
L. brevifolium Smith 13048 (Outgroup)
L. packardiae Ottenlips 32
L. Camas Prairie Lesica 10794
L. packardiae George 91
L. triternatum var. triternatum Ottenlips 74
L. Ottenlips 59
L. packardiae Ottenlips 25
L. Camas Prairie Ottenlips 69
L. Camas Prairie Ottenlips 65
L. Camas Prairie George 102
L. triternatum var. triternatum Ottenlips 77
L. Hell's Canyon Ottenlips 57
L. triternatum var. triternatum Ottenlips 76
L. Camas Prairie Lesica 10798
L. packardiae Mansfield 15152
L. Camas Prairie Ottenlips 62
L. packardiae George 58
L. Mann Creek Mansfield 16036
L. Mann Creek Ottenlips 45
L. packardiae Mansfield 15081
L. Mann Creek Mansfield 7551
L. packardiae Polito 2
L. andrusianum Ottenlips 60
L. packardiae Ottenlips 22
L. East-Central Oregon Ottenlips 36
L. East-Central Oregon Ottenlips 33
L. triternatum var. triternatum Smith 10748
L. Camas Prairie Ottenlips 72
L. East-Central Oregon Ottenlips 35
L. Hell's Canyon Mansfield 17017
L. Mann Creek Mansfield 16037
L. packardiae Truska 38
L. East-Central Oregon Ottenlips 42
L. Mann Creek Stevens 121
L. Mann Creek Stevens 123
L. packardiae Ottenlips 20
L. andrusianum Mansfield 16033
L. andrusianum Mansfield 16031
L. packardiae Carlson 97
L. triternatum var. triternatum Mansfield 16078
L. thompsonii Ottenlips 80 (Outgroup)
L. triternatum var. triternatum Ottenlips 73
L. Western Montana Mansfield 16082
L. Camas Prairie Mansfield 16064
L. Western Montana Lesica 10552
L. Western Montana Lesica 10541
L. East-Central Oregon Ottenlips 42
L. packardiae Ottenlips 29

**Figure 2.3. Bayesian analysis of the chloroplast data set. Support values are Bayesian posterior probabilities. Colors correspond to the clades recovered in the STACEY analysis. Pink represents L. packardiae, yellow 'Mann Creek', brown 'Hell's Canyon, green ' East-Central Oregon', blue 'Camas Prairie', black L. triternatum var. triternatum, gray-blue 'Western Montana, and red L. andrusianum.**

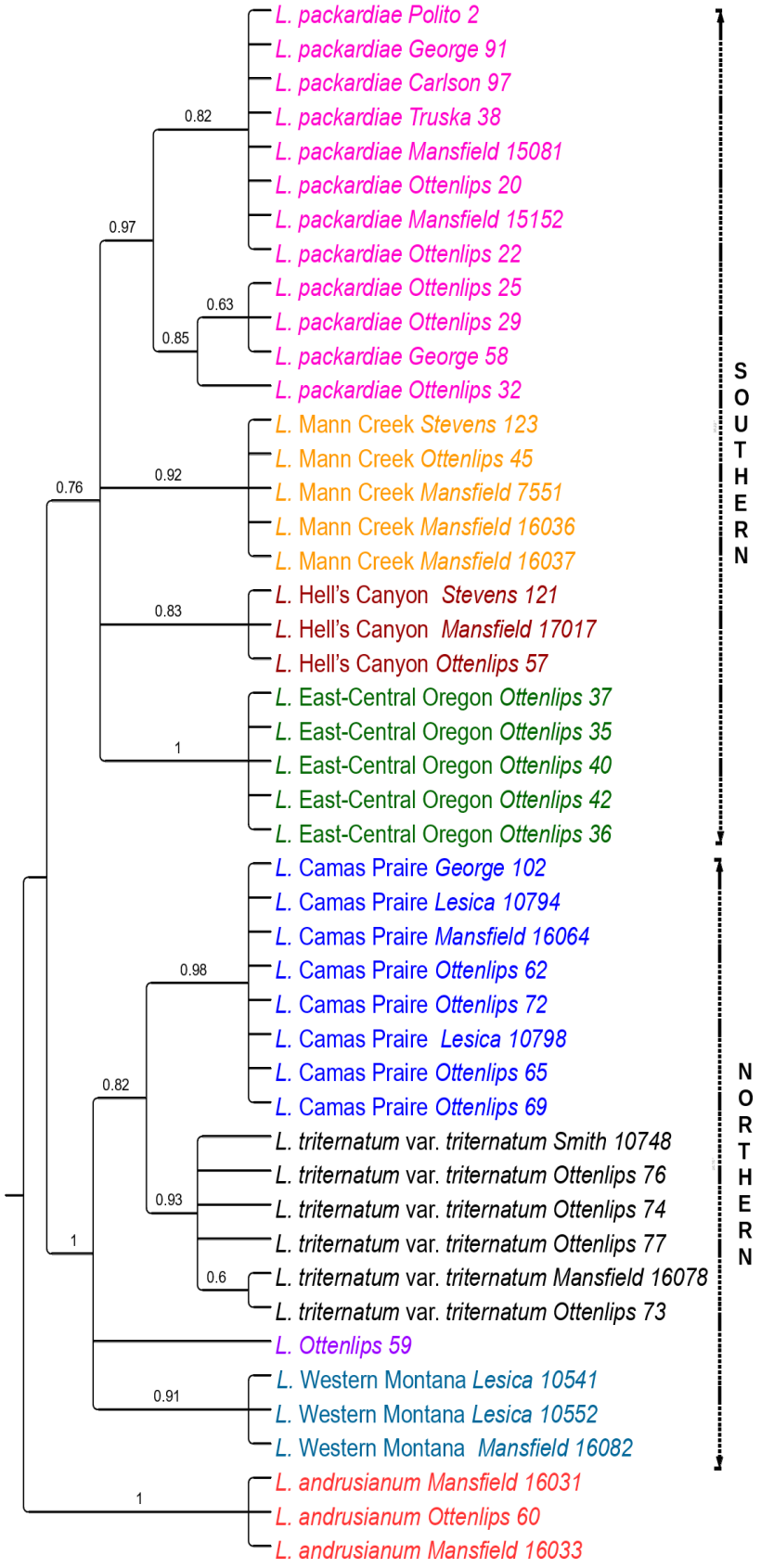
L. packardiae Polito 2
L. packardiae George 91
L. packardiae Carlson 97
L. packardiae Truska 38
L. packardiae Mansfield 15081
L. packardiae Ottenlips 20
L. packardiae Mansfield 15152
L. packardiae Ottenlips 22
L. packardiae Ottenlips 25
L. packardiae Ottenlips 29
L. packardiae George 58
L. packardiae Ottenlips 32
L. Mann Creek Stevens 123
L. Mann Creek Ottenlips 45
L. Mann Creek Mansfield 7551
L. Mann Creek Mansfield 16036
L. Mann Creek Mansfield 16037
L. Hell's Canyon Stevens 121
L. Hell's Canyon Mansfield 17017
L. Hell's Canyon Ottenlips 57
L. East-Central Oregon Ottenlips 37
L. East-Central Oregon Ottenlips 35
L. East-Central Oregon Ottenlips 40
L. East-Central Oregon Ottenlips 42
L. East-Central Oregon Ottenlips 36
L. Camas Praire George 102
L. Camas Praire Lesica 10794
L. Camas Praire Mansfield 16064
L. Camas Praire Ottenlips 62
L. Camas Praire Ottenlips 72
L. Camas Praire Lesica 10798
L. Camas Praire Ottenlips 65
L. Camas Praire Ottenlips 69
L. triternatum var. triternatum Smith 10748
L. triternatum var. triternatum Ottenlips 76
L. triternatum var. triternatum Ottenlips 74
L. triternatum var. triternatum Ottenlips 77
L. triternatum var. triternatum Mansfield 16078
L. triternatum var. triternatum Ottenlips 73
L. Ottenlips 59
L. Western Montana Lesica 10541
L. Western Montana Lesica 10552
L. Western Montana Mansfield 16082
L. andrusianum Mansfield 16031
L. andrusianum Ottenlips 60
L. andrusianum Mansfield 16033
0.82
0.97
0.63
0.85
0.92
0.76
0.83
1
0.98
0.82
0.93
1
0.6
0.91
1
SOUTHERN
NORTHERN

**Figure 2.4. STACEY analysis of 54 introns. Colors correspond to clades described in the discussion and the morphological and climatic analyses. Support values are posterior probabilities. Values under .50 are collapsed into polytomies. The tree is manually rooted on L. andrusianum. Pink represents L. packardiae, yellow 'Mann Creek', brown 'Hell's Canyon, green ' East-Central Oregon', blue 'Camas Prairie', black L. triternatum var. triternatum, gray-blue 'Western Montana, and red L. andrusianum. Th red dots indicate the taxa with incongruent placements in the concatenated Bayesian analysis which agree with geography in the STACEY analysis.**

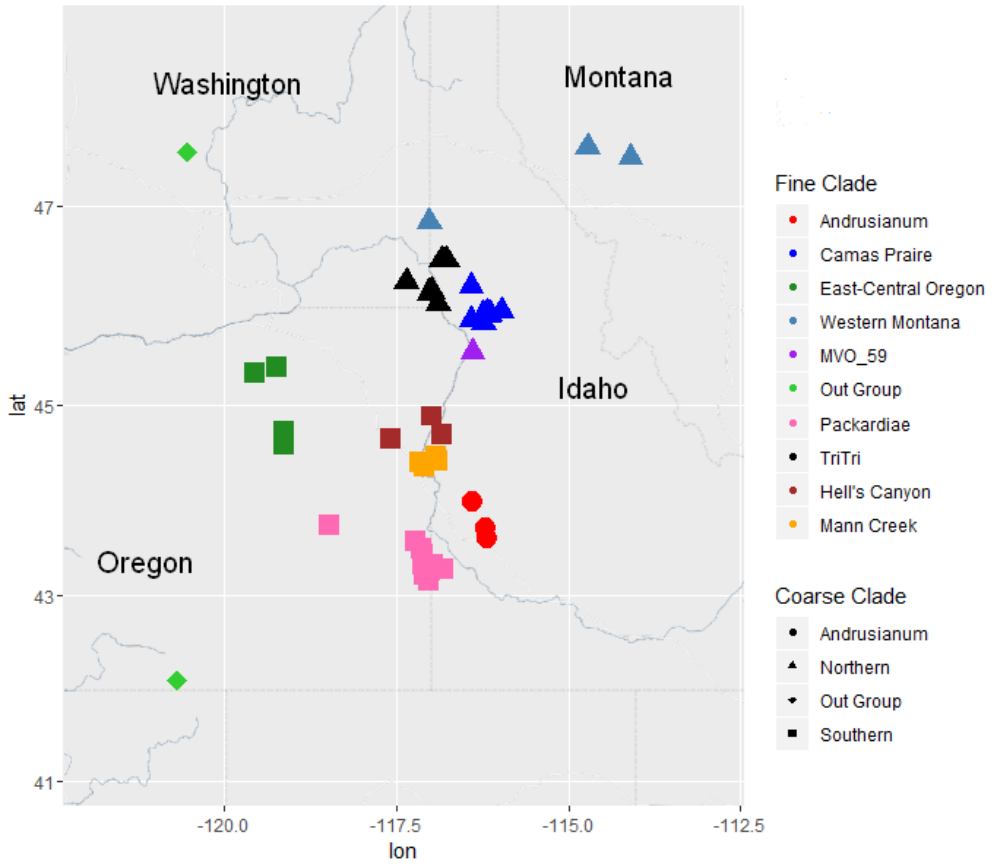


**Figure 2.5. Map depicting locations of the samples and the associated clades uncovered in the STACEY analysis. Outgroups (Ottenlips 80; Smith 13048) from the concatenated BI, chloroplast BI, and ASTRAL analyses are included as light green diamonds. The broader STACEY clades are represented by shapes (Circle for 'Andrusianum'; triangle for 'Northern'; and square for 'Southern'). The finer STACEY clades are color coded(Pink represents L. packardiae, yellow 'Mann Creek', brown 'Hell's Canyon, green ' East-Central Oregon', blue 'Camas Prairie', black L. triternatum var. triternatum, gray-blue 'Western Montana, and red L. andrusianum).**

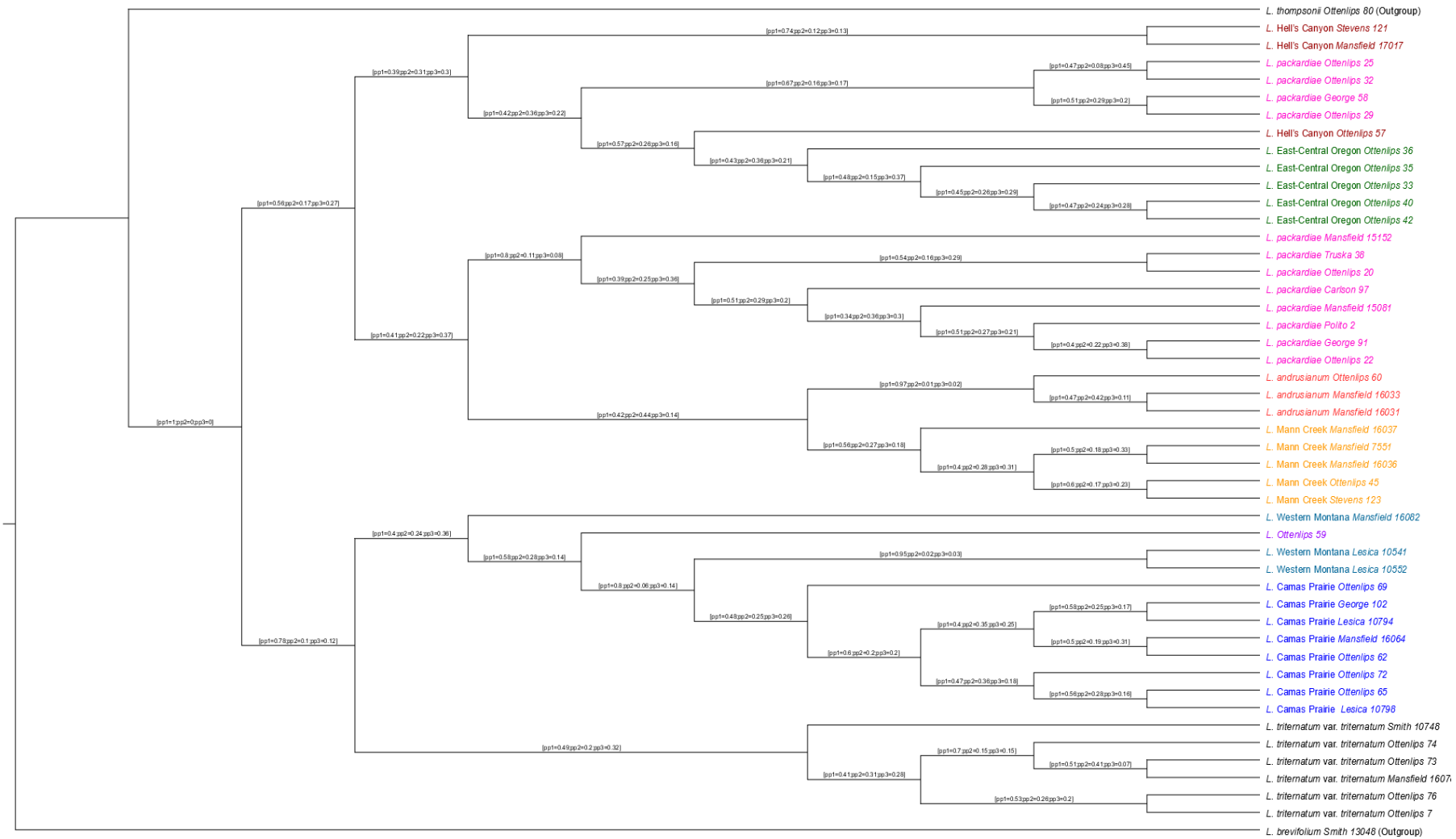
L. thompsonii Ottenlips 80 (Outgroup)
L. Hell's Canyon Stevens 121
L. Hell's Canyon Mansfield 17017
L. packardiae Ottenlips 25
L. packardiae Ottenlips 32
L. packardiae George 58
L. packardiae Ottenlips 29
L. Hell's Canyon Ottenlips 57
L. East-Central Oregon Ottenlips 36
L. East-Central Oregon Ottenlips 35
L. East-Central Oregon Ottenlips 33
L. East-Central Oregon Ottenlips 40
L. East-Central Oregon Ottenlips 42
L. packardiae Mansfield 15152
L. packardiae Truska 38
L. packardiae Ottenlips 20
L. packardiae Carlson 97
L. packardiae Mansfield 15081
L. packardiae Polito 2
L. packardiae George 91
L. packardiae Ottenlips 22
L. andrusianum Ottenlips 60
L. andrusianum Mansfield 16033
L. andrusianum Mansfield 16031
L. Mann Creek Mansfield 16037
L. Mann Creek Mansfield 7551
L. Mann Creek Mansfield 16036
L. Mann Creek Ottenlips 45
L. Mann Creek Stevens 123
L. Western Montana Mansfield 16062
L. Ottenlips 59
L. Western Montana Lesica 10541
L. Western Montana Lesica 10552
L. Camas Prairie Ottenlips 69
L. Camas Prairie George 102
L. Camas Prairie Lesica 10794
L. Camas Prairie Mansfield 16064
L. Camas Prairie Ottenlips 62
L. Camas Prairie Ottenlips 72
L. Camas Prairie Ottenlips 65
L. Camas Prairie Lesica 10798
L. triternatum var. triternatum Smith 10748
L. triternatum var. triternatum Ottenlips 74
L. triternatum var. triternatum Ottenlips 73
L. triternatum var. triternatum Mansfield 1607
L. triternatum var. triternatum Ottenlips 76
L. triternatum var. triternatum Ottenlips 7
L. brevifolium Smith 13048 (Outgroup)

**Figure 2.6. ASTRAL species tree depicting the relationships between the samples. The three support values on each branch are for the quad partition and show three posterior probabilities for each node: one value for the main topology, one value for probability the clade belongs to the sister group, and one value for the probability that the clade belongs to the outgroup. Colors correspond to the clades recovered in the STACEY analysis. Pink represents L. packardiae, yellow 'Mann Creek', brown 'Hell's Canyon, green ' East-Central Oregon', blue 'Camas Prairie', black L. triternatum var. triternatum, gray-blue 'Western Montana, and red L. andrusianum.**

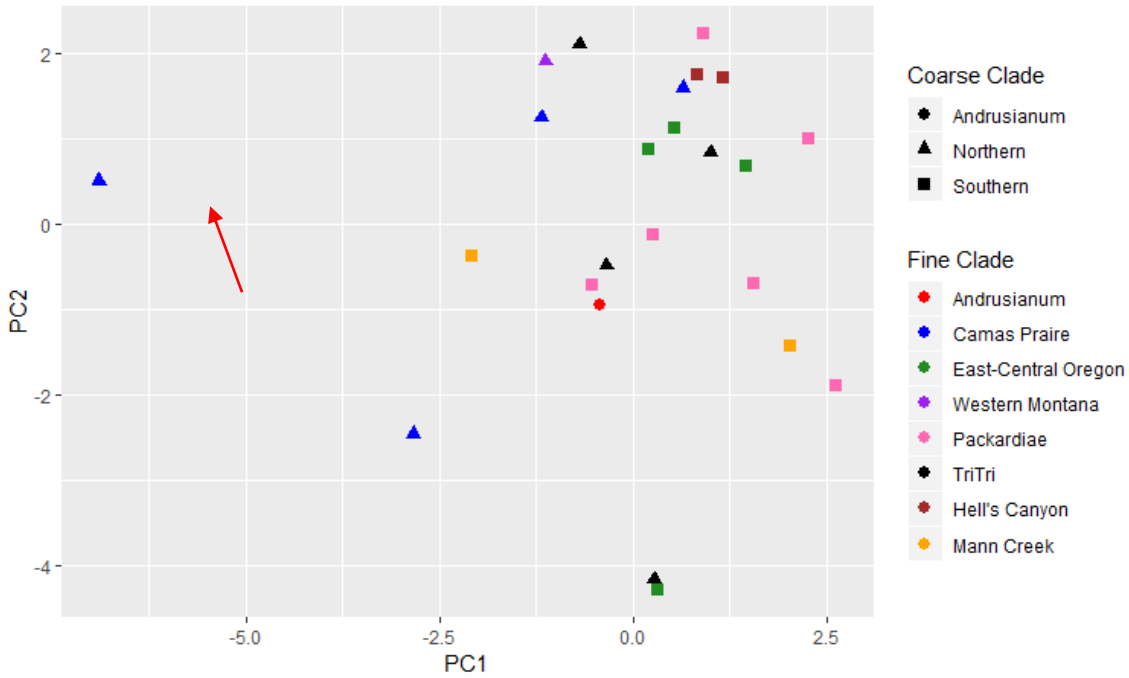


**Figure 2.7. Principal components analysis of soil data. Principal components analysis of averaged, centered, and scaled soil physical and chemical characteristics. The broader STACEY clades are represented by shapes (Circle for 'Andrusianum'; triangle for 'Northern'; and square for 'Southern'). The finer STACEY clades are color coded(Pink represents L. packardiae, yellow 'Mann Creek', brown 'Hell's Canyon, green ' East-Central Oregon', blue 'Camas Prairie', black L. triternatum var. triternatum, gray-blue 'Western Montana, and red L. andrusianum). The red arrow indicates Ottenlips 69in an anomalous position with its placement primarily driven by nitrate and nitrogen content**

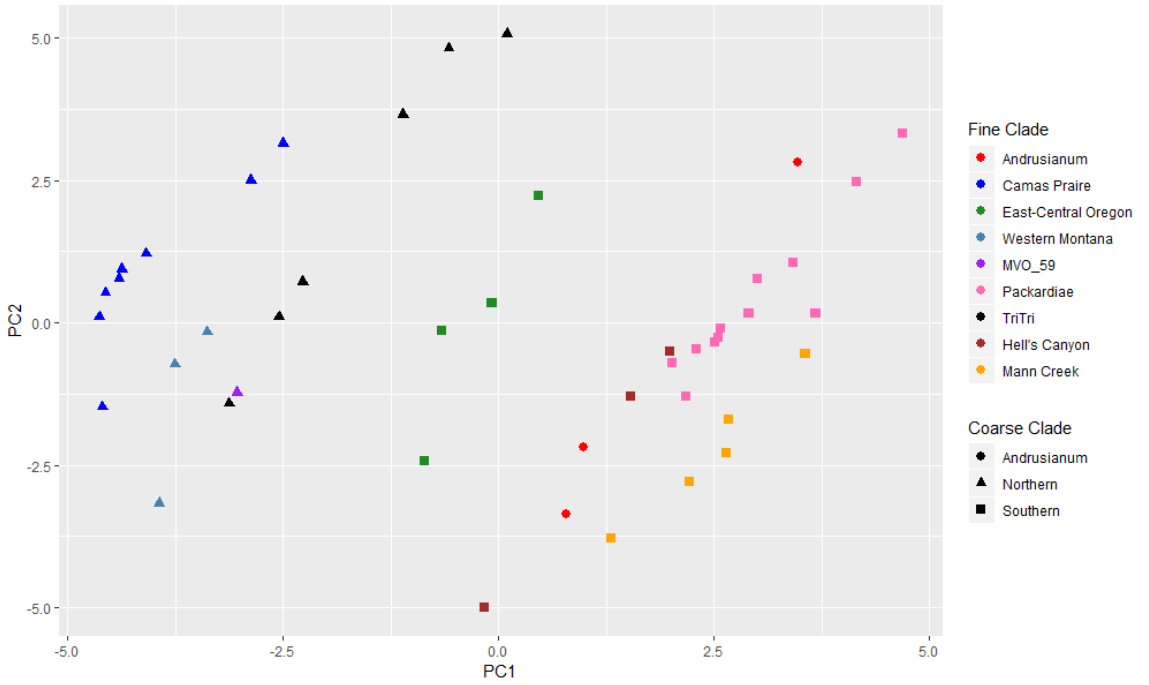


**Figure 2.8. Principal components analysis on 19 centered and scaled bioclimatic variables extracted at 30 arcsecond resolution. The broader STACEY clades are represented by shapes (Circle for 'Andrusianum'; triangle for 'Northern'; and square for 'Southern'). The finer STACEY clades are color coded(Pink represents L. packardiae, yellow 'Mann Creek', brown 'Hell's Canyon, green ' East-Central Oregon', blue 'Camas Prairie', black L. triternatum var. triternatum, gray-blue 'Western Montana, and red L. andrusianum).**

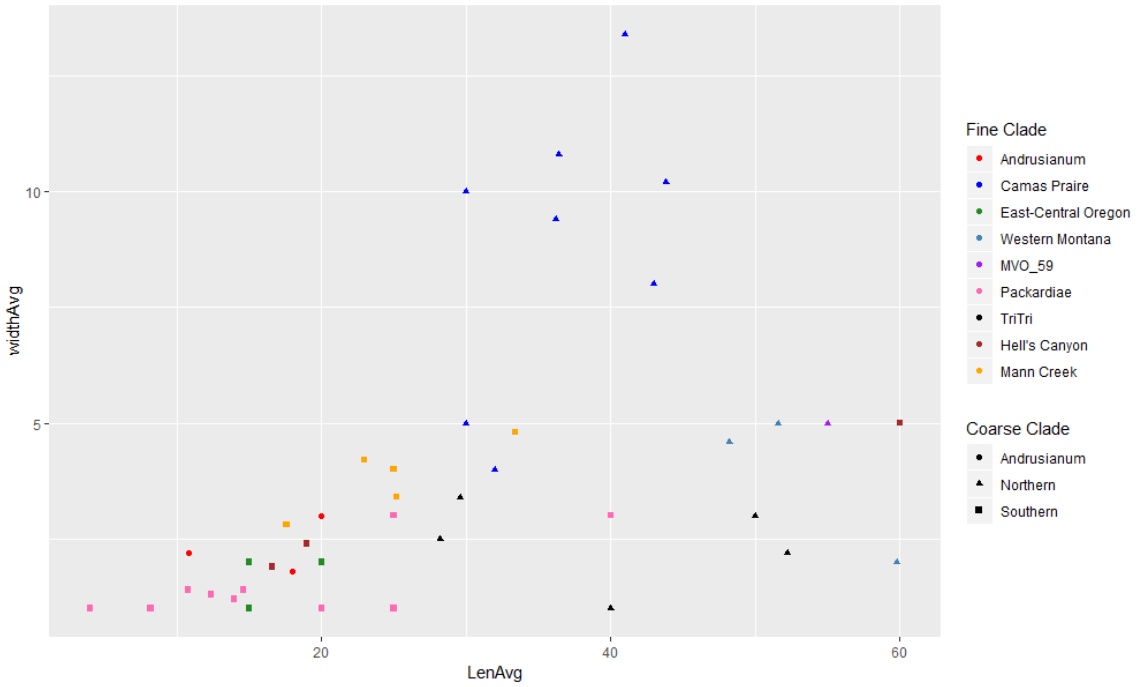


**Figure 2.9. Scatterplot depicting the average leaflet lengths and widths organized by the clades uncovered in the STACEY analysis. The broader STACEY clades are represented by shapes (Circle for 'Andrusianum'; triangle for 'Northern'; and square for 'Southern'). The finer STACEY clades are color coded(Pink represents L. packardiae, yellow 'Mann Creek', brown 'Hell's Canyon, green ' East-Central Oregon', blue 'Camas Prairie', black L. triternatum var. triternatum, gray-blue 'Western Montana, and red L. andrusianum).**

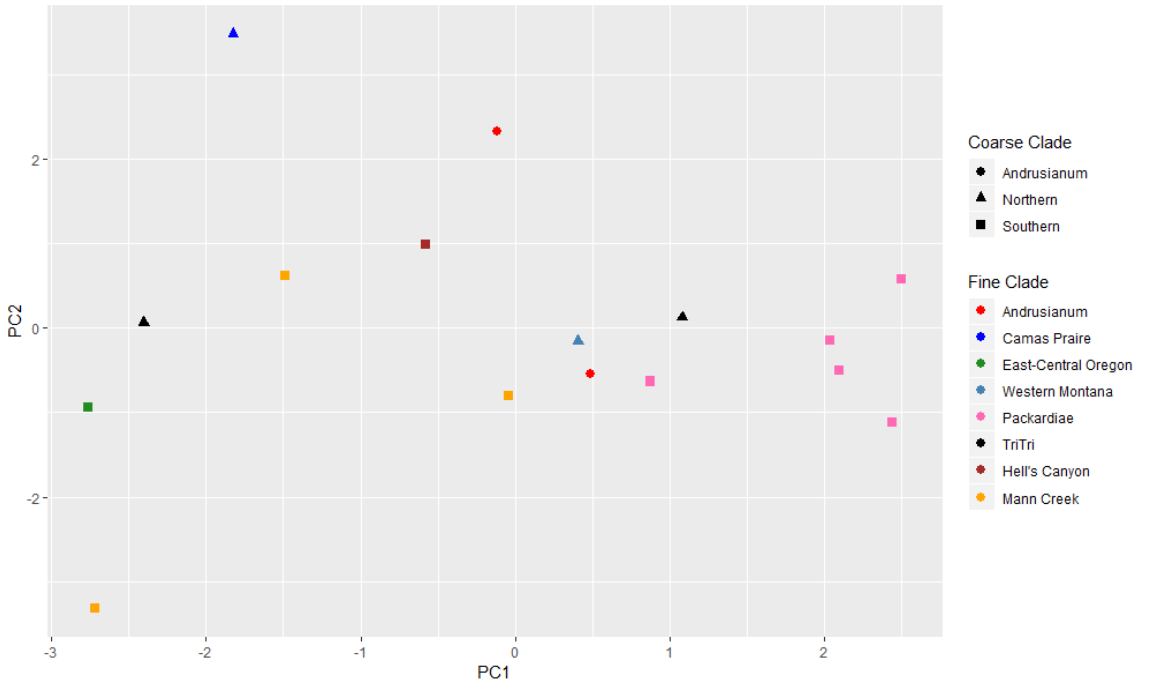


**Figure 2.10. Principal components analysis of eight centered and scaled means of reproductive characters (ray length; mature fruit length; mature fruit width; mature pedicel length; length of primary umbel; width of primary umbel; wing width; fruit length). The broader STACEY clades are represented by shapes (Circle for 'Andrusianum'; triangle for 'Northern'; and square for 'Southern'). The finer STACEY clades are color coded(Pink represents L. packardiae, yellow 'Mann Creek', brown 'Hell's Canyon, green ' East-Central Oregon', blue 'Camas Prairie', black L. triternatum var. triternatum, gray-blue 'Western Montana, and red L. andrusianum)**


**Figure 2.11 Representative digitized herbarium specimens of the clades uncovered in the STACEY analysis. The coarse clades are labeled with the 'Northern' clade on the top row and the 'Southern' clade on the bottom row. L. andrusianum is set off to the far right. A represents 'Camas Prairie' (Ottenlips 62); B represents Lomatium triternatum var. triternatum (Ottenlips 77); C represents Ottenlips 59; D represents 'Western Montana' (Lesica 10541); E represents L. packardiae (Ottenlips 22); F represents 'Mann Creek' (Ottenlips 45); G represents 'Hell's Canyon (Ottenlips 57); H represents 'East-Central Oregon' (Ottenlips 40); I represents L. andrusianum (Mansfield 16031).**

**Table 2.1 Assembly statistics of the 54 introns. Gene number refers to the unique identifier associated with the Angiosperm 353 bait kit target file.**

| Gene number | Alignment length | Missing percent | Percent parsimony informative | Percent variable sites | GC content (percentage) |
|---|---|---|---|---|---|
| 4848 | 729 | 6.076 | 2.5 | 15.2 | 36.3 |
| 4932 | 717 | 3.879 | 2.4 | 8.2 | 31.6 |
| 4992 | 1083 | 5.711 | 5.1 | 15.1 | 32.3 |
| 5116 | 1304 | 6.538 | 19.2 | 23.4 | 32.6 |
| 5271 | 550 | 3.545 | 2.7 | 9.6 | 32.6 |
| 5326 | 439 | 7.422 | 7.5 | 20 | 36 |
| 5333 | 272 | 3.676 | 9.2 | 22.4 | 41.1 |
| 5404 | 727 | 4.149 | 5.1 | 20.1 | 30.7 |
| 5406 | 2890 | 8.284 | 4.9 | 16.7 | 32.1 |
| 5426 | 2661 | 4.129 | 8.9 | 23.6 | 34.8 |
| 5428 | 350 | 6.464 | 2.6 | 13.1 | 44.1 |
| 5464 | 1050 | 6.21 | 2.9 | 16 | 32.4 |
| 5599 | 847 | 7.684 | 5.1 | 20.5 | 36.3 |
| 5614 | 1921 | 5.09 | 4.6 | 23.5 | 33.8 |
| 5639 | 931 | 4.265 | 4 | 13.1 | 32.5 |
| 5664 | 1271 | 3.696 | 8.5 | 16.8 | 33.1 |
| 5822 | 2728 | 7.396 | 3 | 14.4 | 33.9 |
| 5840 | 1250 | 7.793 | 14.3 | 22.7 | 31.3 |
| 5857 | 630 | 6.515 | 2.4 | 18.9 | 37.1 |
| 5899 | 1197 | 8.116 | 9.4 | 23.6 | 33 |
| 5910 | 849 | 6.287 | 9.8 | 20.5 | 41.7 |
| 5913 | 513 | 5.389 | 4.1 | 21.2 | 32.1 |
| 5922 | 2805 | 6.776 | 5.6 | 18.1 | 32.6 |
| 5926 | 545 | 3.437 | 10.1 | 23.5 | 30.9 |
| 5944 | 913 | 1.855 | 1.1 | 13.8 | 33.8 |
| 5974 | 678 | 3.478 | 7.1 | 20.2 | 30.5 |

| | | | | | |
|---|---|---|---|---|---|
| 6026 | 1483 | 5.025 | 7.1 | 16.9 | 32.8 |
| 6041 | 1794 | 4.182 | 11.1 | 24 | 33.6 |
| 6098 | 936 | 4.868 | 7.5 | 18.8 | 32.2 |
| 6295 | 920 | 4.558 | 12.1 | 21.3 | 36.2 |
| 6298 | 616 | 4.522 | 2.9 | 8.6 | 29.9 |
| 6303 | 592 | 3.47 | 7.9 | 24.2 | 30.7 |
| 6366 | 549 | 2.668 | 3.3 | 18.2 | 37.6 |
| 6383 | 808 | 8.97 | 7.8 | 18.8 | 31.7 |
| 6401 | 453 | 3.78 | 3.3 | 14.3 | 34.4 |
| 6406 | 470 | 5.811 | 7.9 | 16.2 | 34.6 |
| 6420 | 1128 | 5.633 | 4 | 13.2 | 32.2 |
| 6450 | 1563 | 6.934 | 6.3 | 18.2 | 32.3 |
| 6460 | 456 | 2.677 | 5.3 | 13.2 | 33.1 |
| 6462 | 1311 | 5.818 | 7 | 24.5 | 31.1 |
| 6494 | 1028 | 3.654 | 8.3 | 18 | 34.4 |
| 6500 | 1459 | 2.659 | 4.9 | 22.3 | 30.7 |
| 6639 | 467 | 2.953 | 7.5 | 18 | 27.1 |
| 6641 | 422 | 4.448 | 9 | 17.8 | 34.2 |
| 6689 | 1294 | 5.422 | 3.5 | 15.8 | 31.9 |
| 6947 | 1568 | 2.473 | 7 | 11.4 | 33.3 |
| 6992 | 557 | 2.528 | 4.1 | 17.8 | 31.1 |
| 7141 | 489 | 4.192 | 6.7 | 23.1 | 32.6 |
| 7174 | 1258 | 9.802 | 2.9 | 14.5 | 33 |
| 7313 | 982 | 5.075 | 6.7 | 22.8 | 33.3 |
| 7324 | 1111 | 3.863 | 8.2 | 16.3 | 33.4 |
| 7333 | 439 | 4.504 | 5.7 | 19.6 | 52.8 |
| 7572 | 430 | 5.15 | 3.7 | 16.5 | 35.4 |
| 7602 | 689 | 4.399 | 8.9 | 15.5 | 35.5 |

**Table 2.2 MrBayes analysis assembly statistics.**

| Alignment name | Alignment length | Missing percent | Percent variable sites | Percent parsimony informative | GC content |
|---|---|---|---|---|---|
| Chloroplast | 150,591 | 1.786 | 6 | 16 | 37.6 |
| Concatenated Introns | 57,596 | 5.361 | 18.3 | 6.7 | 33.4 |

## Works Cited

Albaladejo, R. G., Aguilar, J. F., Aparicio, A., & Feliner, G. N. (2005). Contrasting nuclear-plastidial phylogenetic patterns in the recently diverged Iberian Phlomis crinita and P. lychnitis lineages (Lamiaceae). *Taxon*, *54*(4), 987-998.

Andrews, S. (2010). FastQC: a quality control tool for high throughput sequence data.

Banasiak, Ł., Piwczyński, M., Uliński, T., Downie, S. R., Watson, M. F., Shakya, B., & Spalik, K. (2013). Dispersal patterns in space and time: a case study of Apiaceae subfamily Apioideae. *Journal of Biogeography*, *40*(7), 1324-1335.

Bankevich, A., Nurk, S., Antipov, D., Gurevich, A. A., Dvorkin, M., Kulikov, A. S., ... & Pyshkin, A. V. (2012). SPAdes: a new genome assembly algorithm and its applications to single-cell sequencing. *Journal of computational biology*, *19*(5), 455-477.

Baum, D. A., & Shaw, K. L. (1995). Genealogical perspectives on the species problem. *Experimental and molecular approaches to plant biosystematics*, *53*(289-303), 123-124.

Bickford, D., Lohman, D. J., Sodhi, N. S., Ng, P. K., Meier, R., Winker, K., ... & Das, I. (2007). Cryptic species as a window on diversity and conservation. *Trends in ecology & evolution*, 22(3), 148-155.

Birky, C. W., Fuerst, P., & Maruyama, T. (1989). Organelle gene diversity under migration, mutation, and drift: equilibrium expectations, approach to equilibrium, effects of heteroplasmic cells, and comparison to nuclear genes. *Genetics*, 121(3), 613-627.

Bogarín, D., Pérez-Escobar, O. A., Groenenberg, D., Holland, S. D., Karremans, A. P., Lemmon, E. M., ... & Gravendeel, B. (2018). Anchored hybrid enrichment generated nuclear, plastid and mitochondrial markers resolve the Lepanthes horrida (Orchidaceae: Pleurothallidinae) species complex. *Molecular phylogenetics and evolution*, *129*, 27-47.

Bolger, A. M., Lohse, M., & Usadel, B. (2014). Trimmomatic: a flexible trimmer for Illumina sequence data. *Bioinformatics*, *30*(15), 2114-2120.

Borowiec, M. L. (2016). AMAS: a fast tool for alignment manipulation and computing of summary statistics. *PeerJ*, *4*, e1660.

Bouckaert, R., Heled, J., Kühnert, D., Vaughan, T., Wu, C. H., Xie, D., ... & Drummond, A. J. (2014). BEAST 2: a software platform for Bayesian evolutionary analysis. *PLoS computational biology*, *10*(4), e1003537.

Bouyoucos, G. J. (1962). Hydrometer method improved for making particle size analyses of soils 1. *Agronomy journal*, *54*(5), 464-465.

Bretz, J. H. (1925). The Spokane flood beyond the channeled scablands. The Journal of *Geology*, 33(2), 97-115.

Burger, W. C. (1975). The species concept in Quercus. *Taxon*, 45-50

Chevreux, B. (2007). MIRA: an automated genome and EST assembler.

Chou, J., Gupta, A., Yaduvanshi, S., Davidson, R., Nute, M., Mirarab, S., & Warnow, T. (2015). A comparative study of SVDquartets and other coalescent-based species tree estimation methods. *BMC genomics*, *16*(10), S2.

Cook, J. E., & Halpern, C. B. (2018). Vegetation changes in blown-down and scorched forests 10–26 years after the eruption of Mount St. Helens, Washington, USA. *Plant Ecology*, *219*(8), 957-972.

Cordell, S., Goldstein, G., Mueller-Dombois, D., Webb, D., & Vitousek, P. M. (1998). Physiological and morphological variation in Metrosideros polymorpha, a dominant Hawaiian tree species, along an altitudinal gradient: the role of phenotypic plasticity. *Oecologia*, *113*(2), 188-196.

Criscuolo, A., & Gribaldo, S. (2010). BMGE (Block Mapping and Gathering with Entropy): a new software for selection of phylogenetic informative regions from multiple sequence alignments. *BMC evolutionary biology*, *10*(1), 210.

Cronquist, A. (1992). Nomenclatural innovations in Intermountain Rosidae. *The Great Basin Naturalist*, 75-77.

Cronquist, A. J., Holmgren, N. H., & Holmgren, P. K. (1997). Intermountain flora: Vascular plants of the intermountain west, USA Volume three, part A, subclass Rosidae (except Fabales). *New York: New York Botanical Garden 446p-illus.. ISBN*, *893273759*.

Crowl, A. A., Myers, C., & Cellinese, N. (2017). Embracing discordance: Phylogenomic analyses provide evidence for allopolyploidy leading to cryptic diversity in a Mediterranean Campanula (Campanulaceae) clade. *Evolution*, *71*(4), 913-922.

Darriba, D., Taboada, G. L., Doallo, R., & Posada, D. (2012). jModelTest 2: more models, new heuristics and parallel computing. *Nature methods*, *9*(8), 772.

Darrach, M., Thie, K. K., Wilson, B. L., Brainerd, R. E., & Otting, N. (2010). Lomatium tamanitchii (Apiaceae) a new species from Oregon and Washington state, USA. *Madroño*, 203-208.

Darwin, C. (1862). On the various contrivances by which British and foreign orchids are fertilised by insects: and on the good effects of intercrossing. London: J. Murray.

Davey, J. W., & Blaxter, M. L. (2010). RADSeq: next-generation population genetics. *Briefings in functional genomics*, *9*(5-6), 416-423.

Degnan, J. H., & Rosenberg, N. A. (2009). Gene tree discordance, phylogenetic inference and the multispecies coalescent. *Trends in ecology & evolution*, *24*(6), 332-340.

Denlinger, R. P., & O'Connell, D. R. H. (2010). Simulations of cataclysmic outburst floods from Pleistocene Glacial Lake Missoula. *Bulletin*, *122*(5-6), 678-689.

Eaton, D. A., Hipp, A. L., González-Rodríguez, A., & Cavender-Bares, J. (2015). Historical introgression among the American live oaks and the comparative nature of tests for introgression. *Evolution*, *69*(10), 2587-2601.

Faircloth, B. C., Branstetter, M. G., White, N. D., & Brady, S. G. (2015). Target enrichment of ultraconserved elements from arthropods provides a genomic perspective on relationships among H ymenoptera. *Molecular Ecology Resources*, *15*(3), 489-501.

Feist, M. A. E., Smith, J. F., Mansfield, D. H., Darrach, M., Mcneill, R. P., Downie, S. R., ... & Wilson, B. L. (2017). New combinations in *Lomatium* (Apiaceae, Subfamily Apioideae). *Phytotaxa*, *316*(1), 95-98.

Fick, S.E. and R.J. Hijmans, 2017. Worldclim 2: New 1-km spatial resolution climate surfaces for global land areas. *International Journal of Climatology*

Fishman, L., Kelly, A. J., Morgan, E., & Willis, J. H. (2001). A genetic map in the Mimulus guttatus species complex reveals transmission ratio distortion due to heterospecific interactions. *Genetics*, *159*(4), 1701-1716.

Gagnaire, P. A., Pavey, S. A., Normandeau, E., & Bernatchez, L. (2013). The genetic architecture of reproductive isolation during speciation-with-gene-flow in lake whitefish species pairs assessed by RAD sequencing. *Evolution*, *67*(9), 2483-2497.

George, E. E., Mansfield, D. H., Smith, J. F., Hartman, R. L., Downie, S. R., & Hinchliff, C. E. (2014). Phylogenetic analysis reveals multiple cases of morphological parallelism and taxonomic polyphyly in Lomatium (Apiaceae). *Systematic Botany*, *39*(2), 662-675.

Gernandt, D. S., Aguirre Dugua, X., Vázquez-Lobo, A., Willyard, A., Moreno Letelier, A., Pérez de la Rosa, J. A., ... & Liston, A. (2018). Multi-locus phylogenetics, lineage sorting, and reticulation in Pinus subsection Australes. *American journal of botany*, *105*(4), 711-725.

Hahn, C., Bachmann, L., & Chevreux, B. (2013). Reconstructing mitochondrial genomes directly from genomic next-generation sequencing reads—a baiting and iterative mapping approach. *Nucleic acids research*, *41*(13), e129-e129.

Hebert, P. D., Penton, E. H., Burns, J. M., Janzen, D. H., & Hallwachs, W. (2004). Ten species in one: DNA barcoding reveals cryptic species in the neotropical skipper butterfly Astraptes fulgerator. *Proceedings of the National Academy of Sciences*, *101*(41), 14812-14817.

Hijmans, R. J., & van Etten, J. (2014). raster: Geographic data analysis and modeling. *R package version*, *2*(8).

Hipp, A. L., Eaton, D. A., Cavender-Bares, J., Fitzek, E., Nipper, R., & Manos, P. S. (2014). A framework phylogeny of the American oak clade based on sequenced RAD data. *PLoS One*, *9*(4), e93975.

Hitchcock, C. L., & Cronquist, A. (1973). Flora of the Pacific Northwest. University of Washington Press

Hitchcock, C. L. & Cronquist, A. (2018). Flora of the Pacific Northwest. University of Washington Press

Hooker, M. A. (2018). *Diversification and Phylogeography of Synthyris (Plantaginaceae) in Northwestern North America*(Doctoral dissertation, Washington State University).

Hunn, E. S., & French, D. H. (1981). *Lomatium*: a key resource for Columbia Plateau native subsistence. *Northwest Science*, *55*(2), 87-94.

Izuno, A., Kitayama, K., Onoda, Y., Tsujii, Y., Hatakeyama, M., Nagano, A. J., ... & Isagi, Y. (2017). The population genomic signature of environmental association and gene flow in an ecologically divergent tree species *Metrosideros polymorpha* (Myrtaceae). *Molecular ecology*, *26*(6), 1515-1532.

Jones, G. R. (2014). STACEY: species delimitation and phylogeny estimation under the multispecies coalescent. *BioRxiv*, 010199.

Johnson, M. G., Gardner, E. M., Liu, Y., Medina, R., Goffinet, B., Shaw, A. J., ... & Wickett, N. J. (2016). HybPiper: Extracting coding sequence and introns for phylogenetics from high-throughput sequencing reads using target enrichment. *Applications in plant sciences*, *4*(7), 1600016.

Johnson, M., Pokorny, L., Dodsworth, S., Botigue, L. R., Cowan, R. S., Devault, A., ... & Leebens-Mack, J. H. (2018). A Universal Probe Set for Targeted Sequencing of 353 Nuclear Genes from Any Flowering Plant Designed Using k-medoids Clustering. *bioRxiv*, 361618.

Johnson, S. B., Warén, A., & Vrijenhoek, R. C. (2008). DNA barcoding of Lepetodrilus limpets reveals cryptic species. *Journal of Shellfish Research*, *27*(1), 43-51.

Katoh, K., & Standley, D. M. (2013). MAFFT multiple sequence alignment software version 7: improvements in performance and usability. *Molecular biology and evolution*, *30*(4), 772-780.

Lendvay, B., Höhn, M., Brodbeck, S., Mîndrescu, M., & Gugerli, F. (2014). Genetic structure in Pinus cembra from the Carpathian Mountains inferred from nuclear and chloroplast microsatellites confirms post-glacial range contraction and identifies introduced individuals. *Tree genetics & genomes*, *10*(5), 1419-1433.

Lepofsky, D., & Lertzman, K. (2008). Documenting ancient plant management in the northwest of North America. *Botany*, *86*(2), 129-145.

Léveillé-Bourret, É., Starr, J. R., Ford, B. A., Moriarty Lemmon, E., & Lemmon, A. R. (2017). Resolving rapid radiations within angiosperm families using anchored phylogenomics. *Systematic biology*, *67*(1), 94-112.

Li, H., & Durbin, R. (2010). Fast and accurate long-read alignment with Burrows–Wheeler transform. *Bioinformatics*, *26*(5), 589-595.

Lopes, C., & Mix, A. C. (2009). Pleistocene megafloods in the northeast Pacific. *Geology*, *37*(1), 79-82.

Meng, L., Chen, G., Li, Z., Yang, Y., Wang, Z., & Wang, L. (2015). Refugial isolation and range expansions drive the genetic structure of Oxyria sinensis (Polygonaceae) in the Himalaya-Hengduan Mountains. *Scientific reports*, *5*, 10396.

McGinnis, S., & Madden, T. L. (2004). BLAST: at the core of a powerful and diverse set of sequence analysis tools. *Nucleic acids research*, *32*(suppl_2), W20-W25.

Metzker, M. L. (2010). Sequencing technologies—the next generation. *Nature reviews genetics*, *11*(1), 31.

Meyer, A. (1987). Phenotypic plasticity and heterochrony in Cichlasoma managuense (Pisces, Cichlidae) and their implications for speciation in cichlid fishes. *Evolution*, *41*(6), 1357-1369.

Miller, M. A., Pfeiffer, W., & Schwartz, T. (2011, July). The CIPRES science gateway: a community resource for phylogenetic analyses. In *Proceedings of the 2011 TeraGrid Conference: extreme digital discovery* (p. 41). ACM.

Morales-Briones, D. F., Romoleroux, K., Kolář, F., & Tank, D. C. (2018). Phylogeny and evolution of the Neotropical radiation of *Lachemilla* (Rosaceae): uncovering a history of reticulate evolution and implications for infrageneric classification. *Systematic Botany*, *43*(1), 17-34.

MYcroarray, (2016). MYbaits User Manual Version 3.02.

Nathan, R., Schurr, F. M., Spiegel, O., Steinitz, O., Trakhtenbrot, A., & Tsoar, A. (2008). Mechanisms of long-distance seed dispersal. *Trends in ecology & evolution*, 23(11), 638-647.

Ownbey, M. (1950). Natural hybridization and amphiploidy in the genus *Tragopogon*. American Journal of Botany, 37(7), 487-499.

Paris, C. A., F. S. Wagner, and W. H. Wagner. 1989. Cryptic species, species delimitation, and taxonomic practice in the homosporous ferns. *American Fern Journal* 79: 46–54.

Peery, R. M. 2015 Understanding angiosperm genome interactions and evolution: insights from sacred lotus (*Nelumbo nucifera*) and the carrot family (Apiaceae). University of Illinois. PhD Dissertation.

Perkins, M. E., & Nash, B. P. (2002). Explosive silicic volcanism of the Yellowstone hotspot: The ash fall tuff record. *Geological Society of America Bulletin*, 114(3), 367-381.

R Core Team (2018). R Foundation for Statistical Computing; Vienna, Austria: 2014. *R: A language and environment for statistical computing*, 2013.

Rambaut, A. (2007). FigTree, a graphical viewer of phylogenetic trees. *See http://tree. bio. ed. ac. uk/software/figtree*.

Rambaut, A., & Drummond, A. (2003). Tracer: a program for analysing results from Bayesian MCMC programs such as BEAST & MrBayes. *University of Edinburgh, UK*.

Rambaut, A., & Drummond, A. J. (2013). TreeAnnotator v1. 7.0. Available as part of the BEAST package at http://beast. bio. ed. ac. uk.

Rambaut, A., & Drummond, A. J. (2013). LogCombiner v1. 8.0.

Rautenberg, A., Hathaway, L., Oxelman, B., & Prentice, H. C. (2010). Geographic and phylogenetic patterns in Silene section Melandrium (Caryophyllaceae) as inferred from chloroplast and nuclear DNA sequences. *Molecular Phylogenetics and Evolution*, *57*(3), 978-991.

Ronquist, F., Teslenko, M., Van Der Mark, P., Ayres, D. L., Darling, A., Höhna, S., ... & Huelsenbeck, J. P. (2012). MrBayes 3.2: efficient Bayesian phylogenetic inference and model choice across a large model space. *Systematic biology*, *61*(3), 539-542.

Stubbs, R. L., Folk, R. A., Xiang, C. L., Soltis, D. E., & Cellinese, N. (2018). Pseudo-parallel patterns of disjunctions in an Arctic-alpine plant lineage. *Molecular phylogenetics and evolution*, *123*, 88-100.

Schield, D. R., Card, D. C., Adams, R. H., Jezkova, T., Reyes-Velasco, J., Proctor, F. N., ... & Castoe, T. A. (2015). Incipient speciation with biased gene flow between two lineages of the Western Diamondback Rattlesnake (*Crotalus atrox*). *Molecular Phylogenetics and Evolution*, *83*, 213-223.

Schlessman, M. A. (1982). Expression of andromonoecy and pollination of tuberous *Lomatiums* (Umbelliferae). *Systematic Botany*, 134-149.

Slater, G. S. C., & Birney, E. (2005). Automated generation of heuristics for biological sequence comparison. *BMC bioinformatics*, *6*(1), 31.

Smith, J. F., Mansfield, D. H., Stevens, M., Sosa, E., Feist, M. A. E., Downie, S. R., ... & Darrach, M. (2018). Try Tri again? Resolving species boundaries in the Lomatium triternatum (Apiaceae) complex. *Journal of Systematics and Evolution*, *56*(3), 218-230.

Sobel, J. M., & Streisfeld, M. A. (2015). Strong premating reproductive isolation drives incipient speciation in Mimulus aurantiacus. *Evolution*, *69*(2), 447-461.

Soltis, D. E., & Soltis, P. S. (1989). Allopolyploid speciation in Tragopogon: insights from chloroplast DNA. *American Journal of Botany*, *76*(8), 1119-1124.

Soltis, P. S., Plunkett, G. M., Novak, S. J., & Soltis, D. E. (1995). Genetic variation in Tragopogon species: additional origins of the allotetraploids T. mirus and T. miscellus (Compositae). *American Journal of Botany*, *82*(10), 1329-1341.

Soltis, D. E., Soltis, P. S., PIRES, J. C., Kovarik, A., Tate, J. A., & Mavrodiev, E. (2004). Recent and recurrent polyploidy in *Tragopogon* (Asteraceae): cytogenetic, genomic and genetic comparisons. *Biological Journal of the Linnean Society*, *82*(4), 485-501.

Stamatakis, A. (2014). RAxML version 8: a tool for phylogenetic analysis and post-analysis of large phylogenies. *Bioinformatics*, *30*(9), 1312-1313.

Stevens, M., Mansfield, D. H., Smith, J. F., & Feist, M. A. E. (2018). Resolving the Anomaly of *Lomatium anomalum*: Discovery of a New Species in Southwestern Idaho (USA), *Lomatium andrusianum* (Apiaceae). *Journal of the Botanical Research Institute of Texas.*

Stöver, B. C., & Müller, K. F. (2010). TreeGraph 2: combining and visualizing evidence from different phylogenetic analyses. *BMC bioinformatics*, *11*(1), 7.

Stubbs, R. L., Soltis, D. E., & Cellinese, N. (2018). The future of cold- adapted plants in changing climates: *Micranthes* (Saxifragaceae) as a case study. *Ecology and evolution*, 8(14), 7164-7177.

Sun, F. J., & Downie, S. R. (2010). Phylogenetic analyses of morphological and molecular data reveal major clades within the perennial, endemic western North American Apiaceae subfamily Apioideae. *The Journal of the Torrey Botanical Society*, 133-156.

Tang, Y., Horikoshi, M., & Li, W. (2016). ggfortify: unified interface to visualize statistical result of popular R packages. *RJ*, *8*(2), 474-485.

Wan, Q., Zheng, Z., Huang, K. et al. *Tree Genetics & Genomes* (2017) 13: 73.

Whittall, J. B., & Hodges, S. A. (2007). Pollinator shifts drive increasingly long nectar spurs in columbine flowers. Nature, 447(7145), 706.

Wickham, H. (2016). ggplot2: elegant graphics for data analysis. Springer.

Williams, E. W., Farrar, D. R., & Henson, D. (2016). Cryptic speciation in allotetraploids: Lessons from the *Botrychium matricariifolium* complex. *American Journal of Botany*, *103*(4), 740-753.

Zhang, C., Sayyari, E., & Mirarab, S. (2017). ASTRAL-III: increased scalability and impacts of contracting low support branches. In *RECOMB International Workshop on Comparative Genomics* (pp. 53-75). Springer, Cham.

# APPENDIX A

**Samples and Genbank Accession Numbers for Chapter 1**

***Aletes filifolius,*** R. C. Sivinski 4561 (RM), Socorro, New Mexico, tbd, tbd, tbd, tbd, tbd, tbd, tbd

***Angelica lineariloba* A. Gray,** A. Thiehm 11344 (NY), Esmeralda, Nevada, tbd, tbd, tbd, tbd, tbd, tbd, tbd

***Arracacia donnell-smithii* J.M. Coult. & Rose,** D.E. Breedlove 22815 (NY), Chiapas , Mexico, tbd, tbd, tbd, tbd, tbd, tbd, tbd

***Arracacia atropurpurea* (Lehm.) Hemsl,** A. ventura 479 (NY), Tepepulco, Mexico, tbd, tbd, tbd, tbd, tbd, tbd, tbd

***Cymopterus* sp. nov.,** D. Roth 1380 (NAVA), Navajo, Arizona, tbd, tbd, tbd, tbd, tbd, tbd, tbd

**Cymopterus beckii,** J. Anderson 87-149, D. Atwood and B. Thompson (RM), San Juan, Utah, tbd, tbd, tbd, tbd, tbd, tbd, tbd

***Cymopterus evertii,*** H. Marriott 10806 (RM), Park, Wyoming, tbd, tbd, tbd, tbd, tbd, tbd, tbd

***Cymopterus lapidosus,*** B. E. Nelson 35207 (RM), Uinta, Wyoming, tbd, tbd, tbd, tbd, tbd, tbd, tbd

**Cymopterus bakeri,** B. Franklin 3947 (RM), San Juan, Utah, tbd, tbd, tbd, tbd, tbd, tbd, tbd

***Lomatium planosum* (Oster.) Mansfield & S. R. Downie,** C. E. Hinchliff 1322 (SRP, Delta, Colorado, KF619617, tbd, KF619891, KF619754, tbd, tbd, tbd

***Cymopterus ripleyi* Barneby,** C. E. Hinchliff 1310 (SRP), Lincoln, Nevada, KF619616, tbd, KF619894, KF619757, tbd, tbd, tbd

***Cymopterus glomeratus* var. *fendleri* (A. Gray) R.L. Hartm,** C. E. Hinchliff 1314 (CIC), Mesa, Colorado, KF619882, tbd, KF619745, KF620018, tbd, tbd, tbd

***Cymopterus glomeratus* var. *greeleyorum* (J.W. Grimes & P.L. Packard) R.L. Hartm,** E. George 087 (CIC), Malheur , Oregon, tbd, tbd, tbd, tbd, tbd, tbd, tbd

***Cymopterus longilobus* (Rydb.) W.A. Weber,** B. Ertter 22416 (SRP), Teton, Wyoming, tbd, tbd, tbd, tbd, tbd, tbd, tbd

***Cymopterus nivalis* S. Watson,** C E. Hinchliff 1348 (CIC), Beaverhead, Montana, tbd, tbd, tbd, tbd, tbd, tbd, tbd

***Donnellsmithia juncea* (Humb. & Bonpl. ex Spreng.) Mathias & Constance,** T.R. VanDevender 98-999 (NY), Sonora, Mexico, tbd, tbd, tbd, tbd, tbd, tbd, tbd

***Harbouria trachypleura* (A. Gray) J.M. Coult. & Rose,** K. Marlow 113 (CIC), Boulder, Colorado, tbd, tbd, tbd, tbd, tbd, tbd, tbd

***Lomatium ambiguum* (Nutt.) J.M. Coult. & Rose,** B. Ertter 22278 (SRP), British Columbia, Canada, MH131697, MH131898, MH132102, MH132294, MH132480, MH132647, MH132843

***Lomatium anomalum* M.E. Jones ex J.M. Coult. & Rose,** M. Darrach 645 (CIC), Grant, Oregoon, MH131719, MH131922, MH132126, MH132315, MH132503, MH132671, MH132861

***Lomatium anomalum* M.E. Jones ex J.M. Coult. & Rose,** M. Darrach 656 (CIC), Asotin, Washington, MH131720, MH131923, MH132316, MH132316, MH132504, MH132672, MH132862

***Lomatium anomalum* M.E. Jones ex J.M. Coult. & Rose,** D. Mansfield 07-011 (CIC), Malheur, Oregon, X, MH131905, MH132109, MH132299, MH132487, MH132654, MH132848
***Lomatium anomalum* M.E. Jones ex J.M. Coult. & Rose,** D. Mansfield 07-055 (CIC), Washington, Idaho, MH131708, MH131911, MH132115, MH132305, MH132493, MH132660, MH132852
***Lomatium anomalum* M.E. Jones ex J.M. Coult. & Rose,** D. Mansfield 15-001 (CIC), Malheur, Oregon, MH131703, MH131906, MH132110, MH132300, MH132488, MH132655, MH132849
***Lomatium anomalum* M.E. Jones ex J.M. Coult. & Rose,** D. Mansfield 15-152 (CIC), Owyhee, Idaho, MH131705, MH131908, MH132112, MH132302, MH132490, MH132657, MH132851
***Lomatium anomalum* M.E. Jones ex J.M. Coult. & Rose,** E. George & J. Reichel 058 (CIC), Malheur, Oregon, KF619689, MH131912, KF619961, KF619824, MH132494, MH132661, MH132853
***Lomatium anomalum* M.E. Jones ex J.M. Coult. & Rose,** E. George & J. Reichel 066 (CIC), Washington, Idaho, MH131710, MH131913, MH132117, MH132307, MH132495, MH132662, MH132854
***Lomatium anomalum* M.E. Jones ex J.M. Coult. & Rose,** E. George & D. Mansfield 091 (CIC), Malheur, Oregon, KF619690, MH131915, KF619962, KF619825, MH132497, MH132664, MH132856
***Lomatium anomalum* M.E. Jones ex J.M. Coult. & Rose,** E. George 102 (CIC), Idaho, Idaho, MH131711, MH131914, MH132118, MH132308, MH132496, MH132663, MH132855
***Lomatium anomalum* M.E. Jones ex J.M. Coult. & Rose,** C. E. Hinchliff 1252 (SRP), Morrow, Oregon, MH131700, MH131902, MH132106, MH132297, MH132484, MH132651, MH132846
***Lomatium anomalum* M.E. Jones ex J.M. Coult. & Rose,** C. L. Hitchcock 23492 (WTU), Asotin, Washington, MH131701, MH131903, MH132107, X, MH132485, MH132652, X
***Lomatium anomalum* M.E. Jones ex J.M. Coult. & Rose,** P. Lesica 10794 (CIC), Idaho, Idaho, MH131724, MH131927, MH132131, MH132320, MH132508, MH132676MH132866,
***Lomatium anomalum* M.E. Jones ex J.M. Coult. & Rose,** P. Lesica 10798 (CIC), Idaho, Idaho, MH131725, MH131928, MH132132, MH132321, MH132509, MH132677, MH132867
***Lomatium anomalum* M.E. Jones ex J.M. Coult. & Rose,** C. V. Piper sn (WTU:88603), Whitman, Washington, MH131702, MH131904, MH132108, MH132298, MH132486, MH132653, MH132847
***Lomatium anomalum* M.E. Jones ex J.M. Coult. & Rose,** L. Polito et al. 002 (CIC), Owyhee, Idaho, MH131715, MH131918, MH132122, MH132312, MH132500, MH132667, MH132858
***Lomatium anomalum* M.E. Jones ex J.M. Coult. & Rose,** L. Polito et al. 003 (CIC), Owyhee, Idaho, MH131716, MH131919, MH132123, MH132313, MH132501, MH132668, MH132859

***Lomatium anomalum* M.E. Jones ex J.M. Coult. & Rose,** L. Polito et al. 004 (CIC), Owyhee, Idaho, MH131717, MH131920, MH132124, MH132314, MH132502, MH132669, MH132860
***Lomatium anomalum* M.E. Jones ex J.M. Coult. & Rose,** J. F. Smith et al. 10748 (SRP), Nez Perce , Idaho, MH131713, MH131916, MH132120, MH132310, MH132498, MH132665, MH132857
***Lomatium anomalum* M.E. Jones ex J.M. Coult. & Rose,** A. Truksa & S. Truksa 38 (CIC), Malheur, Oregon, MH131726, MH131929, MH132133, MH132322, MH132510, MH132678, MH132868
***Lomatium roneorum,*** D. Mansfield 11493 (CIC), Kittitas, Washington, tbd, tbd, tbd, tbd, tbd, tbd, tbd
***Lomatium roneorum,*** M. Darrach 649 (CIC), Chelan, Washington, tbd, tbd, tbd, tbd, tbd, tbd, tbd
***Vesper constancei* (R.L. Hartm.) R.L. Hartm. & G.L. Nesom,** C. E. Hinchliff 1224 (CIC), Bernalillo, New Mexico, tbd, tbd, tbd, tbd, tbd, tbd, tbd
***Lomatium attenuatum,*** E. Evert 16359 (RM), Park, Wyoming, KF619624, tbd, KF619897, KF619761, tbd, tbd, tbd
***Lomatium basalticum* Mansfield & M. Stevens,** C. E. Hinchliff 891 (CIC), Baker, Oregon, MH131727, MH131930, MH132134, MH132323, MH132511, MH132679, MH132869
***Lomatium basalticum* Mansfield & M. Stevens,** L. Polito et al. 043 (CIC), Adams, Idaho, MH131728, MH131931, MH132135, MH132324, MH132512, MH132680, MH132870
***Lomatium basalticum* Mansfield & M. Stevens,** L. Polito et al. 044 (CIC), Adams, Idaho, MH131729, MH131932, MH132136, MH132325, MH132513, MH132681, MH132871
***Lomatium basalticum* Mansfield & M. Stevens,** L. Polito et al. 045 (CIC), Adams, Idaho, MH131730, MH131933, MH132137, MH132326, MH132514, MH132682, MH132872
***Lomatium basalticum* Mansfield & M. Stevens,** M. Darrach 1115 (CIC), Wallowa, Oregon, MH131731, MH131934, MH132138, MH132327, MH132515, MH132683, MH132873
***Lomatium bentonitum* K. Carlson & D. Mansfield,** E. George & D. Mansfield 089 (CIC), Malheur, Oregon, KF619625, MH131935, KF619899, KF619762, MH132516, MH132684, MH132874
***Lomatium bicolor* (S. Watson) J.M. Coult. & Rose var. *bicolor*,** B. Moseley 1768 (ID), Franklin, Idaho, KF619626, MH131936, KF619900, KF619763, MH132517, MH132685, MH132875
***Lomatium bicolor* (S. Watson) J.M. Coult. & Rose var. *leptocarpum* (Torr. & A. Gray) Schlessman,** E. George & J. Reichel 064 (CIC), Washington, Idaho, KF619629, MH131937, KF619903, KF619766, MH132518MH132686, , MH132876
***Lomatium brevifolium* (J.M. Coult. & Rose) J.M. Coult. & Rose,** D. French 2759 (WTU), Klickitat, Washington, X, MH131944, MH132147, MH132337, X, MH132694, MH132883

***Lomatium brevifolium* (J.M. Coult. & Rose) J.M. Coult. & Rose,** M. Darrach 1056 (CIC), Klickitat, Washington, MH131759, MH131963, MH132163, MH132351, MH132531, MH132711, MH132903
***Lomatium brevifolium* (J.M. Coult. & Rose) J.M. Coult. & Rose,** B. Ertter 7572 (WTU), Klickitat, Washington, MH131736, MH132711, X, MH132331, MH132519, MH132878, X
***Lomatium brevifolium* (J.M. Coult. & Rose) J.M. Coult. & Rose,** B. Legler 1798 (WTU), Kittitas, Washington, MH131737, MH131940, MH132142, MH132332, MH132520, MH132689, MH132879
***Lomatium brevifolium* (J.M. Coult. & Rose) J.M. Coult. & Rose,** G. N. Jones 1554 (WTU), Yakima, Washington, MH131745, MH131949, MH132150, MH132341, X, MH132699, MH132889
***Lomatium brevifolium* (J.M. Coult. & Rose) J.M. Coult. & Rose,** C. E. Hinchliff 1267 (SRP), Klickitat, Washington, MH131739, MH131942, MH132144, MH132334, MH132522, MH132691, MH132881
***Lomatium brevifolium* (J.M. Coult. & Rose) J.M. Coult. & Rose,** S. Gage & S. Rodman 227 (WTU), Yakima, Washington, MH131766, MH131970, MH132170, MH132356, X, MH132718, MH132909
***Lomatium brevifolium* (J.M. Coult. & Rose) J.M. Coult. & Rose,** C. L. Hitchcock 20278 (WTU), Kittitas, Washington, MH131740, X, MH132145, MH132335, MH132523, MH132692, MH132882
***Lomatium brevifolium* (J.M. Coult. & Rose) J.M. Coult. & Rose,** J. G. Smith 152 (WTU), Kittitas, Washington, MH131751, MH131955, X, MH132156, MH132529, MH132705, MH132895
***Lomatium brevifolium* (J.M. Coult. & Rose) J.M. Coult. & Rose,** J. W. Thompson 11577 (WTU), Kittitas, Washington, MH131754, MH131958, MH132159, MH132347, X, MH132707, MH132897
***Lomatium brevifolium* (J.M. Coult. & Rose) J.M. Coult. & Rose,** M. A. Schlessman 211 (WTU), Kittitas, Washington, MH131758, MH131962, MH132162, MH132350, X, MH132710, MH132902
***Lomatium brevifolium* (J.M. Coult. & Rose) J.M. Coult. & Rose,** D. Mansfield 11-491 (CIC), Kittitas, Washington, MH131741, MH131945, MH132148, MH132338, MH132524, MH132695, MH132884
***Lomatium brevifolium* (J.M. Coult. & Rose) J.M. Coult. & Rose,** F. A. Warren 1562 (WTU), Pierce, Washington, MH131742, MH131946, MH132149, MH132339, X, MH132696, MH132886
***Lomatium brevifolium* (J.M. Coult. & Rose) J.M. Coult. & Rose,** F. A. Warren 1609 (WTU) , Pierce, Washington, MH131743, MH131947, X, MH132340, X, MH132697, MH132887
***Lomatium brevifolium* (J.M. Coult. & Rose) J.M. Coult. & Rose,** J. W. Thompson 12577a (WTU), Pierce, Washington, MH131752, MH131956, MH132157, MH132346, MH132530, MH132706, MH132898
***Lomatium brevifolium* (J.M. Coult. & Rose) J.M. Coult. & Rose,** K. A. Beck 200101 (WTU), Klickitat, Washington, MH131757, MH131961, MH132160, MH132349, X, MH132709, MH132901

***Lomatium brevifolium* (J.M. Coult. & Rose) J.M. Coult. & Rose,** P. F. Zika 24419 (SRP), Klickitat, Washington, MH131763, MH131967, MH132167, MH132354, MH132535, MH132715, MH132906
***Lomatium brevifolium* (J.M. Coult. & Rose) J.M. Coult. & Rose,** M. Darrach 304 (SRP), Klickitat, Washington, MH131760, MH131964, MH132164, X, MH132532, MH132712, X
***Lomatium brevifolium* (J.M. Coult. & Rose) J.M. Coult. & Rose,** D. H. French 1883 (CIC), Wasco, Oregon, X, MH131943, MH132146, MH132336, X, MH132693, MH132885
***Lomatium brevifolium* (J.M. Coult. & Rose) J.M. Coult. & Rose,** I. C. Otis 1903 (WTU), Thurston, Washington, MH131746, MH131950, MH132151, X, X, MH132700, MH132890
***Lomatium brevifolium* (J.M. Coult. & Rose) J.M. Coult. & Rose,** P. P. Lowry 712 (WTU), Skamania, Washington, MH131764, MH131968, MH132168, MH132355, X, MH132716, MH132907
***Lomatium brunsfeldianum* Kemper & R.P. McNeill,** C. R. Bjork 6481 (ID), Kootenai, Idaho, KF619633, MH131971, KF619906, KF619769, MH132537, MH132719, MH132910
***Lomatium brunsfeldianum* Kemper & R.P. McNeill,** T. Kemper 93 (CIC), Idaho, Idaho, MH131772, MH131976, MH132176, MH132362, MH132542, MH132724, MH132925
***Lomatium brunsfeldianum* Kemper & R.P. McNeill,** P. Brunsfeld et al. 6426 (ID), Shosone, Idaho, MH131770, MH131974, MH132174, MH132360, MH132540, MH132722, MH132926
***Lomatium brunsfeldianum* Kemper & R.P. McNeill,** S. Walker 218 (ID), Idaho, Idaho, KF619634, MH131975, KF619907, KF619770, MH132541, MH132723, X
***Lomatium brunsfeldianum* Kemper & R.P. McNeill,** T. Spribille 14241 (ID), Shosone, Idaho, X, MH131977, MH132177, MH132363, MH132543, MH132725, MH132927
***Lomatium canbyi* (J.M. Coult. & Rose) J.M. Coult. & Rose,** E. George & D. Mansfield 086 (CIC), Malheur, Oregon, KF619639, MH131978, KF619911, KF619775, MH132544, MH132726, MH132928
***Lomatium caruifolium,*** R. McNeill sn (CIC), Madera, California, tbd, tbd, tbd, tbd, tbd, tbd, tbd
***Lomatium columbianum* Mathias & Constance,** C. E. Hinchliff 1265 (SRP), Klickitat, Washington, KF619642, MH131979, KF619915, KF619778, MH132545, MH132727, X
***Lomatium cous* (S. Watson) J.M. Coult. & Rose,** D. Mansfield 11-010 (CIC), Umatilla, Oregon, KF619647, MH131980, KF619920, KF619783, MH132546, MH132728, MH132929
***Lomatium cous* (S. Watson) J.M. Coult. & Rose.,** C. Johnson 7260 (WTU), Wallowa, Oregon, tbd, tbd, tbd, tbd, tbd, tbd, tbd
***Lomatium cusickii* (S. Watson) J.M. Coult. & Rose,** B. E. Nelson 50572 (CIC), Idaho, Idaho, KF619648, tbd, KF619921, KF619784, tbd, tbd, tbd
***Lomatium cuspidatum,*** G. Patrick sn (WTU), Chelan, Washington, tbd, tbd, tbd, tbd, tbd, tbd, tbd
***Lomatium cuspidatum,*** G. Patrick sn (WTU), Chelan, Washington, tbd, tbd, tbd, tbd, tbd, tbd, tbd

***Lomatium cuspidatum,*** P. Elvaneter 1000 (WTU), Kittitas, Washington, tbd, tbd, tbd, tbd, tbd, tbd, tbd
***Lomatium dissectum,*** J. T. Duncan 11 (CIC), Jackson, Oregon, KF619652, tbd, KF619925, KF619788, tbd, tbd, tbd
***Lomatium dissectum,*** R. Helliwell 3957 (CIC), Douglas, Oregon, KF619654, tbd, KF619927, KF619790, tbd, tbd, tbd
***Lomatium donnellii* (J.M. Coult. & Rose) J.M. Coult. & Rose,** C. E. Hinchliff 1258 (CIC), Jefferson, Oregon, KF619656, MH131983, KF619929, KF619792, MH132549, MH132731, MH132932
***Lomatium gormannii* (Howell) J.M. Coult. & Rose,** C. E. Hinchliff 1212 (CIC), Walla Walla, Washington, KF619664, MH131984, KF619937, KF619800, MH132550, MH132732, MH132933
***Lomatium grayi* (J.M. Coult. & Rose) J.M. Coult. & Rose ,** C. E. Hinchliff 1240 (CIC), Yakima, Washington, KF619670, MH131986, KF619943, KF619806, MH132552, MH132734, MH132935
***Lomatium grayi* (J.M. Coult. & Rose) J.M. Coult. & Rose ,** C. E. Hinchliff 1264 (SRP), Klickitat, Washington, MH131782, MH131987, MH132187, MH132373, MH132553, MH132735, MH132936
***Lomatium grayi* (J.M. Coult. & Rose) J.M. Coult. & Rose ,** C. E. Hinchliff 898 (SRP), Baker, Oregon, MH131783, MH131988, MH132188, MH132374, MH132554, MH132736, MH132937
***Lomatium grayi* (J.M. Coult. & Rose) J.M. Coult. & Rose ,** D. Mansfield et al. 12-444 (CIC), Owyhee, Idaho, MH131785, MH131990, MH132190, MH132376, X, MH132738, MH132939
***Lomatium grayi* (J.M. Coult. & Rose) J.M. Coult. & Rose ,** D. Mansfield 15-155 (CIC), Owyhee, Idaho, MH131784, MH131989, MH132189, MH132375, MH132555, MH132737, MH132938
***Lomatium grayi* (J.M. Coult. & Rose) J.M. Coult. & Rose ,** J. F. Smith et al. 10766 (SRP), Nez Perce, Idaho, MH131786, MH131991, MH132191, MH132377, X, MH132739, MH132940
***Lomatium grayi* (J.M. Coult. & Rose) J.M. Coult. & Rose ,** J. F. Smith et al. 11591 (SRP), Gem, Idaho, MH131787, MH131992, MH132192, MH132378, MH132556, MH132740, MH132941
***Lomatium grayi* (J.M. Coult. & Rose) J.M. Coult. & Rose ,** M. Stevens & J. Avitia 067 (CIC), Washington, Idaho, MH131789, MH131994, MH132194, MH132380, MH132558, MH132742, MH132943
***Lomatium macrocarpum* (Hook. & Arn.) J.M. Coult. & Rose,** D. Mansfield 07-329 (CIC), Harney, Oregon, MH131791, MH131996, X, MH132382, MH132559, MH132744, MH132945
***Lomatium macrocarpum* (Hook. & Arn.) J.M. Coult. & Rose,** E. George 101 (CIC), Nez Perce, Idaho, MH131792, MH131997, MH132196, MH132383, MH132560, MH132745, MH132946
***Lomatium macrocarpum* (Hook. & Arn.) J.M. Coult. & Rose,** R. Helliwell 3952 (CIC), Josephine, Oregon, MH131798, MH132003, MH132202, MH132389, MH132566, MH132751, MH132952

***Lomatium nevadense* (S. Watson) J.M. Coult. & Rose var. nevadense,** D. Mansfield 11-081 (CIC), Elko, Nevada, KF619682, MH132005, KF619954, KF619817, MH132568, MH132753, MH132953
***Lomatium nevadense* (S. Watson) J.M. Coult. & Rose var. parishii (J.M. Coult. & Rose) Jeps.,** C. E. Hinchliff 1283 (CIC), Apache, Arizona, KF619681, MH132006, KF619953, KF619816, X, MH132754, MH132954
***Lomatium oreganum,*** B. Bafus 402 (WTU), Baker, Oregon, tbd, tbd, tbd, tbd, tbd, tbd, tbd
***Lomatium oreganum,*** C. Johnson sn (WTU), Wallowa, Oregon, tbd, tbd, tbd, tbd, tbd, tbd, tbd
***Lomatium simplex* (Nutt. ex S. Watson) J.F. Macbr.,** B. Ertter 21062 & A. DiNicola (CIC), Adams, Idaho, MH131808, MH132013, MH132212, MH132399, MH132575, MH132761, MH132961
***Lomatium simplex* (Nutt. ex S. Watson) J.F. Macbr.,** B. Ertter 22285 (SRP), British Columbia, Canada, MH131806, MH132011, MH132210, MH132397, MH132573, MH132759, MH132959
***Lomatium simplex* (Nutt. ex S. Watson) J.F. Macbr.,** B. Ertter 22286 (SRP), British Columbia, Canada, MH131807, MH132012, MH132211, MH132398, MH132574, MH132760, MH132960
***Lomatium simplex* (Nutt. ex S. Watson) J.F. Macbr.,** D. Giblin 5208 (WTU), Kittitas, Washington, MH131812, MH132017, MH132216, MH132403, MH132576, MH132764, MH132964
***Lomatium simplex* (Nutt. ex S. Watson) J.F. Macbr.,** C. A. Morrow sn (WTU), Gallatin, Montana, MH131809, MH132014, MH132213, MH132400, X, MH132762, MH132962
***Lomatium simplex* (Nutt. ex S. Watson) J.F. Macbr.,** J. F. Smith 5428 (SRP), Blaine, Idaho, MH131822, MH132027, MH132226, MH132413, MH132586, MH132774, MH132973
***Lomatium simplex* (Nutt. ex S. Watson) J.F. Macbr.,** D. Mansfield 11-007 (CIC), Harney, Oregon, KF619715, MH132021, KF619988, KF619851, MH132580, MH132768, MH132968
***Lomatium simplex* (Nutt. ex S. Watson) J.F. Macbr.,** D. Mansfield et al. 14-009 (CIC), Ada, Idaho, MH131813, MH132018, MH132217, MH132404, MH132577, MH132765, MH132965
***Lomatium simplex* (Nutt. ex S. Watson) J.F. Macbr.,** D. Mansfield et al. 14-110 (CIC), Ada, Idaho, MH131814, MH132019, MH132218, MH132405, MH132578, MH132766, MH132966
***Lomatium simplex* (Nutt. ex S. Watson) J.F. Macbr.,** R. Goff 99-18 (WTU), Ferry, Washington, MH131824, MH132029, MH132228, X, X, MH132776, MH132975
***Lomatium simplex* (Nutt. ex S. Watson) J.F. Macbr.,** C. E. Hinchliff 1345 (SRP), Lemhi, Idaho, MH131810, MH132015, MH132214, MH132401, X, MH132763, MH132963
***Lomatium simplex* (Nutt. ex S. Watson) J.F. Macbr.,** C. L. Hitchcock 9288 (WTU), Lemhi, Idaho, MH131811, MH132016, MH132215, MH132402, X, X, MH133032
***Lomatium peckianum,*** Forman and Butts 73573 (WTU), Lake, Oregon, tbd, tbd, tbd, tbd, tbd, tbd, tbd

***Lomatium* sp,** J. W. Thompson 9763.5 (WTU), Kittitas, Washington, tbd, tbd, tbd, tbd, tbd, tbd, tbd
***Lomatium andrusianum* McK. Stevens & Mansfield,** B. Ertter 20719 (CIC), Ada, Idaho, MH131826, MH132031, MH132230, MH132416, MH132589, MH132778, MH132915
***Lomatium andrusianum* McK. Stevens & Mansfield,** B. Ertter 20748 (CIC), Ada, Idaho, MH131827, MH132032, MH132231, MH132417, MH132590, MH132779, MH132976
***Lomatium andrusianum* McK. Stevens & Mansfield,** D. Johnson & T. Day 026-1 (CIC), Gem, Idaho, MH131836, MH132040, MH132240, MH132426, MH132599, MH132788, MH132978
***Lomatium andrusianum* McK. Stevens & Mansfield,** D. Johnson & T. Day 026-2 (CIC), Gem, Idaho, MH131837, MH132041, MH132241, MH132427, MH132600, MH132789, MH132979
***Lomatium andrusianum* McK. Stevens & Mansfield,** D. Mansfield 16004 (CIC), Payette, Idaho, MH131828, MH132033, MH132232, MH132418, MH132591, MH132780, MH132916
***Lomatium andrusianum* McK. Stevens & Mansfield,** J. F. Smith et al. 11580 (SRP), Boise, Idaho, MH131831, MH132035, MH132235, MH132421, MH132594, MH132783, MH132977
***Lomatium andrusianum* McK. Stevens & Mansfield,** M. Stevens et al. 106 (CIC)*F, Ada, Idaho, NA, NA, NA, NA, NA, NA, NA
***Lomatium* sp. nov. 2,** M. Darrach 627 (CIC), Morrow, Oregon, MH131838, MH132042, MH132242, MH132428, MH132601, MH132790, MH132980
***Lomatium* sp. nov. 3,** C. L. Hitchcock 8397 (WTU), Latah, Idaho, MH131841, MH132079, MH132273, MH132457, X, MH132821, X
***Lomatium* sp. nov. 3,** C. L. Hitchcock 17794 (WTU), Lake, Montana, MH131840, MH132044, MH132244, MH132430, MH132603, MH132792, MH132981
***Lomatium* sp. nov. 3,** P. Lesica 10541 (CIC), Sanders, Montana, MH131857, MH132060, MH132256, MH132439, MH132611, MH132804, MH132992
***Lomatium* sp. nov. 3,** P. Lesica 10552 (CIC), Lake, Montana, MH131858, MH132061, MH132257, MH132440, MH132612, MH132805, MH132993
***Lomatium* sp. nov. 3,** I. C. Otis 1940 (WTU: 2nd sheet), Whitman , Washinton, MH131849, MH132052, MH132250, X, X, MH132797, MH133033
***Lomatium* sp. nov. 3,** J. W. Oppe 71 (WTU), Latah, Idaho, MH131851, MH132054, MH132251, MH132436, MH132608, MH132798, X
***Lomatium* sp. nov. 3,** M. A. Schlessman 423 (WTU), Whitman, Washington, MH131853, MH132056, MH132253, MH132437, MH132609, MH132800, MH132990
***Lomatium* sp. nov. 3,** M. A. Schlessman 589 (WTU) â€ , Nez Perce, Idaho, MH131853, MH132056, MH132253, MH132437, MH132609, MH132800, MH132990
***Lomatium* sp. nov. 3,** M. A. Schlessman 651 (WTU), Nez Perce, Idaho, MH131856, MH132059, MH132255, MH132438, MH132610, MH132803, MH132991
***Lomatium* sp. nov. 3,** L. M. Umbach 425 (WTU), Yakima, Washington, MH131852, MH132055, MH132252, X, X, MH132799, X
***Lomatium* sp. nov. 3,** I. C. Otis 1940 (WTU) â€ , Whitman, Washington, MH131848, MH132051, MH132249, X, X, X, MH132988

***Lomatium* sp. nov. 4,** R. G. Olmstead 096-55 (WTU), Lake, Oregon, MH131871, MH132073, MH132267, MH132451, MH132621, MH132815, MH133004
***Lomatium* sp. nov. 4,** M. Friend sn (SRP), Plumas, California, MH131870, MH132072, MH132266, MH132450, X, MH132814, X
***Lomatium* sp. nov. 5,** R. Helliwell 3953 (CIC), Josephine, Oregon, MH131876, MH132078, MH132272, MH132456, MH132626, MH132820, MH133009
***Lomatium* sp. nov. 5,** A. R. Kruckeberg 1891 (WTU), Josephine, Oregon, MH131872, MH132074, MH132268, MH132452, MH132622, MH132816, MH133005
***Lomatium* sp. nov. 5,** M. F. Denton 2433 (ID), Josephine, Oregon, MH131875, MH132077, MH132271, MH132455, MH132625, MH132819, MH133008
***Lomatium watsonii* (J.M. Coult. & Rose) J.M. Coult. & Rose,** B. Legler 13650 (WTU), Yakima, Washington, tbd, tbd, tbd, tbd, tbd, tbd, tbd
***Lomatium suksdorfii* (S. Watson) J.M. Coult. & Rose ,** M. Darrach 900 (CIC), Wasco, Oregon, MH131878, MH132081, MH132275, MH132459, MH132628, MH132823, MH133011
***Lomatium suksdorfii* (S. Watson) J.M. Coult. & Rose ,** C. E. Hinchliff 1363 (SRP), Klickitat, Washington, MH131877, MH132080, MH132274, MH132458, MH132627, MH132822, MH133010
***Lomatium swingerae* R.P. McNeill,** R. P. McNeill sn (CIC), Idaho, Idaho, MH131879, MH132082, X, MH132460, MH132629, MH132824, MH133012
***Lomatium swingerae* R.P. McNeill,** R. P. McNeill sn (CIC), Idaho, Idaho, MH131880, MH132083, X, MH132461, MH132630, MH132825, MH133013
***Lomatium tamanitchii* Darrach & Thie,** M. Darrach 624 (CIC), Klickitat, Washington, MH131881, MH132085, MH132277, MH132463, MH132632, MH132827, MH133015
***Lomatium tamanitchii* Darrach & Thie,** C. E. Hinchliff 1268 (SRP), Klickitat, Washington, X, MH132084, MH132276, MH132462, MH132631, MH132826MH133014,
***Lomatium thompsonii* (Mathias) C.L. Hitchc.,** D. French 2513 (CIC), Chelan, Washington, MH131884, MH132088, MH132280, MH132466, MH132635, MH132830, MH133018
***Lomatium thompsonii* (Mathias) C.L. Hitchc.,** C. E. Hinchliff 1355 (CIC), Kittitas, Washington, KF619711, MH132087, KF619984, KF619087, MH132634, MH132829, MH133017
***Lomatium triternatum,*** J. T. Duncan 05(CIC), Jackson, Oregon, tbd, tbd, tbd, tbd, tbd, tbd, tbd
***Lomatium grayi* (J.M. Coult. & Rose) J.M. Coult. & Rose ,** Brill sn (WTU), Yakima, w, MH131780, , MH131985, , MH132185, , MH132371, , MH132551, , MH132733,, MH132934
***Lomatium triternatum,*** J. Benca 08-62 (WTU), Granite, Montana, tbd, tbd, tbd, tbd, tbd, tbd, tbd
***Lomatium triternatum* (Pursh) J.M. Coult. & Rose,** K. Carlson & E. Valdes 097 (CIC), Owyhee, Idaho, MH131886, MH132090, MH132282, MH132468, MH132637, MH132832, MH133020
***Lomatium tuberosum* Hoover,** C. E. Hinchliff 1270 (WS), Yakima, Washington, KF619716, MH132091, KF619989, KF619852, MH132638, MH132833, MH133021

***Lomatium utriculatum* (Nutt. ex Torr. & A. Gray) J.M. Coult. & Rose,** R. P. McNeill sn, Kern, California, MH131888, MH132092, MH132284, MH132470, MH132639, X, MH133023
***Lomatium vaginatum* J.M. Coult. & Rose,** R. Helliwell 3956 (CIC), Douglas, Oregon, MH131892, MH132096, MH132288, MH132474, X, MH132837, MH133022
***Lomatium vaginatum* J.M. Coult. & Rose,** D. Mansfield 11-005 (CIC), Harney, Oregon, KF619717, MH132093, KF619990, KF619853, MH132640, MH132834, MH133024
***Lomatium vaginatum* J.M. Coult. & Rose,** D. Mansfield 11-006 (CIC), Harney, Oregon, KF619719, MH132094, KF619992, KF619855, MH132641, MH132835, MH133025
***Lomatium watsonii* (J.M. Coult. & Rose) J.M. Coult. & Rose,** C. E. Hinchliff 1269 (CIC), Klickitat, Washington, KF619720, MH132097, KF619993, KF619856, MH132643, MH132838, MH133027
***Lomatium ambiguum* (Nutt.) J.M. Coult. & Rose,** C. E. Hinchliff 1273 (CIC), Idaho, Idaho, KF619621, tbd, KF619895, KF619758, tbd, tbd, tbd
***Lomatium ambiguum* (Nutt.) J.M. Coult. & Rose,** J.F. Smith 9561 (SRP), Gem, Idaho, KF619622, tbd, KF619896, KF619759, tbd, tbd, tbd
***Lomatium ambiguum* (Nutt.) J.M. Coult. & Rose,** J.F. Smith 9720 (SRP), Adams, Idaho, tbd, tbd, tbd, tbd, tbd, tbd, tbd
***Lomatium ambiguum* (Nutt.) J.M. Coult. & Rose,** Frank H. Rose 1536 (MONTU), Missoula, Montana, tbd, tbd, tbd, tbd, tbd, tbd, tbd
***Lomatium attenuatum* Evert,** C.E. Hinchhliff 1349 (SRP), Beaverhead, Montana, KF619623, tbd, KF619898, KF619760, tbd, tbd, tbd
***Lomatium erythrocarpum* Meinke & Constance,** Michael Murray sn (OSC), Baker, Oregon, tbd, tbd, tbd, tbd, tbd, tbd, tbd
***Lomatium erythrocarpum* Meinke & Constance,** Meinke 3201 (OSC), Baker, Oregon, tbd, tbd, tbd, tbd, tbd, tbd, tbd
***Lomatium foeniculaceum* var. *fimbriatum* (W.L. Theob.) B. Boivin,** K. Carlson 002 (CIC), Malheur, Oregon, HQ426076, tbd, HQ426127, HQ426102, tbd, tbd, tbd
***Lomatium foeniculaceum* var. *macdougalii* (J.M. Coult. & Rose) Cronquist,** C. E. Hinchliff 1306 (SRP), Lincoln, Nevada, KF619659, tbd, KF619932, KF619795, tbd, tbd, tbd
***Lomatium foeniculaceum* var. *macdougalii* (J.M. Coult. & Rose) Cronquist,** D. Mansfield 07001 (CIC), Canyon, Idaho, KF619660, tbd, KF619933, KF619796, tbd, tbd, tbd
***Lomatium greenmanii* Mathias ,** R. D. Kratz & R. Sines sn (WTU), Wallowa, Oregon, tbd, tbd, tbd, tbd, tbd, tbd, tbd
***Lomatium greenmanii* Mathias ,** Jessie Johanson 02-118 (WTU), Wallowa, Oregon, tbd, tbd, tbd, tbd, tbd, tbd, tbd
***Lomatium greenmanii* Mathias ,** Jessie Johanson 02-118 (OSC), Wallowa, Oregon, tbd, tbd, tbd, tbd, tbd, tbd, tbd
***Lomatium greenmanii* Mathias ,** G.D. Carr 1565 (OSC), Wallowa , Oregon, tbd, tbd, tbd, tbd, tbd, tbd, tbd
***Lomatium greenmanii* Mathias ,** Jessie Johanson 02-112 (WTU), Wallowa , Oregon, tbd, tbd, tbd, tbd, tbd, tbd, tbd

***Lomatium hallii* (S. Watson) J.M. Coult. & Rose ,** Porter P. Lowry II 569 (WTU), Multnomah, Oregon, tbd, tbd, tbd, tbd, tbd, tbd, tbd
***Lomatium multifidum* (Nutt.) R.P. McNeill & Darrach,** C.E. Hinchhliff 1249 (SRP), Asotin, Washington, KF619650, tbd, KF619926, KF619789, tbd, tbd, tbd
***Lomatium multifidum* (Nutt.) R.P. McNeill & Darrach,** C.E. Hinchhliff 1296 (SRP), Coconino, Arizona, KF619651, tbd, KF619924, KF619787, tbd, tbd, tbd
***Lomatium multifidum* (Nutt.) R.P. McNeill & Darrach,** D. Mansfield 7048c (CIC), Elmore, Idaho, tbd, tbd, tbd, tbd, tbd, tbd, tbd
***Lomatium multifidum* (Nutt.) R.P. McNeill & Darrach,** D. Mansfield 07391 (CIC), Malheur, Oregon, tbd, tbd, tbd, tbd, tbd, tbd, tbd
***Lomatium multifidum* (Nutt.) R.P. McNeill & Darrach,** E. George 059 (CIC), Washington, Idaho, KF619653, tbd, KF619926, KF619789, tbd, tbd, tbd
***Lomatium multifidum* (Nutt.) R.P. McNeill & Darrach,** Emma George 100 (CIC), Nez Perce, Idaho, tbd, tbd, tbd, tbd, tbd, tbd, tbd
***Lomatium multifidum* (Nutt.) R.P. McNeill & Darrach,** B. Chavez 028 (CIC), Owyhee, Idaho, tbd, tbd, tbd, tbd, tbd, tbd, tbd
***Lomatium oreganum* (J.M. Coult. & Rose) J.M. Coult. & Rose,** Rachel Sines sn (OSC), Wallowa, Oregon, tbd, tbd, tbd, tbd, tbd, tbd, tbd
***Lomatium oreganum* (J.M. Coult. & Rose) J.M. Coult. & Rose,** Roy Sines sn (OSC), Baker, Oregon, tbd, tbd, tbd, tbd, tbd, tbd, tbd
***Lomatium oreganum* (J.M. Coult. & Rose) J.M. Coult. & Rose,** Ann Kratz s.n. (WTU), Baker, Oregon, tbd, tbd, tbd, tbd, tbd, tbd, tbd
***Lomatium tracyi* Mathias & Constance,** J. Duncan 2013-4 (CIC), Curry, Oregon, tbd, tbd, tbd, tbd, tbd, tbd, tbd
***Musineon divaricatum,*** P. Lesica 11295 (CIC), Granite, Montana, tbd, tbd, tbd, tbd, tbd, tbd, tbd
***Musineon tenuifolia,*** B. E. Nelson 25258 (RM), Niobara, Wyoming, tbd, tbd, tbd, tbd, tbd, tbd, tbd
***Musineon vaginatum,*** P. Lesica 11285 (CIC), Missoula, Montana, tbd, tbd, tbd, tbd, tbd, tbd, tbd
***Musineon glaucescens* Lesica,** P. Lesica 11308 ICIC), Lewis & Clark, Montana, tbd, tbd, tbd, tbd, tbd, tbd, tbd
**Neoparrya lithophila Mathias ,** C.E. Hinchliff 1275, Taos, New Mexico, KF619725, tbd, KF619998, KF619861, tbd, tbd, tbd
***Pteryxia terebinthina* var. *terebinthina* (Hook.) J.M. Coult. & Rose ,** B. Ertter 22298 (SRP), Grant, Washington, MH131894, MH132101, MH132293, MH132479, MH132646, MH132842, MH133031
***Pteryxia terebinthina* var. *terebinthina* (Hook.) J.M. Coult. & Rose ,** C. E. Hinchliff 1271 (CIC), Grant, Washington, KF619733, MH132098, KF620007, KF619870, X, MH132839, MH133028
***Pteryxia terebinthina* var. *terebinthina* (Hook.) J.M. Coult. & Rose ,** L. Polito 038 (CIC), Boise, Idaho, MH131897, MH132100, MH132292, MH132478, MH132645, MH132841, MH133030
***Pteryxia terebinthina* var. *terebinthina* (Hook.) J.M. Coult. & Rose ,** J. F. Smith 11038 (SRP), Blaine, Idaho, MH131896, MH132099, MH132291, MH132477, MH132644, MH132840, MH133029

***Lomatium lithosolamans* J.F. Sm. & M.A. Feist,** C.E. Hinchliff 1237 (CIC), Yakima, Washington, KF619737, MH131995, KF620011, KF619874, X, MH132743, MH132944
***Tauschia stricklandii,*** B. Legler 3597 (WTU), Pierce, Washington, tbd, tbd, tbd, tbd, tbd, tbd, tbd
***Lomatium tenuissimum* (Geyer ex Hook.) Feist & G.M. Plunkett,** C. E. Hinchliff 1272 (SRP), Shoshone, Idaho, KF619738, MH132086, KF620012, KF619875, MH132633, MH132828, MH133016
***Tauschia texana,*** F. R. Barrie 1435 (RM), Gonzalez, Texas, tbd, tbd, tbd, tbd, tbd, tbd, tbd
***Tauschia glauca* (J.M. Coult. & Rose) Mathias & Constance ,** R. Spellenberg 10254 (ID), Trinity, California, tbd, tbd, tbd, tbd, tbd, tbd, tbd
**Tauschia stricklandii (J.M. Coult. & Rose) Mathias & Constance,** David Giglin 5362 (WTU), Yakima, Washington, tbd, tbd, tbd, tbd, tbd, tbd, tbd
***Thaspium trifoliatum,*** R.B. Clarkson 2474 (RM), Burnet, Texas, tbd, tbd, tbd, tbd, tbd, tbd, tbd
***Vesper multinervatus,*** M. Darrach 622 (CIC), Clark, Nevada, tbd, tbd, tbd, tbd, tbd, tbd, tbd
***Zizia aurea,*** R. L. McGregor 32892 (RM), Cherokee, Kansas, tbd, tbd, tbd, tbd, tbd, tbd, tbd
***Zosima absinthifolia* Link,** C. Davidson 12429 (SRP), , , tbd, tbd, tbd, tbd, tbd, tbd, tbd

# APPENDIX B

**Table depicting voucher information and which specimens were available for each analysis. (Chapter 2)**

| Accession | Collection | Location | Vegetative | Sanger | Environmental | Soil | NGS |
|---|---|---|---|---|---|---|---|
| *Ottenlips 80* | MVO_80 | Chelan County, Washington | Y | N | Y | Y | Y |
| *Mansfield 16031* | DM_16031 | Ada County, Idaho | N | Y | Y | N | Y |
| *Mansfield 16033* | DM_16033 | Ada County. Idaho | N | Y | Y | N | Y |
| *Mansfield 16078* | DM_16078 | Nez Perce County, Idaho | N | Y | Y | N | Y |
| *Carlson 97* | KC_097 | Owyhee County, Idaho | N | Y | Y | N | Y |
| *Lesicia 10552* | PL_10552 | Lake County, Montana | N | Y | Y | N | Y |
| *Lesicia 10541* | PL_10541 | Sanders County, Montana | N | Y | Y | N | Y |
| *Mansfield 16082* | DM_16082 | Latah County, Idaho | N | Y | Y | N | Y |
| *George 102* | EG_102 | Idaho County, Idaho | N | Y | Y | N | Y |
| *Lesicia 10978* | PL_10978 | Idaho County, Idaho | N | Y | Y | N | Y |
| *Lesicia 10794* | PL_10794 | Idaho County, Idaho | N | Y | Y | N | Y |
| *Ottenlips 65* | MVO_65 | Idaho County, Idaho | Y | N | Y | Y | Y |
| *Mansfield 16036* | DM_16036 | Washington County, Idaho | N | Y | Y | N | Y |
| *Mansfield 7055* | DM_7-55 | Washington County, Idaho | N | Y | Y | N | Y |
| *George 58* | EG_58 | Malheur County, Oregon | N | Y | Y | N | Y |
| *Smith 13048* | JFS_13048 | Lake County, Oregon | N | Y | Y | N | Y |
| *Ottenlips 42* | MVO_42 | Morrow County, Oregon | Y | N | Y | Y | Y |
| *Ottenlips 40* | MVO_40 | Morrow County, Oregon | Y | N | Y | Y | Y |

| | | | | | | | |
|---|---|---|---|---|---|---|---|
| *Truska 38* | Truska_38 | Malheur County, Oregon | N | Y | Y | N | Y |
| *Mansfield 15088* | DM_15088 | Owyhee County, Idaho | N | Y | Y | N | Y |
| *Pollito 002* | LP_002 | Owyhee County, Idaho | N | Y | Y | N | Y |
| *George 91* | EG_91 | Malheur County, Oregon | N | Y | Y | N | Y |
| *Ottenlips 74* | MVO_74 | Asotin County, Washington | Y | N | Y | Y | Y |
| *Ottenlips 76* | MVO_76 | Asotin County, Washington | N | N | Y | Y | Y |
| *Ottenlips 77* | MVO_77 | Asotin County, Washington | N | N | Y | Y | Y |
| *Ottenlips 25* | MVO_25 | Malheur County, Oregon | Y | N | Y | Y | Y |
| *Ottenlips 69* | MVO_69 | Idaho County, Idaho | Y | N | Y | Y | Y |
| *Mansfield 15152* | DM_15152 | Owyhee County, Idaho | N | Y | Y | N | Y |
| *Smith 10748* | JFS_10748 | Nez Perce County, Idaho | N | Y | Y | N | Y |
| *Mansfield 16037* | DM_16037 | Washington County, Idaho | N | Y | Y | Y | Y |
| *Ottenlips 32* | MVO_32 | Harney County, Oregon | N | N | Y | Y | Y |
| *Ottenlips 60* | MVO_60 | Gem County, Idaho | Y | N | Y | Y | Y |
| *Ottenlips 57* | MVO_57 | Washington County, Idaho | Y | N | Y | Y | Y |
| *Ottenlips 35* | MVO_35 | Grant County, Oregon | Y | N | Y | Y | Y |
| *Ottenlips 33* | MVO_33 | Grant County, Oregon | Y | N | Y | Y | Y |
| *Ottenlips 29* | MVO_29 | Malheur County, Oregon | Y | N | Y | Y | Y |
| *Ottenlips 22* | MVO_22 | Malheur County, Oregon | Y | N | Y | Y | Y |
| *Ottenlips 59* | MVO_59 | Idaho County, Idaho | Y | N | Y | Y | Y |
| *Mansfield 16064* | DM_16064 | Idaho County, Idaho | N | Y | Y | N | Y |
| *Ottenlips 45* | MVO_45 | Washington County, Idaho | Y | N | Y | Y | Y |

| | | | | | | | |
|---|---|---|---|---|---|---|---|
| *Ottenlips 62* | MVO_62 | Idaho County, Idaho | Y | N | Y | Y | Y |
| *Ottenlips 20* | MVO_20 | Owyhee County, Idaho | Y | N | Y | Y | Y |
| *Stevens 121* | MS_121 | Baker County, Oregon | N | Y | Y | Y | Y |
| *Stevens 123* | MS_123 | Washington County, Oregon | N | Y | Y | Y | Y |
| *Ottenlips 36* | MVO_36 | Grant County, Oregon | Y | N | Y | Y | Y |
| *Mansfield 17017* | DM_17017 | Baker County, Oregon | N | Y | Y | N | Y |
| *Ottenlips 73* | MVO_73 | Nez Perce County, Idaho | Y | N | Y | Y | Y |
| *Ottenlips 72* | MVO_72 | Nez Perce County, Idaho | Y | N | Y | Y | Y |

# APPENDIX C

**Box blot from pilot study of pocket-penetrometer efficacy (Chapter 2)**

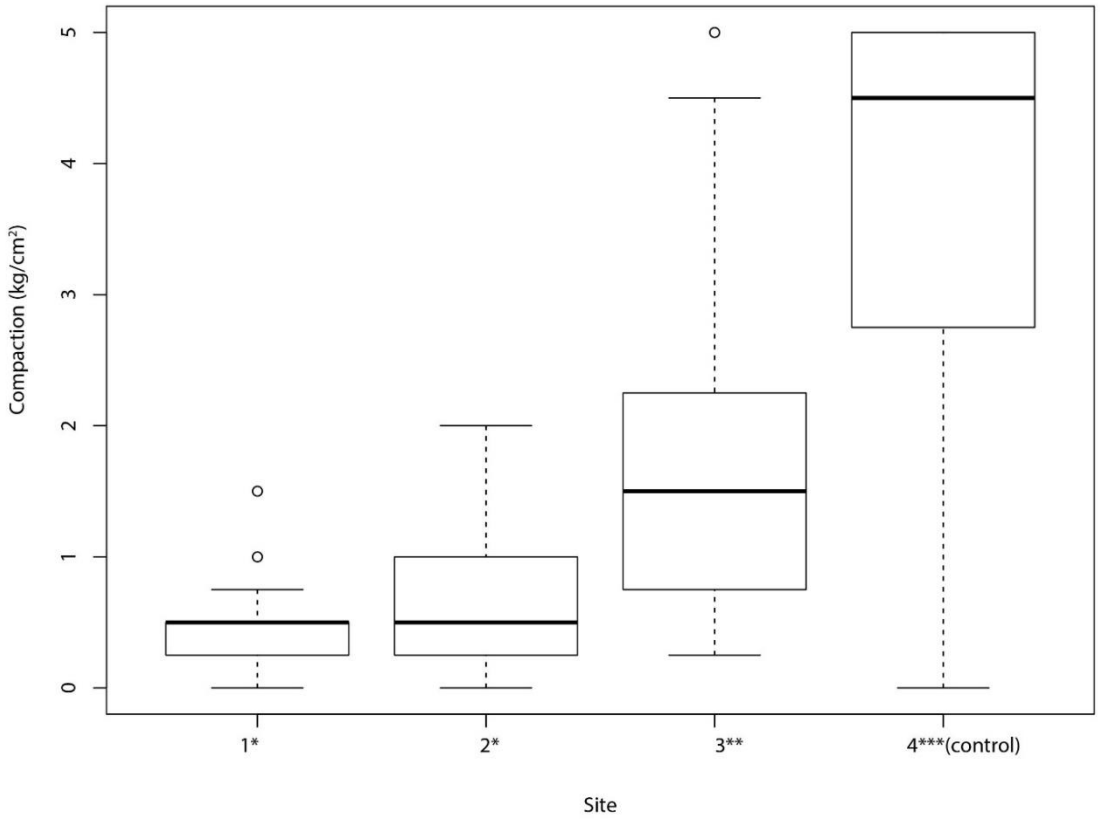


Box plot depicting the differences and variability of soil compaction readings between sites. The ranks of the sums are significantly different (Kruskal-Wallis chi-squared = 166.26, df = 3, p-value < .01) Different numbers of asterisks denote significance from the Wilcoxon rank sum pairwise comparisons. The dark line in the middle of the box represents the mean. The top and bottom bounds of the box represent the 25th and 75th percentiles, respectively. The whiskers at the end of the dotted line represent the 5th and 95th percentiles. The hollow dots represent the outliers.

# APPENDIX D

**Raw soil chemistry and physical properties data (Chapter 2)**

| Collection | Soil_pH | P_ppm | Bray1_K_ppm | Ca_ppm | Mg_ppm | Na_ppm | CEC_sum | OM | Sulfate_ppm | Soluble_salts | N | nitrate | amonia | gravel | clay | sand_and_silt |
|---|---|---|---|---|---|---|---|---|---|---|---|---|---|---|---|---|
| MVO_20 | 6.9 | 48 | 653 | 3247 | 401 | 89 | 18 | 3.80161 | 4.1 | 0.35 | 1755.77 | 19.9 | 7 | 60.7895 | 37.9658 | 62.0342 |
| MVO_22 | 7.1 | 36 | 405 | 3499 | 1044 | 164 | 18 | 3.86001 | 2.7 | 0.22 | 1336.79 | 3.1 | 6.8 | 67.4234 | 48.0144 | 51.9856 |
| MVO_25 | 7.6 | 16 | 336 | 2759 | 621 | 231 | 15 | 2.2705 | 1.4 | 0.29 | 843.468 | 3.7 | 3.6 | 30.5889 | 34 | 66 |
| MVO_29 | 7.1 | 66 | 545 | 2907 | 723 | 48 | 16 | 3.73674 | 2.3 | 0.21 | 1801.1 | 10.9 | 4 | 16.1484 | 40.008 | 59.992 |
| MVO_32 | 7.1 | 27 | 192 | 4153 | 630 | 88 | 20 | 2.18951 | 0.8 | 0.28 | 672.357 | 3.1 | 4.1 | 1.83552 | 68.0068 | 31.9932 |
| MVO_33 | 6.7 | 21 | 172 | 3089 | 1058 | 31 | 16 | 3.96606 | 2.8 | 0.21 | 1790.05 | 8.5 | 7.1 | 10.1006 | 35.9928 | 64.0072 |
| MVO_35 | 7.1 | 20 | 140 | 3227 | 1092 | 34 | 14 | 2.79122 | 2.9 | 0.25 | 1041.03 | 6.4 | 9.1 | 40.0951 | 37.9962 | 62.0038 |
| MVO_36 | 6.9 | 13 | 171 | 2334 | 1047 | 35 | 10 | 3.17588 | 1.7 | 0.15 | 1534.95 | 6.4 | 7.6 | 38.7924 | 28.9913 | 71.0087 |
| MVO_40 | 7.8 | 34 | 214 | 6624 | 437 | 24 | 34 | 3.66231 | 19.6 | 0.27 | 1589.21 | 4.5 | 7.4 | 19.499 | 40.9918 | 59.0082 |
| MVO_42 | 6.9 | 24 | 258 | 2610 | 649 | 45 | 13 | 3.15615 | 4.2 | 0.21 | 1437.26 | 9.9 | 7.9 | 38.9585 | 33.0066 | 66.9934 |
| MVO_45 | 7 | 54 | 258 | 3519 | 1162 | 43 | 20 | 2.99615 | 1.5 | 0.23 | 812.527 | 2 | 11.4 | 29.4146 | 57.9826 | 42.0174 |
| MVO_57 | 6.7 | 29 | 244 | 2484 | 496 | 220 | 16 | 3.40369 | 2.8 | 0.14 | 1441.36 | 2.4 | 11.6 | 41.5451 | 24.985 | 75.015 |

| | | | | | | | | | | | | | | | | |
|---|---|---|---|---|---|---|---|---|---|---|---|---|---|---|---|---|
| MVO_59 | 6.4 | 44 | 183 | 2127 | 276 | 15 | 12 | 4.47077 | 5 | 0.12 | 2352.36 | 10.8 | 6.3 | 39.6089 | 25.9844 | 74.0156 |
| MVO_60 | 6.5 | 45 | 235 | 3408 | 856 | 29 | 20 | 4.95427 | 4.2 | 0.25 | 2077.94 | 2.5 | 12.3 | 30.7358 | 47.976 | 52.024 |
| MVO_62 | 6.3 | 7 | 83 | 3280 | 1049 | 41 | 17 | 2.97109 | 1.3 | 0.2 | 1216.15 | 16.2 | 3.3 | 26.803 | 32.3069 | 67.6931 |
| MVO_65 | 5.9 | 16 | 153 | 2339 | 601 | 48 | 15 | 4.54464 | 5.4 | 0.2 | 2126.82 | 26.6 | 4.8 | 41.3407 | 37.9507 | 62.0493 |
| MVO_69 | 5.8 | 5 | 261 | 2759 | 809 | 19 | 20 | 7.71278 | 5.5 | 0.6 | 4292.75 | 153 | 3.4 | 20.7059 | 31.1495 | 68.8505 |
| MVO_72 | 6.3 | 35 | 335 | 3958 | 407 | 28 | 25 | 6.24873 | 4.2 | 0.31 | 2941.42 | 36.4 | 44.3 | 40.8583 | 43.9341 | 56.0659 |
| MVO_73 | 6.9 | 24 | 355 | 7158 | 816 | 19 | 34 | 3.57964 | 2.5 | 0.25 | 1498.02 | 11.3 | 44.4 | 44.0935 | 43 | 57 |
| MVO_74 | 6.9 | 20 | 209 | 4180 | 671 | 17 | 19 | 2.58565 | 1.4 | 0.15 | 1246.68 | 8.4 | 2.9 | 32.9555 | 27.8996 | 72.1004 |
| MVO_76 | 6.7 | 47 | 363 | 3861 | 497 | 17 | 22 | 4.35281 | 2 | 0.12 | 2325.18 | 4.5 | 6.1 | 29.5254 | 38.1986 | 61.8014 |
| MVO_77 | 6 | 24 | 184 | 1893 | 392 | 19 | 13 | 3.39382 | 2.4 | 0.16 | 1920.26 | 21.4 | 3 | 0.12565 | 33.8949 | 66.1051 |
| MS_121 | 7 | 22 | 156 | 2731 | 1076 | 40.4 | 14.4531 | 1.8 | 2.9 | 0.33 | 796 | 2.8 | 14.5 | 23.6749 | 22.1343 | 77.8657 |
| DM_16037 | 6.6 | 123 | 612 | 2843 | 807 | 40.4 | 19.2827 | 4.6 | 4.4 | 0.43 | 2515.8 | 4.5 | 12.6 | 20.8075 | 25.3416 | 74.6584 |

# APPENDIX E

**Climatic variables for each collection. Codes correspond to the variable in the key: bio1_12 = Annual Mean Tempature (°C); bio2_12= Mean Diurnal Range (°C); bio3_12 = Isothermality (°C); bio5_12 = Max Temperature of the Warmest Month (°C); bio6_12 = Min Temperature of the Coldest Month (°C); bio7_12 = Temperature Annual Range (°C); bio8_12 = Mean Temperature of the Wettest Quarter (°C); bio9_12 = Mean Temperature of the Driest Quarter (°C); bio11_12 = Mean Temperature of the Warmest Quarter (°C); bio12_12 = Mean Temperature of the Coldest Quarter (°C); bio13_12 = Annual Precipitation (mm); bio14_12 = Precipitation of the Wettest Month (mm); bio16_12 = Precipitation of the Driest Month (mm); bio19_12 = Precipitation of the Wettest Quarter (mm). (Chapter 2)**

| Collection | bio1_12 | bio2_12 | bio3_12 | bio4_12 | bio5_12 | bio6_12 | bio7_12 | bio8_12 | bio9_12 | bio10_12 | bio11_12 | bio12_12 | bio13_12 | bio14_12 | bio15_12 | bio16_12 | bio17_12 | bio18_12 | bio19_12 |
|---|---|---|---|---|---|---|---|---|---|---|---|---|---|---|---|---|---|---|---|
| MVO_80 | 95 | 139 | 36 | 8336 | 308 | -68 | 376 | -7 | 195 | 201 | -14 | 448 | 88 | 8 | 72 | 241 | 36 | 37 | 220 |
| DM_16031 | 76 | 149 | 38 | 8149 | 301 | -88 | 389 | -18 | 178 | 183 | -27 | 486 | 70 | 11 | 46 | 199 | 50 | 57 | 188 |
| DM_16033 | 106 | 140 | 36 | 8346 | 327 | -56 | 383 | 7 | 209 | 215 | -1 | 330 | 42 | 8 | 38 | 121 | 37 | 43 | 111 |
| DM_16078 | 116 | 129 | 37 | 7620 | 321 | -26 | 347 | 25 | 211 | 215 | 21 | 445 | 48 | 19 | 25 | 143 | 67 | 80 | 132 |
| KC_097 | 72 | 159 | 40 | 7731 | 297 | -91 | 388 | -17 | 169 | 175 | -24 | 354 | 40 | 11 | 31 | 120 | 46 | 59 | 112 |
| PL_10552 | 72 | 126 | 35 | 7914 | 277 | -79 | 356 | 112 | 26 | 176 | -28 | 439 | 59 | 25 | 28 | 150 | 88 | 124 | 97 |
| PL_10541 | 48 | 136 | 37 | 7708 | 261 | -104 | 365 | -42 | 143 | 149 | -48 | 575 | 65 | 30 | 22 | 182 | 110 | 128 | 172 |
| DM_16082 | 77 | 125 | 37 | 6893 | 275 | -57 | 332 | -5 | 164 | 166 | -10 | 614 | 80 | 21 | 37 | 234 | 77 | 90 | 217 |

| | | | | | | | | | | | | | | | | | | | |
|---|---|---|---|---|---|---|---|---|---|---|---|---|---|---|---|---|---|---|---|
| EG_102 | 77 | 132 | 38 | 7085 | 278 | -63 | 341 | 106 | 167 | 172 | -9 | 586 | 77 | 28 | 29 | 205 | 103 | 125 | 125 |
| PL_10978 | 74 | 134 | 38 | 7095 | 276 | -68 | 344 | 102 | 164 | 169 | -13 | 600 | 77 | 29 | 27 | 207 | 105 | 128 | 130 |
| PL_10794 | 102 | 137 | 38 | 7592 | 315 | -43 | 358 | 96 | 197 | 203 | 8 | 600 | 71 | 26 | 26 | 195 | 97 | 116 | 140 |
| MVO_65 | 79 | 132 | 38 | 7151 | 280 | -62 | 342 | 108 | 169 | 174 | -9 | 569 | 74 | 28 | 28 | 198 | 101 | 123 | 121 |
| DM_16036 | 90 | 151 | 36 | 8948 | 321 | -90 | 411 | -18 | 198 | 206 | -27 | 361 | 53 | 9 | 43 | 149 | 41 | 50 | 139 |
| DM_7-55 | 82 | 155 | 37 | 8877 | 315 | -98 | 413 | -24 | 188 | 196 | -36 | 433 | 65 | 10 | 47 | 184 | 45 | 55 | 173 |
| EG_58 | 102 | 157 | 39 | 8121 | 330 | -65 | 395 | 4 | 200 | 208 | -2 | 244 | 26 | 8 | 27 | 76 | 36 | 46 | 70 |
| JFS_13048 | 73 | 143 | 41 | 6668 | 273 | -68 | 341 | -4 | 158 | 161 | -10 | 442 | 56 | 13 | 36 | 163 | 54 | 63 | 145 |
| MVO_42 | 88 | 140 | 41 | 6651 | 286 | -50 | 336 | 12 | 174 | 176 | 7 | 373 | 47 | 11 | 34 | 133 | 45 | 55 | 118 |
| MVO_40 | 75 | 163 | 41 | 7714 | 303 | -89 | 392 | -14 | 172 | 178 | -20 | 346 | 40 | 12 | 30 | 117 | 46 | 59 | 108 |
| Truska_38 | 73 | 164 | 41 | 7701 | 301 | -90 | 391 | -15 | 170 | 176 | -22 | 346 | 39 | 12 | 30 | 115 | 46 | 59 | 107 |
| DM_15088 | 80 | 162 | 41 | 7679 | 305 | -83 | 388 | -10 | 175 | 182 | -17 | 315 | 34 | 11 | 28 | 100 | 43 | 56 | 93 |
| LP_002 | 82 | 166 | 42 | 7673 | 310 | -82 | 392 | -9 | 176 | 183 | -15 | 301 | 32 | 11 | 27 | 92 | 43 | 55 | 85 |
| EG_91 | 68 | 133 | 39 | 6974 | 269 | -71 | 340 | -13 | 157 | 159 | -19 | 587 | 72 | 20 | 34 | 213 | 77 | 91 | 196 |
| MVO_74 | 77 | 131 | 38 | 7156 | 279 | -64 | 343 | -7 | 168 | 170 | -12 | 522 | 55 | 22 | 25 | 163 | 81 | 97 | 148 |
| MVO_76 | 73 | 132 | 38 | 7136 | 275 | -69 | 344 | -11 | 163 | 166 | -17 | 537 | 57 | 22 | 25 | 170 | 83 | 99 | 155 |
| MVO_77 | 94 | 160 | 40 | 7939 | 321 | -71 | 392 | -1 | 190 | 199 | -7 | 264 | 28 | 9 | 27 | 82 | 38 | 50 | 76 |
| MVO_25 | 88 | 132 | 38 | 7290 | 292 | -53 | 345 | 118 | 181 | 185 | -1 | 519 | 66 | 25 | 26 | 177 | 91 | 111 | 114 |
| MVO_69 | 70 | 156 | 40 | 7735 | 293 | -91 | 384 | -18 | 168 | 174 | -26 | 363 | 42 | 11 | 32 | 126 | 46 | 59 | 117 |
| DM_15152 | 105 | 131 | 37 | 7515 | 311 | -37 | 348 | 137 | 200 | 204 | 12 | 420 | 48 | 19 | 23 | 130 | 70 | 84 | 108 |

| | | | | | | | | | | | | | | | | | | | |
|---|---|---|---|---|---|---|---|---|---|---|---|---|---|---|---|---|---|---|---|
| JFS_10748 | 80 | 152 | 37 | 8773 | 309 | -98 | 407 | -25 | 186 | 193 | -35 | 389 | 57 | 11 | 43 | 159 | 46 | 57 | 149 |
| DM_16037 | 80 | 164 | 41 | 7988 | 308 | -92 | 400 | -15 | 178 | 185 | -22 | 283 | 36 | 11 | 32 | 102 | 41 | 50 | 92 |
| MVO_32 | 70 | 155 | 39 | 8235 | 297 | -100 | 397 | -27 | 170 | 177 | -37 | 513 | 72 | 12 | 45 | 210 | 54 | 63 | 198 |
| MVO_60 | 58 | 155 | 38 | 8397 | 287 | -116 | 403 | -39 | 160 | 167 | -52 | 547 | 79 | 15 | 43 | 222 | 62 | 76 | 212 |
| MVO_57 | 72 | 157 | 44 | 6524 | 281 | -72 | 353 | -3 | 154 | 159 | -9 | 406 | 47 | 16 | 28 | 137 | 61 | 73 | 119 |
| MVO_35 | 53 | 159 | 43 | 6688 | 264 | -98 | 362 | -23 | 138 | 142 | -30 | 443 | 55 | 17 | 31 | 157 | 65 | 78 | 138 |
| MVO_33 | 67 | 161 | 41 | 7822 | 294 | -98 | 392 | -24 | 164 | 170 | -32 | 360 | 43 | 12 | 31 | 125 | 48 | 61 | 116 |
| MVO_29 | 76 | 164 | 41 | 7686 | 305 | -87 | 392 | -12 | 173 | 179 | -19 | 330 | 37 | 11 | 30 | 109 | 44 | 56 | 101 |
| MVO_22 | 63 | 146 | 39 | 7404 | 275 | -91 | 366 | 94 | 156 | 160 | -30 | 583 | 64 | 24 | 25 | 178 | 91 | 112 | 159 |
| MVO_59 | 76 | 133 | 38 | 7107 | 277 | -65 | 342 | 105 | 166 | 171 | -11 | 589 | 77 | 28 | 28 | 206 | 103 | 126 | 126 |
| DM_16064 | 68 | 154 | 37 | 8664 | 299 | -109 | 408 | -34 | 173 | 180 | -46 | 480 | 71 | 12 | 45 | 200 | 52 | 64 | 190 |
| MVO_45 | 59 | 141 | 39 | 7125 | 264 | -89 | 353 | 87 | 149 | 153 | -29 | 621 | 74 | 28 | 25 | 201 | 104 | 126 | 154 |
| MVO_62 | 74 | 163 | 41 | 7721 | 302 | -90 | 392 | -15 | 171 | 177 | -22 | 353 | 41 | 12 | 31 | 120 | 46 | 59 | 111 |
| MVO_20 | 87 | 154 | 38 | 8471 | 313 | -84 | 397 | -14 | 189 | 195 | -25 | 470 | 67 | 13 | 43 | 193 | 54 | 66 | 179 |
| MS_121 | 78 | 154 | 37 | 8818 | 310 | -102 | 412 | -27 | 184 | 191 | -39 | 450 | 67 | 11 | 47 | 190 | 47 | 57 | 180 |
| MS_123 | 72 | 157 | 44 | 6524 | 281 | -72 | 353 | -3 | 154 | 159 | -9 | 406 | 47 | 16 | 28 | 137 | 61 | 73 | 119 |
| MVO_36 | 74 | 152 | 39 | 8140 | 295 | -93 | 388 | -24 | 174 | 178 | -32 | 337 | 42 | 14 | 29 | 118 | 53 | 68 | 108 |
| DM_17017 | 102 | 125 | 36 | 7360 | 303 | -37 | 340 | 15 | 195 | 198 | 10 | 474 | 51 | 20 | 25 | 152 | 72 | 86 | 139 |
| MVO_73 | 68 | 129 | 37 | 7060 | 268 | -72 | 340 | 97 | 158 | 162 | -19 | 597 | 71 | 27 | 24 | 190 | 101 | 119 | 148 |
| MVO_72 | 67 | 158 | 44 | 6682 | 275 | -81 | 356 | -7 | 154 | 155 | -14 | 436 | 58 | 11 | 40 | 164 | 46 | 58 | 154 |

# APPENDIX F

**Summary of reproductive character measurements. Each cell is the mean of 5 replicate measures. (Chapter 2)**

| Collection | STACEY fine clade | Ray length | Mature Fruit length | Mature Fruit Width | Mature Pedicel Length | Length of primary umbel | Width of primary umbel | Wing width | Fruit length |
|---|---|---|---|---|---|---|---|---|---|
| DM_16031 | Andrusianum | 8.1 | 12.6 | 4.8 | 4.4 | 7 | 8 | 1 | 4 |
| DM_16033 | Andrusianum | 10.6 | 10.6 | 4.2 | 4.2 | 13.5 | 12.5 | 1 | 4.5 |
| DM_16078 | TriTri | 7.1 | 14.8 | 6 | 8.8 | 10 | 14 | 1 | 5.5 |
| DM_16082 | Western Montana | 7.6 | 9.2 | 4.6 | 7.4 | 8.5 | 9 | 1 | 4 |
| DM_16036 | Mann Creek | 3.8 | 18.4 | 6.4 | 4.8 | 7 | 6 | 2 | 6 |
| MVO_42 | East-Central Oregon | 6.2 | 11.2 | 6 | 7 | 9 | 13 | 2 | 6 |
| DM_15088 | Packardiae | 5.4 | 7.8 | 4.2 | 4.6 | 8 | 9 | 0.75 | 3 |
| EG_91 | Packardiae | 5.7 | 9.4 | 4 | 5.2 | 11 | 4 | 1 | 5 |
| MVO_25 | Packardiae | 5.4 | 7.6 | 3.6 | 4.8 | 7 | 6 | 1 | 3 |
| DM_15152 | Packardiae | 6.6 | 9 | 4 | 4.2 | 8 | 9 | 0.75 | 3 |
| DM_16037 | Mann Creek | 8.6 | 14.8 | 5.7 | 6.6 | 11 | 12.5 | 1 | 4.5 |
| DM_16064 | Camas Prairie | 11.8 | 10.6 | 4.6 | 4.4 | 17 | 15 | 1.25 | 6 |
| MVO_20 | Packardiae | 6.8 | 6.4 | 3 | 4.8 | 8 | 10 | 0.5 | 4 |
| MS_121 | Hell's Canyon | 10.2 | 15.4 | 4.2 | 8 | 13 | 7 | 1 | 4 |
| MS_123 | Mann Creek | 6.9 | 13.2 | 4.6 | 8 | 8 | 8 | 1 | 4 |
| MVO_73 | TriTri | 6.8 | 8.2 | 3.8 | 6 | 9 | 10 | 1 | 4 |

# APPENDIX G

**The mean of 5 replicate measurements for leaflet width and length taken from Herbarium collections. (Chapter 2)**

| Collection | Length | Width |
|---|---|---|
| DM_15088 | 8.2 | 1 |
| DM_16031 | 18 | 1.8 |
| DM_16033 | 10.8 | 2.2 |
| DM_16036 | 25.2 | 3.4 |
| DM_16037 | 17.6 | 2.8 |
| DM_16064 | 41 | 13.4 |
| DM_16078 | 29.6 | 3.4 |
| DM_16082 | 59.8 | 2 |
| DM_17017 | 16.6 | 1.9 |
| DM_7-55 | 23 | 4.2 |
| EG_102 | 36.4 | 10.8 |
| EG_58 | 14.6 | 1.4 |
| EG_91 | 14 | 1.2 |
| KC_097 | 10.8 | 1.4 |
| MS_121 | 19 | 2.4 |
| MS_123 | 33.4 | 4.8 |
| MVO_32 | 12.4 | 1.3 |
| MVO_76 | 28.2 | 2.5 |
| MVO_77 | 52.2 | 2.2 |
| PL_10541 | 48.2 | 4.6 |
| PL_10552 | 51.6 | 5 |
| PL_10794 | 36.2 | 9.4 |
| PL_10978 | 43.8 | 10.2 |
| MVO_65 | 30 | 5 |
| MVO_42 | 20 | 2 |
| MVO_40 | 20 | 1 |
| MVO_74 | 40 | 1 |
| MVO_25 | 4 | 1 |
| MVO_69 | 32 | 4 |
| MVO_60 | 20 | 3 |
| MVO_57 | 60 | 5 |
| MVO_35 | 15 | 2 |
| MVO_33 | 15 | 1 |
| MVO_29 | 40 | 3 |
| MVO_22 | 20 | 1 |
| MVO_59 | 55 | 5 |
| MVO_45 | 25 | 4 |
| MVO_62 | 30 | 10 |

| | | |
|---|---|---|
| MVO_20 | 25 | 3 |
| MVO_36 | 25 | 1 |
| MVO_73 | 50 | 3 |
| MVO_72 | 43 | 8 |